

© Copyright 2013
Nora Lee

The Role of Organic Cation Transporter 3 in Metformin Disposition during Pregnancy

Nora Lee

A dissertation

submitted in partial fulfillment of the

requirements for the degree of

Doctor of Philosophy

University of Washington

2013

Reading Committee:

Joanne Wang, Chair

Kenneth E. Thummel

Mary F. Hebert

Program Authorized to Offer Degree:

Pharmaceutics

University of Washington

Abstract

The Role of Organic Cation Transporter 3 in Metformin Disposition during Pregnancy

Nora Lee

Chair of the Supervisory Committee:

Professor Joanne Wang

Department of Pharmaceutics

Metformin, a front line drug for type 2 diabetes mellitus, has been recently introduced as an alternative therapy for insulin in treatment of gestational diabetes mellitus. Despite clinical enthusiasm for the drug, there are still concerns about the effects of metformin on maternal and neonatal outcomes. A clinical study conducted by Obstetric-fetal Pharmacology Research Network showed that metformin renal clearance was significantly increased during pregnancy. Moreover, metformin readily crosses the placental barrier and its concentration in fetal circulation can be as high as maternal concentrations. The overall goal of this dissertation is to understand mechanisms involved in maternal and fetal disposition of metformin. The studies were designed to 1) determine the mechanism of altered maternal metformin disposition during pregnancy; 2) elucidate the role of OCT3 in fetal exposure to metformin and in tissue distribution of metformin in both pregnant and non-pregnant states.

To evaluate the effect of pregnancy on expression of polyspecific organic cation transporters, we measured mRNA and protein expression of major organic cation transporters in

kidney, liver and placenta in pregnant mice and in human placentas. The overall effect of pregnancy on renal and hepatic expression of organic cation transporters was moderate, suggesting that increased renal clearance of metformin in pregnant women might be due to other pregnancy-associated changes. OCT3/Oct3 were highly expressed in human and mouse placentas. Interestingly, the expression of mouse placental Oct3 significantly increased from mid gestational stage to term whereas OCT3 in human placenta only showed a moderate increase in mid-to-late pregnancy. The role of OCT3/Oct3 in metformin tissue specific distribution was determined by performing an *in vivo* study in *Oct3* gene deletion mice. The *in vivo* study results suggest that Oct3 profoundly affects metformin plasma kinetics and distribution in peripheral tissues including salivary gland, heart and skeletal muscle, which highly express OCT3/Oct3. Our findings demonstrate that OCT3/Oct3 is responsible for high accumulation of metformin in the salivary glands, which potentially accounts for the taste disturbance caused by metformin in type 2 diabetic patients taking this drug. In order to determine the role of OCT3 in fetal exposure to metformin, immunolocalization study in human term placenta and *in vivo* study in pregnant Oct3^{-/-} mice were carried out. OCT3 was concentrated to the basal membrane of syncytiotrophoblast in human placenta. Pregnant Oct3^{-/-} mice showed reduced fetal exposure to metformin, suggesting that OCT3/Oct3 facilitates transport of metformin from the placenta to the fetal compartment.

In summary, findings from this dissertation research have greatly contributed our understanding of the mechanisms involved in maternal and fetal disposition of metformin. Importantly, our studies uncovered a novel molecular mechanism underlying taste disturbance caused by metformin and identified OCT3 as an important determinant of fetal exposure to metformin.

Table of Contents

List of figures.....	iv
List of tables.....	vi
Chapter 1. Introduction	1
1.1. Background	1
1.1.1. Pharmacotherapy in pregnant women	1
1.1.2. Gestational diabetes mellitus and metformin	3
1.1.3. Metformin disposition during pregnancy	6
1.1.3.1. Polyspecific organic cation transporters and the roles in metformin PK/PD.....	6
1.1.3.2. Metformin maternal and fetal disposition during pregnancy	9
1.1.3.3. Potential importance of OCT3 in metformin disposition	10
1.2. Hypothesis and Specific Aims	11
1.3. Research Focus and Overall Significance	12
Chapter 2. Pregnancy induced metformin pharmacokinetic change in a mouse model	18
2.1. Introduction	18
2.2. Materials and methods	19
2.2.1. Animals	20
2.2.2. <i>In vivo</i> study	20
2.2.3. Statistical and pharmacokinetics analysis	20
2.3. Results	21
2.4. Discussion	22
Chapter 3. Effect of gestational age on mRNA and protein expression of polyspecific organic cation transporters during pregnancy	26
3.1. Introduction	26
3.2. Materials and methods	28
3.2.1. Animals and tissue harvest	28
3.2.2. Human placenta source	29
3.2.3. RNA isolation, cDNA synthesis and quantitative real-time PCR assays	29

3.2.4. Membrane protein preparation and quantification of transporters by LC-MS/MS analysis	31
3.2.5. Data analysis	33
3.3. Results	33
3.3.1. Fluctuation of house-keeping genes in various tissues during pregnancy	33
3.3.2. mRNA quantification of renal and hepatic mOct and mMate transporters in non-pregnant and pregnant mice at different gestational ages	34
3.3.3. Protein quantification of renal and hepatic mOct and mMate transporters in non-pregnant and pregnant mice at different gestational age.....	35
3.3.4. mRNA expression pattern of OC transporters in human and mouse placenta	35
3.3.5. mOct3 mRNA and protein expression in mouse placenta at various gestational stages	36
3.3.6. hOCT3 mRNA and protein expression in human placenta at different trimesters ..	37
3.4. Discussion.....	38

Chapter 4. Taste of pill: Organic cation transporter 3 mediates salivary gland

accumulation of metformin	50
4.1. Introduction	50
4.2. Materials and methods	51
4.2.1. Animals	51
4.2.2. Human salivary glands	51
4.2.3. RNA preparation and real-time PCR	52
4.2.4. Drug uptake in hOCT3 expressing cells	52
4.2.5. Membrane protein preparation and LC-MS/MS analysis	53
4.2.6. <i>In vivo</i> study in mice	54
4.2.7. Immunofluorescent labeling of hOCT3 in human submandibular salivary glands...	56
4.2.8. Pharmacokinetic data analysis	57
4.2.9. Statistical analysis	57
4.3. Results	58
4.3.1. Metformin transport kinetics by OCT3.....	59
4.3.2. Predominant expression of OCT3 in salivary glands	59
4.3.3. OCT3 protein expression and localization in salivary glands	60

4.3.4. Altered metformin pharmacokinetics in Oct3 ^{-/-} mice	61
4.3.5. Depleted metformin accumulation in salivary glands of Oct3 ^{-/-} mice	62
4.4. Discussion	63
Chapter 5. Organic cation transporter 3 facilitates fetal disposition of metformin during pregnancy	81
5.1. Introduction	81
5.2. Materials and methods	81
5.2.1. Animals and tissue harvest	83
5.2.2. Human placenta source	83
5.2.3. Immunolocalization studies in human placenta	83
5.2.4. Expression of organic cation transporters and monoamine transporters in mouse placenta	84
5.2.5. <i>In vivo</i> study	84
5.2.6. Pharmacokinetic data analysis	85
5.3. Results	86
5.3.1. Localization of OCT3 in human term placenta	88
5.3.2. Expression of polyspecific organic cation transporters and monoamine transporters in placenta of pregnant Oct3 ^{+/+} and Oct3 ^{-/-} mice	88
5.3.3. Maternal plasma kinetics of metformin in Oct3 ^{+/+} and Oct3 ^{-/-} mice	88
5.3.4. Fetal exposure to metformin in Oct3 ^{+/+} and Oct3 ^{-/-} mice	89
5.3.5. Peripheral tissue distribution of metformin in Oct3 ^{+/+} and Oct3 ^{-/-} mice	90
5.4. Discussion	90
Chapter 6. Conclusions and future direction	103
Bibliography	106

List of figures

Figure 1.1 Cellular models of renal (A) and hepatic (B) organic cation transport	15
Figure 2.1. Dose-normalized plasma concentration-time profile of metformin in wild-type FVB non-pregnant (□) and pregnant (■) mice	25
Figure 3.1. Ct values of different housekeeping genes in kidney and liver from pregnant mice at different gestational ages	44
Figure 3.2. mRNA and protein expression of mouse OC transporters in kidney (A and C) and liver (B and D) at different gestational ages	45
Figure 3.3. mRNA expression of various OC transporters in human term placenta (A) and mouse placenta at gd 19 (B)	46
Figure 3.4. mOct3 mRNA and protein expression in mouse placenta at different gestational ages	47
Figure 3.5. Quantification of hOCT3 mRNA (A) and protein (B) in human placentas at different gestational stages and correlation analysis of mRNA and protein expression (C)	48
Figure 4.1. Metformin transport kinetics in human OCT3-expressing HEK cells	70
Figure 4.2. Expression of polyspecific organic cation transporters in various tissues of Oct3 ^{+/+} (solid bar) and Oct3 ^{-/-} (open bar) mice	71
Figure 4.3. Oct3 mRNA expression in various mouse tissues (A) and mRNA expression of various transporters in mouse salivary glands (B)	72
Figure 4.4. mRNA expression of various transporters in human salivary glands (A) and OCT3 mRNA expression in three human salivary gland regions (B).....	73
Figure 4.5. Protein expression of OCT3 in three human salivary glands regions	74
Figure 4.6. Dual-color immunofluorescence staining in human submandibular glands	75
Figure 4.7. Metformin plasma kinetics in female Oct3 ^{+/+} and Oct3 ^{-/-} mice	76
Figure 4.8. Metformin plasma kinetics in male Oct3 ^{+/+} and Oct3 ^{-/-} mice	77

Figure 4.9. Accumulation of metformin in salivary glands of female and male Oct3 ^{+/+} and Oct3 ^{-/-} mice	78
Figure 4.10. Plasma and salivary glands metformin concentration in female and male Oct3 ^{+/+} (A) and Oct3 ^{-/-} (B) mice	79
Figure 4.11. Proposed model for OCT3-mediated organic cation transport in salivary gland epithelial cells	80
Figure 5.1. Dual-color immunofluorescence staining in human term placenta	98
Figure 5.2. Expression of various organic cation transporters in the placentas of Oct3 ^{+/+} and Oct3 ^{-/-} mice	99
Figure 5.3. The plasma concentration-time curve of metformin after an oral dose in pregnant Oct3 ^{+/+} mice (□) and Oct3 ^{-/-} mice (■) (n=3-5 at each time point) at gd 19	100
Figure 5.4. Fetal concentration-time curve of metformin after an oral dose in pregnant Oct3 ^{+/+} mice (■) and Oct3 ^{-/-} mice (□) (n=3-5 at each time point) at gd 19	101
Figure 5.5. Proposed cellular model of metformin transport at the maternal-fetal interface ...	102

List of tables

Table 1.1. Effect of physiological changes on pharmacokinetics during pregnancy	16
Table 1.2. Apparent binding affinities of OCT1-3, MATE1/2K and PMAT toward metformin	17
Table 2.1. Dose-normalized pharmacokinetic parameters of metformin in pregnant and non- pregnant wild-type FVB mice	24
Table 3.1. Optimized MS/MS parameters of proteotypic peptides selected for targeted analysis of mOct1, mOct2, mOct3, mMate1 and hOCT3	43
Table 3.2. hOCT3 mRNA and protein quantification in human placentas from first, second trimesters and at term	44
Table 4.1. Metformin pharmacokinetic parameters from female Oct3 ^{+/+} and Oct3 ^{-/-} mice	67
Table 4.2. Metformin pharmacokinetic parameters from male Oct3 ^{+/+} and Oct3 ^{-/-} mice	68
Table 4.3. Tissue AUC _{0-8hr} from female and male Oct3 ^{+/+} and Oct3 ^{-/-} mice	69
Table 5.1. Maternal metformin pharmacokinetic parameters from pregnant Oct3 ^{+/+} and Oct3 ^{-/-} mice	95
Table 5.2. Fetal exposure to metformin in Oct3 ^{+/+} and Oct3 ^{-/-} pregnant mice	96
Table 5.3. Various tissue AUCs in Oct3 ^{+/+} and Oct3 ^{-/-} pregnant mice	97

Acknowledgement

This dissertation is a milestone in my academic career. I have been fortunate to build a solid foundation of scientific theories and skills which would have been impossible if I had not met a number of people who have guided and supported me throughout my research journey.

Foremost, I would like to express my sincerest gratitude to my doctoral advisor, Dr. Joanne Wang, for her everlasting patience, support and guidance. She has been a dedicated scientific advisor as well as a great mentor on life and career. She knows and understands my strengths and weaknesses, and has guided me to enhance my strengths and overcome my weaknesses in a scientific context. I would not have been able to successfully complete this dissertation research and develop into a mature scientist without her unremitting dedication of time and effort.

I would also like to offer my sincere appreciation to my doctoral supervisory committee: Drs. Thummel, Hebert, Shen, Mao and Rettie for their insights and guidance on my dissertation research. I am deeply grateful for their questions, comments and suggestions that they provided to me during the examinations. Their advice and comments have helped to drive my research to move forward and have contributed to my scientific development.

In my daily work, I have been fortunate to be surrounded by a friendly group of experienced scientist and researchers. My sincere thanks especially go to Dr. Horace Ho and Dr. Haichuan Duan, who are always willing to help me to learn new scientific techniques and provide insightful discussion and comments on my research design and data interpretation.

Lastly, I would like to thank the faculty, staff and students in the Departments of Pharmaceutics and Medicinal Chemistry who have supported and encouraged me to believe in myself and my own abilities. They have helped me through various situations, allowing me to reach this accomplishment.

Dedication

To my mom and dad,

Thank you for your unconditional love and support through not only my graduate study, but also my entire life. Your sincerity and diligence always inspire me to become a better person.

To my sister Hanna,

We were apart for many years, but you are always in my thoughts. Thank you for your love and advice on my career.

To Michelle and Clara,

I feel lucky that I have encountered you two dearest friends in Seattle. I will always cherish the time that we spent together for the past five years.

To Peter, Eunice, Hyojung, Sylvia, Minkyung, Jinhyun, Kyunghwa, Yoojung, Jennifer, Sunhyung, and Hyeyeon,

Thank you all for always being there for me no matter where you are and helping me through this long journey.

Chapter 1. Introduction

1.1. Background

1.1.1. Pharmacotherapy in pregnant women

About 60% of pregnant women in the United States take at least one prescription medication other than a vitamin or mineral supplement and majority of these prescribed drugs are category C drugs, drugs for which human safety during pregnancy has not been established (Adam et al., 2011; Andrade et al., 2004; Glover et al., 2003). Due to safety concerns for both pregnant women and their developing fetuses, many drugs have never been tested in the pregnant population. Therefore, information on the pharmacokinetics (PK) and pharmacodynamics (PD) of many drugs in pregnant women, as well as potential effect on the fetus, are rather limited.

Because of the lack of PK/PD data in the pregnant population, drug selection and dosage regimens for pregnant women are mostly empirically derived and based on information obtained from non-pregnant population. However, during pregnancy there are extensive physiological changes occurring that could alter maternal drug absorption, distribution, metabolism and excretion (Table 1.1), which presents complexity and challenges for pharmacotherapy during pregnancy. Pregnancy-associated physiological changes include decreased intestinal motility, increased gastric pH, an increase in cardiac output and plasma volume, reduced plasma albumin concentrations, and increased renal blood flow and glomerular filtration rate (Isoherranen and Thummel, 2013). In addition, there are substantial changes in the expression and activity of drug metabolizing enzymes including cytochrome P450 (CYP) and UDP glucuronosyltransferase (UGT) and drug transporters in a gestational age-dependent manner during pregnancy (Isoherranen and Thummel, 2013). For instance, it was previously reported that clearance of

midazolam was greater in third trimester of pregnancy than postpartum, suggesting an increased CYP3A4 activity in pregnancy (Hebert et al., 2008). In contrast, the activity of CYP1A2 was shown to decrease throughout pregnancy (Tracy et al., 2005). Other drug metabolizing enzymes including CYP2B6, 2D6 and 2C9 and UGT1A4 and 2B7 are also shown to be influenced by pregnancy (Isoherranen and Thummel, 2013). Although the effect of pregnancy on the expression and activity of drug transporters is less known, several studies have shown that drug transporters can be also affected by pregnancy. Previously, it was reported that renal secretion clearance of digoxin increased in pregnant women, indicating an increased P-glycoprotein (P-gp) activity during pregnancy (Hebert et al., 2008). In a mouse model, the expression of placental P-gp was found to be dependent on gestational age. (Mathias et al., 2005). Also, a recent clinical study showed increased renal clearance of metformin in pregnant women, suggesting possible alteration of renal organic cation transporter (OCT) by pregnancy (Eyal et al., 2010).

Another aspect that challenges drug therapy in pregnant women is the potential harmful effect of drugs on the developing fetus. The cases of thalidomide and isotretinoin have clearly demonstrated that fetal exposure to certain drugs can cause detrimental birth defects (Shehata and Nelson-Piercy, 2001). Nevertheless, the fetal exposure and teratogenic risks for more than 90% of drugs have not been determined in humans (Adam et al., 2011). There have been considerable efforts made by government agencies, pharmaceutical industries and academic researchers to gather information about the potential teratogenic risks of prescription drugs and prevent the adverse birth defects from use of drugs in pregnancy (Adam et al., 2011). Despite these efforts, the available data on fetal exposure and drug teratogenicity are still very limited; therefore leaving the developing embryo and fetus at risk to the vast majority of drugs used during pregnancy.

Pregnancy-induced changes in drug disposition and potential teratogenicity make safe and effective drug therapy in pregnant women challenging. However, it is almost impossible to entirely avoid drug treatment during pregnancy because maternal illnesses including hypertension, pre-eclampsia and gestational diabetes mellitus can endanger both the mother and the fetus if they are not treated properly. Thus, it is important to understand maternal and fetal drug disposition and response during pregnancy, which would inform rational drug selection and dosage for pregnant women to achieve optimal drug efficacy while minimizing toxicity. Basic research to elucidate the molecular mechanisms of altered drug disposition, response and teratogenic effects during pregnancy is indispensable. These research based studies can further provide information on potential pregnancy-induced changes in PK/PD and teratogenicity in order to optimize drug therapy and prevent adverse events that may occur while utilizing pharmacotherapy during pregnancy.

1.1.2. Gestational diabetes mellitus and metformin

Diabetes mellitus, or simply diabetes, is a major metabolic disease affecting an estimated 285 million people worldwide (Qaseem et al., 2012). In the United States, diabetes is the seventh leading cause of death, and its incidence is increasing substantially due to an increasing obesity rate (Qaseem et al., 2012). Diabetes is classified into four broad categories: type 1, type 2, gestational diabetes and other specific types, with type 2 being the most common form making up about 90% of all cases (Qaseem et al., 2012). Diabetes increase the risk of long-term complications, including microvascular (retinopathy, nephropathy and neuropathy) and macrovascular (coronary artery, cerebrovascular, and peripheral vascular disease) complications (Qaseem et al., 2012). Gestational diabetes mellitus (GDM) is characterized by glucose

intolerance that starts or is first diagnosed during pregnancy. GDM complicates about 5% of pregnancies. Women with uncontrolled GDM can be at increased risk of cesarean delivery, pre-eclampsia, and long-term diabetes and her offspring are prone to develop childhood obesity and type 2 diabetes (Langer et al., 2005). In the non-pregnant diabetic population, the standard therapy is insulin. Oral glucose lowering agents have also been widely used to achieve glycemic control, especially in type 2 diabetes. Similar to type 2 diabetes, the hallmark of GDM is insulin resistance which is likely resulted by placental hormones including human placental lactogen, cortisol, estrogen, progesterone, and tumor necrosis factor α (Berggren and Boggess, 2013). Insulin is the only Federal Drug Administration-approved therapy for GDM treatment yet (Berggren and Boggess, 2013) and has been the mainstay of GDM treatment. However, recently oral hypoglycemic agents received attention and are increasingly used as alternatives to insulin therapy due to lower cost, no need for self-injections, and comparable efficacy (Berggren and Boggess, 2013).

Metformin is an oral hypoglycemic drug used as a front line drug for the treatment of type 2 diabetes (Johnson et al., 2002). Metformin is an 'insulin sensitizer', because it decreases glucose levels without increasing insulin secretion. Its major mechanism of action involves suppression of hepatic glucose production by stimulating AMP-activated protein kinase (AMPK) and inhibiting complex 1 of the mitochondrial respiratory chain (Hundal and Inzucchi, 2003). In addition, metformin stimulates peripheral glucose uptake by skeletal muscle and adipose tissue, decreases intestinal glucose absorption, and improves insulin secretion by pancreatic β cells (Hundal and Inzucchi, 2003).

Metformin is a polar and water soluble biguanide with a log P of -0.5 and pKa of 12.4. It has an oral bioavailability of 40-60 %, a wide volume of distribution (63-276 L), and minimal

protein binding (Scheen, 1996). This drug is known to be highly accumulated in the tissues including liver, kidney, small intestine and salivary glands (Hundal and Inzucchi, 2003; Scheen, 1996). Metformin does not undergo hepatic metabolism and is predominantly eliminated by kidney (Hundal and Inzucchi, 2003; Scheen, 1996) with renal clearance (335-615 mL/min) about four times glomerular filtration rate (GFR) (Scheen, 1996). The most common side effect of metformin is gastrointestinal upset, which occurs in 20-30 % of patients (Zolk, 2012). Clinically, there are large variations in the patient-to-patient pharmacokinetics and antidiabetic response to metformin (Tzvetkov et al., 2009; Zolk, 2012).

Recently, metformin has been introduced as an alternative therapy to insulin in GDM treatment due to its comparable efficacy and safety, easier route of administration, lower cost, as well as improved patient's satisfaction (Langer et al., 2000; Rowan et al., 2008). In the treatment of GDM, metformin can be used as monotherapy or in combination with insulin. Some patients with multiple risk factors for insulin resistance (e.g higher body mass index (BMI), higher baseline glucose) may require supplementary insulin to meet the treatment goals (Lautatzis et al., 2013; Rowan et al., 2008). Although its use in pregnancy is on the rise, there are concerns because of the limited data on metformin's effect on maternal and neonatal outcomes (Gui et al., 2013; Mesdaghinia et al., 2013). Metformin disposition in pregnant population was shown to be profoundly different from that in non-pregnant population (Eyal et al., 2010). Metformin renal clearance was increased significantly in mid- and late- pregnancy compared with postpartum (Eyal et al., 2010). These findings suggest that dose may need to be adjusted upward in pregnant women to achieve sufficient glycemic control. Metformin readily crosses the placental barrier and metformin concentration in fetal circulation can reach as high as maternal concentrations (Eyal et al., 2010; Kovo et al., 2008). In contrast, infant exposure to metformin by breastfeeding

is low (Eyal et al., 2010). Theoretically metformin could increase fetal insulin sensitivity and consequently reduce fetal insulin production, an effect that might restrict the fetal growth and cause neonatal hypoglycemia (Kovo et al., 2008; Vanky et al., 2005). So far, no adverse fetal effects have been reported among women treated with metformin during pregnancy. However, long-term outcome and complications of exposed fetuses requires further evaluation. For the safe and effective use of metformin in pregnant women, mechanistic studies are required to better understand maternal and fetal disposition of metformin, as well as its potential teratogenicity and long-term effects.

1.1.3. Metformin disposition during pregnancy

1.1.3.1. Polyspecific organic cation transporters and the roles in metformin PK/PD

Organic cation transporters (OCTs) in the solute carrier 22 (SLC22) family play an important role in the disposition and detoxification of various endogenous compounds and xenobiotics. OCTs transport relatively small and hydrophilic organic cations with diverse chemical structures. OCT-mediated transport is electrogenic, Na^+ independent and bi-directional (Koepsell et al., 2003; Wright and Dantzler, 2004). The classic OCT substrates include MPP⁺ (1-methyl-4-phenyl-pyridinium), TEA (tetraethylammonium), biogenic amines, and a number of clinically used drugs (Wright and Dantzler, 2004). The three major OCT isoforms, OCT1-3, display a large overlap in substrate and inhibitor specificity. In humans, OCT1 is mainly expressed in the liver. Localized to the sinusoidal membrane of hepatocytes, OCT1 mediates organic cation uptake from the blood into hepatocytes (Fig. 1.1) (Koepsell, 2004). OCT2 is primarily expressed in the kidney and is localized to the basolateral membrane of renal proximal tubular cells. By transporting organic cations from the blood into the proximal tubular cells,

OCT2 mediates the first step in renal secretion of many cation drugs (Fig. 1.1) (Koepsell, 2004). OCT3 is highly expressed in the placenta and also widely distributed in various tissues. OCT3 has been implicated in the clearance of endogenous monoamines, but its roles in transport of xenobiotic OCs have not been adequately investigated.

After being transported into the hepatocytes (by OCT1) or renal tubular cells (by OCT2), organic cations are further excreted into the bile or urine by the multidrug and toxin extrusion (MATE) proteins in SLC47 family (Fig. 1.1) (Moriyama et al., 2008). In humans, there are two isoforms: hMATE1 (SLC 47A1) and hMATE2-K (SLC47A2) (Masuda et al., 2006; Otsuka et al., 2005; Tsuda et al., 2009b). MATE1 is highly expressed in the kidney, adrenal gland, liver, skeletal muscle and several other tissues, whereas MATE2-K is kidney specific (Otsuka et al., 2005). The MATEs are H^+ /OC antiporters and mediate electroneutral exchange of H^+ and an OC substrate. The MATE proteins are localized on the apical membrane of renal and hepatic cells, and are responsible for the final step of excretion of OCs (Otsuka et al., 2005). Not surprisingly, the MATEs share a large substrate overlap with the OCTs (Hiasa et al., 2006; Otsuka et al., 2005).

In addition to OCTs and MATEs, a novel polyspecific organic cation transporter, plasma membrane monoamine transporter (PMAT), was cloned and characterized by our laboratory (Engel and Wang, 2005; Engel et al., 2004; Xia et al., 2007; Zhou et al., 2007). The substrates and inhibitors specificity of PMAT largely overlap with those of the OCTs (Engel and Wang, 2005). PMAT mRNA is widely expressed in a number of human tissues including small intestine, brain, kidney, liver and heart (Barnes et al., 2006; Engel et al., 2004; Xia et al., 2007). Currently, the role and significance of PMAT in organic cation disposition is largely unknown.

In vitro studies have demonstrated that metformin is a substrate for OCT1-3, MATE1-2, and PMAT (Dresser et al., 2002; Kimura et al., 2005; Masuda et al., 2006; Nies et al., 2009; Suhre et al., 2005; Zhou et al., 2007). The apparent binding affinities (K_m) of these transporters towards metformin are summarized in Table 1.2. OCT1-3, PMAT and MATE2-K have similar K_m values towards metformin, in low mM range, whereas MATE1 has a relatively higher affinity. The therapeutic concentrations of metformin was reported to range between 3 ~12 μ M (Scheen, 1996). OCT1 transports metformin into the hepatocyte, which is the major site of metformin action. It was reported that patients with low-activity genetic variants of OCT1 (SLC22A1) (R61C, G401S, M420del, or G465R) had a reduced therapeutic response to metformin due to a decreased hepatic uptake, suggesting that OCT1-mediated hepatic uptake is an important determinant of the glucose-lowering effect of metformin (Shu et al., 2008; Shu et al., 2007). The renal clearance of metformin is about 4 times GFR, suggesting that active tubular secretion is the major route for metformin elimination (Dunn and Peters, 1995; Li et al., 2006). OCT2, expressed at the basolateral membrane of renal proximal tubular cell, mediates metformin uptake from the peritubular capillary blood into the tubular cells (Fujita et al., 2006; Wright and Dantzler, 2004). Once inside the cells, metformin is further transported into the tubular lumen by the apical MATE1 and MATE2-K (Tsuda et al., 2009b). It was reported that in carriers of a variant form of the *OCT2* gene (SLC22A2), metformin renal clearance and its area under the concentration-time curve (AUC) were altered (Chen et al., 2009; Song et al., 2008; Wang et al., 2008). More recently, Choi et al. reported that a common 5'-UTR (untranslated region) variant in *MATE2-K* gene is associated with poor response to metformin (Choi et al., 2011). However, conflicting results were also reported and genetic polymorphisms in *OCT1-2* and *MATE* genes alone cannot fully explain the large inter-individual differences in metformin PK/PD observed

clinically (Chen et al., 2009; Song et al., 2008; Tzvetkov et al., 2009; Wang et al., 2008; Zolk, 2012).

1.1.3.2. Metformin maternal and fetal disposition during pregnancy

Recently, a clinical study in pregnant women has been conducted by the Obstetric-Fetal Pharmacology Research Unit (OPRU) at the University of Washington. Metformin renal clearance was found to be significantly increased in mid (by 52 %) and late (by 31 %) pregnancy compared with postpartum (Eyal et al., 2010). Creatinine clearance and net secretion clearance of metformin increased during pregnancy (Eyal et al., 2010), suggesting that the altered metformin PK in pregnant women can be attributed to changes in renal filtration and tubular secretion of metformin during pregnancy. Enhanced metformin tubular secretion during pregnancy could be due to altered expression and activity of renal organic cation transporters. However, currently little is known about the expression and activity of polyspecific organic cation transporters during pregnancy.

Clinical studies and *ex vivo* perfusion study have also shown that metformin crosses the human placenta, and its fetal blood concentrations at delivery can reach the maternal concentrations (Charles et al., 2006; Eyal et al., 2010; Kovo et al., 2008; Vanky et al., 2005). While a carrier-mediated pathway has been suggested (Kovo et al., 2008), the molecular mechanisms of metformin transport at the placental barrier is unclear. Among all known metformin transporters, only OCT3 is highly expressed in human placenta (Otsuka et al., 2005). The localization of OCT3 in the human placental syncytiotrophoblast has not been clearly defined, yet it is suggested to be localized to the basal membrane facing the fetal blood (Sata et al., 2005; Vahakangas and Myllynen, 2009). Results from an *ex vivo* perfusion study indicate

that metformin transport across the placenta is concentration-dependent, saturable and possibly mediated by a bi-directional organic cation transporter (Kovo et al., 2008). When pregnant Oct3 (-/-) mice were given an intravenous dose of MPP⁺, a 3-fold reduction in fetal MPP⁺ accumulation was observed in homozygous Oct3(-/-), compared to wild-type, embryos (Zwart et al., 2001b), suggesting that OCT3 mediates maternal-to-fetal transport of OCs. However, in contrast, results from a recent study in a rat model showed high expression of rMate1 in the rat placenta and suggested that rOct3 and rMate1 work together sequentially to mediate fetal-to-maternal transport of MPP⁺ (Ahmadimoghaddam et al., 2012). These mixed results compel further investigation to elucidate the precise transport mechanism of metformin and other OCs at the human placental barrier.

1.1.3.3. Potential importance of OCT3 in metformin disposition

OCT3, also known as the extraneuronal monoamine transporter (EMT), is generally believed to play a role in extraneuronal uptake of monoamine neurotransmitters. OCT3 is expressed in the placenta, liver, kidney, small intestine, skeletal muscle, heart, lung, brain and salivary glands. Similar to OCT1-2, OCT3 transports MPP⁺, catecholamines, and other type I OCs (Koepsell et al., 2003). A previous *in vivo* study with Oct3 (-/-) mice using MPP⁺ as a prototypical substrate suggests that Oct3 may also play a role in disposition of xenobiotic organic cations (Zwart et al., 2001b). We and others recently showed that metformin is transported by hOCT3 with apparent affinity (K_m) comparable to those reported for hOCT1 and hOCT2 (Chen et al., 2010; Nies et al., 2009) (Lee and Wang, unpublished data). However, the exact *in vivo* role of OCT3 in metformin disposition and action has not yet been established. Interestingly, in addition to the placenta, OCT3 is also highly expressed in those tissues known to highly

accumulate metformin that include liver, kidney, small intestine and salivary glands. Moreover, OCT3 is expressed in skeletal muscle cells, which is a secondary site of metformin action.

Based upon these observations, OCT3 may play an important role not only in of the transport of metformin across the placental barrier and into the fetus, but also in tissue-specific distribution of metformin, which may in turn affect metformin pharmacology *in vivo*.

1.2. Hypothesis and specific aims

The goal of my thesis research is to improve our understanding of the role of OCT3 in metformin disposition, especially under the pregnant state. To that end, the following three hypotheses will be tested the execution of the associated specific aims:

Hypothesis 1. Expression of renal/hepatic organic cation transporters is altered during pregnancy, affecting maternal metformin pharmacokinetic (PK) behavior.

Specific aim 1.1. To confirm that mouse pregnancy can recapitulate metformin PK in human pregnancy.

Specific aim 1.2. To determine if the mRNA/protein expression of organic cation transporters in kidney, liver and placenta is up-regulated by pregnancy.

Hypothesis 2. OCT3 plays an important role in the tissue-specific distribution of metformin, which influences metformin pharmacokinetics and pharmacodynamic response *in vivo*.

Specific aim 2.1. To determine metformin transport kinetics by hOCT3 stably expressed HEK293 cells.

Specific aim 2.2. To determine the expression profile and localization of Oct3 in mice.

Specific aim 2.3. To determine if metformin PK is altered in the Oct3 knockout mouse model.

Hypothesis 3. OCT3 plays an important role in placental transport and fetal exposure to metformin during pregnancy.

Specific aim 3.1. To determine the membrane localization of OCT3 in human term placenta.

Specific aim 3.2. To determine if fetal exposure to metformin is reduced in pregnant Oct3 knockout mice.

1.3. Research focus and overall significance

The first goal of my thesis research is to determine if the expression of polyspecific organic cation transporters is altered during pregnancy that may affect metformin and other cationic drug disposition during pregnancy. Because obtaining tissues from pregnant women is not feasible, we used a mouse model with timed-pregnancy to evaluate the effect of pregnancy on the expression of various organic cation transporters. In order to validate the animal model, and show that pregnancy has a similar effect on metformin disposition in human and mice, we first characterized metformin disposition *in vivo* in non-pregnant and pregnant mice. Our results presented in Chapter 2 confirmed that pregnancy altered metformin PK in pregnant mice in a manner similar to that seen in humans, demonstrating that mouse pregnancy can recapitulate metformin PK changes observed in human pregnancy.

In Chapter 3, we determined the effect of pregnancy and gestational age on mRNA and protein expression of major organic cation transporters in kidney, liver and placenta in pregnant mice and human placentas using quantitative real-time PCR and LC-MS/MS targeted proteomics. Overall, the effect of pregnancy on the expression of renal and hepatic organic cation transporters was moderate and non-significant with the exception of reduced mMate1 expression in mouse kidney during pregnancy.

OCT3/Oct3 were highly (and selectively) expressed in human and mouse placenta. Moreover, the expression of mouse placental mOct3 greatly increased after gestational day (gd) 10, whereas human placenta only showed a moderate increase in the expression of OCT3 in mid- and late- pregnancy. These data suggest an important role of OCT3 in OC transporter at the maternal-fetal placental interface. In addition, our results suggest that an altered renal expression of OC transporters may not be the reason underlying the observed increase in renal clearance of metformin during pregnancy. Other pregnancy-associated changes, such as elevations in renal blood flow and glomerular filtration, might better explain the increased total renal clearance of metformin in pregnancy.

The second goal my dissertation research is to investigate the role of OCT3 in tissue specific distribution of metformin. As reported in Chapter 4, we determined the expression profile of Oct3 in various mouse tissues and investigated its role in metformin disposition *in vivo* using wild-type and Oct3 gene deletion mice. The results suggest that OCT3 profoundly affects metformin plasma PK and its distribution in peripheral tissues including salivary gland, heart and skeletal muscle, which all show high expression of OCT3. Importantly, our *in vivo* study revealed that OCT3 is responsible for high accumulation of metformin in the salivary glands,

which underlies the taste disturbance effect of metformin, a commonly reported adverse effect of the drug.

In Chapter 5, we determined the role of OCT3 in maternal and fetal disposition of metformin during pregnancy and elucidated the mechanism governing fetal exposure to metformin. We first determined the membrane localization of OCT3 in human placenta and showed that the transporter is primarily localized to the basal membrane of placental syncytiotrophoblast cells and in placental endothelial cells of fetal origin. We then determined the *in vivo* impact of Oct3 in metformin disposition across the placental barrier using pregnant Oct3 knockout and wild-type mice. Our data showed that the overall fetal exposure to metformin was reduced in pregnant Oct3^{-/-} mice, even after normalizing to maternal plasma AUC. These results suggest that OCT3 facilitates metformin entry from maternal side into the fetal compartment and is an important determinant of fetal exposure to metformin and possibly other organic cation drugs.

Findings from this dissertation research improve our mechanistic understanding of how pregnancy affects the expression of polyspecific organic cation transporter. Moreover, the current studies provide novel information regarding the role and *in vivo* significance of OCT3 in the distribution and pharmacological response of metformin in both non-pregnant and pregnant states. Importantly, our studies uncovered a novel molecular mechanism underlying taste disturbance of metformin and revealed OCT3 as a key factor influencing fetal exposure to metformin. Together, these results greatly enhance our understanding of the mechanisms involved in the maternal and fetal disposition of metformin. Knowledge gained from these studies will help to pave the way for optimizing metformin pharmacotherapy in the treatment of type 2 diabetes as well as GDM in pregnant women.

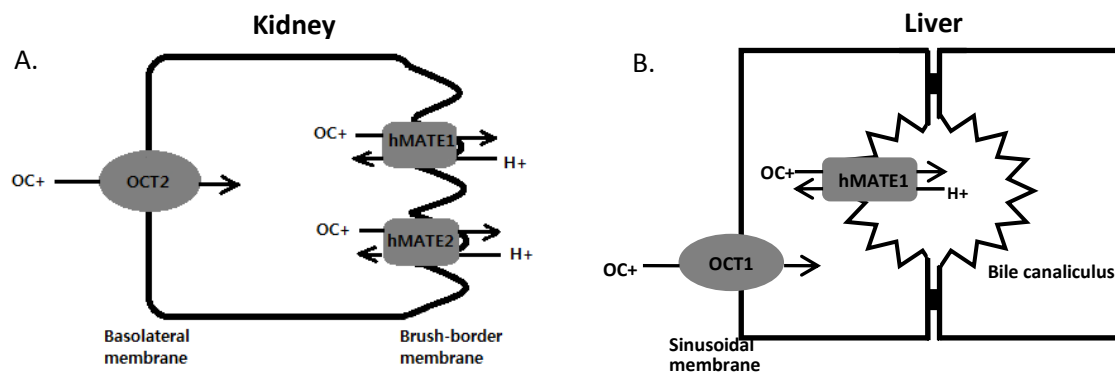


Figure 1.1. Cellular models of renal (A) and hepatic (B) organic cation transport.

Table 1.1. Effect of physiological changes on pharmacokinetics during pregnancy

Absorption	Distribution	Metabolism	Excretion
<ul style="list-style-type: none"> ▪ ↓ Intestinal motility ▪ ↑ Gastric pH 	<ul style="list-style-type: none"> ▪ ↑ Cardiac output, plasma volume, total body water ▪ Change in protein binding (↓albumin) e.g. phenytoin, valporic acid (epilepsy) 	<ul style="list-style-type: none"> ▪ Change in CYP450 enzymes ↑CYP3A4, 2D6, 2C9 ↓CYP1A2, 2C19 e.g. indinavir (HIV), metoprolol (hypertension), phenytoin (epilepsy) 	<ul style="list-style-type: none"> ▪ ↑ Renal blood flow ▪ ↑ Glomerular filtration e.g. ampicillin (antibiotics), metformin (diabetes)

Table 1.2. Apparent binding affinities of OCT1-3, MATE1/2K and PMAT toward metformin.

	K_m (μM)
hOCT1	1,470 (Kimura et al., 2005)
hOCT2	990, 1,380 (Dresser et al., 2002; Kimura et al., 2005)
hOCT3	2,260, 1,090 (Chen et al., 2010; Nies et al., 2009)
MATE1	212 (Chen et al., 2007)
MATE2-K	1,050 (Masuda et al., 2006)
PMAT	1,320 (Zhou et al., 2007)

Chapter 2. Pregnancy induced metformin pharmacokinetic change in a mouse model

2.1. Introduction

In a recent clinical study performed by the Obstetric Pharmacology Research Unit (OPRU) at the University of Washington, investigators reported a change in metformin pharmacokinetics in pregnant women (Eyal et al., 2010). Metformin renal clearance increased significantly in mid (723 ± 243 ml/min, $P < 0.01$) and late pregnancy (625 ± 130 ml/min, $P < 0.01$) compared with postpartum (477 ± 132 ml/min) (Eyal et al., 2010). This increased renal clearance of metformin in pregnant women is likely to the result of increases in renal filtration and tubular secretion of metformin. The molecular mechanisms underlying these changes during pregnancy are unclear. Because transepithelial transport of metformin in the nephron tubules is mediated by the sequential action of polyspecific organic cation transporter 2 (OCT2) and the multidrug and toxin extrusion proteins (MATEs), the increased secretory clearance may be due to increased expression and activity of these renal transporters in pregnancy. A major goal of my dissertation research is to determine whether expression of polyspecific organic cation transporters is altered during pregnancy, thereby affecting cationic drug disposition during pregnancy. Because it is unrealistic to directly examine gene expression in kidney and liver tissues collected from pregnant women, mice with timed-pregnancy will be used to investigate the effect of pregnancy on the expression of polyspecific organic cation transporters.

Mice with timed-pregnancy are commonly used as an animal model of human pregnancy – specifically for *in vivo* characterization of drug disposition and *ex vivo* gene profiling. For example, P-gp expression in human placenta was shown to be up-regulated in early pregnancy,

and a similar trend was found in mouse placenta showing highest placental P-gp expression at gestational day (gd) 10 (Zhang et al., 2008). Also, the expression of hepatic Cyp3a isoforms increased in pregnant mice, which is consistent with an increased CYP3A activity in human pregnancy (Zhang et al., 2008). The increased Cyp3a expression in mice was at least in part responsible for the increased systemic clearance of glyburide in pregnant mice, providing a molecular understanding for pregnancy-induced pharmacokinetic (PK) alterations of glyburide in pregnant women (Koh et al., 2011; Zhou et al., 2008). These findings suggest that mice can serve as an appropriate animal model to evaluate the pregnancy effect on certain CYP enzymes and drug transporters. Moreover, the availability of mice with targeted gene deletion provides a unique opportunity to dissect the molecular mechanism involved in drug handling *in vivo*.

Our genes of interest are polyspecific organic cation transporters including OCT1-3, MATE1-2K and PMAT. Little is known about the regulation of organic cation transporters during pregnancy. In order to examine the effect of pregnancy on these transporters and elucidate the mechanisms behind the increased clearance of metformin in pregnancy, our studies were designed to first characterize renal expression of various polyspecific organic cation transporters in tissues from pregnant mice during timed-pregnancies. However, it is important to validate that the alterations in metformin disposition in human pregnancy is appropriately replicated in pregnant mice. Therefore, we first carried out a metformin *in vivo* PK study in non-pregnant and pregnant mice to evaluate the effect of pregnancy on metformin disposition and to determine if the changes observed in mice recapitulate the PK changes seen in human pregnancy.

2.2. Materials and methods

2.2.1. Animals

Adult (8-10 weeks of age) wild-type FVB mice (Taconic) were housed in the specific pathogen free (SPF) facility at the University of Washington. The animal studies were approved by the Institutional Animal Care and Use Committee (IACUC) of the University of Washington. To obtain pregnant mice at gestational day (gd) 19 (term in mice is ~20-21 days), timed mating was carried out. The date that a vaginal plug was observed was assigned as gestational day 1.

2.2.2. *In vivo* study

Non-pregnant (virgin) and pregnant mice at gd 19 were fasted for 5-10 hours and administered 15 mg/kg metformin containing 0.2 mCi/kg of [^{14}C] labeled metformin by oral gavage. At 15, 30, 45, 60, 120, 180, 240, and 480 min, blood was collected. For each time point, 3-5 mice were used. The non-pregnant and pregnant mice were sacrificed using CO_2 . The blood samples were obtained in heparinized microhematocrit capillary tubes (Fisher) by cardiac puncture and plasma was separated by centrifugation for 1 minute at 5000 x g. Metformin concentrations in the plasma were determined by scintillation counting using the method described by Wilcock et al. with minor modification (Wilcock and Bailey, 1994). In brief, plasma samples were placed in scintillation vials with 1 mL 1 M NaOH and incubated at 55~70°C for 1~2 hours. After cooling, H_2O_2 was added to decolorize the samples. After several hours, 15 mL of Eco-scintillation buffer was added first, followed by 1 mL 1 M HCL to neutralize the solutions. The samples were stored overnight before counting. The amounts of radioactivity were expressed as ng/ml for plasma.

2.2.3. Statistical and pharmacokinetics analysis.

Non-compartment analysis was conducted using WinNonlin 5.2 (Pharsight Corporation, Moutian View, CA) to estimate the drug pharmacokinetic parameters. Metformin was administered to non-pregnant and pregnant mice based on body weight (mg per kg body weight). The average body weights for non-pregnant and pregnant mice were 20 g and 35 g respectively. Due to the difference in body weights between the two mouse groups, the dose given to the pregnant mice was about 1.8 times greater than that given to the non-pregnant mice. Therefore, we calculated the dose-normalized area under the concentration-time curve (AUC) and oral clearance using the following equations (Zhou et al., 2010):

$$AUC_{\text{dose-normalized}} = AUC_{0-8h} / (\text{mean dose for respective mouse group})$$

$$CL/F = \text{mean dose for respective mouse group} / AUC_{0-8h}$$

The data are expressed as mean \pm S.D. Statistical significance was determined by Student's *t* test using *n*=3 for each time point. A *p*-value less than 0.05 was considered significant.

2.3. Results

The plasma concentration-time profile of metformin following an oral 15 mg/kg dose in non-pregnant and pregnant mice is shown in Figure 2.1. The dose-normalized plasma concentrations at most time points in pregnant mice were lower than those in non-pregnant mice. Pharmacokinetic parameters of metformin are summarized in Table 2.1. The dose normalized AUC and C_{max} in pregnant mice was 37% and 30% lower than those in non-pregnant mice, respectively. The calculated oral clearance (CL/F) in the pregnant mouse showed a 57% increase, compared to the non-pregnant state. In contrast, the terminal half-life ($T_{1/2, \beta}$) and oral volume of distribution (V_{β}/F) in pregnant and non-pregnant mice was not significantly different.

2.4. Discussion

In a recent clinical study performed by OPRU investigators at the University of Washington, women were given 500 mg of metformin twice daily during their pregnancy and postpartum, for therapeutic reasons that included preexisting diabetes, gestational diabetes, and polycystic ovary syndrome (PCOS) (Eyal et al., 2010). When plasma steady-state PK parameters were determined, metformin AUCs in early-, mid- and late-pregnancy were respectively 33%, 37% and 29% lower than those postpartum (Eyal et al., 2010). Consequently, the apparent oral clearances were increased by 57%, 76% and 38% in early, mid and late pregnancy respectively (Eyal et al., 2010). The overall renal clearance was found to be increased by 26-71% throughout gestation (Eyal et al., 2010).

In the current study, the wild-type FVB pregnant mice at gd 19 showed a 37% decrease in the dose normalized AUC and a 57% increase in oral clearance of metformin compared to the non-pregnant mice. The magnitude of the changes in dose-normalized AUC and oral clearance of metformin in the pregnant mice was found to be comparable to those in the pregnant women receiving a standard dose of 500 mg. These data suggest that pregnancy has a similar effect on plasma metformin PK in humans and mice. Due to technical challenges, we did not measure renal clearance in the mouse study. However, similar to human, metformin is primarily eliminated by the kidney via filtration and OCT/MATE mediated tubular secretion in mice. Assuming no changes in oral bioavailability, the increased oral clearance of metformin during mouse pregnancy most likely resulted from an increase in renal clearance of the drug.

Multiple polyspecific organic cation transporters are known to play important roles in metformin tissue distribution and renal excretion, affecting metformin response in both humans

and mice. It is unknown whether these transporters are regulated in a similar manner during human and mouse pregnancy. However, because our data showed that pregnancy has a similar effect on plasma metformin PK in humans and mice, the mechanisms involved in metformin disposition are likely to be similar and affected by pregnancy in a similar manner. Moreover, the availability of mice with targeted deletion of individual organic cation transporters provides an added strength for using this animal model to understand drug transport mechanisms *in vivo*. Thus, the mouse may represent a valid animal model to study the effect of pregnancy on the expression of various polyspecific organic cation transporters involved in metformin disposition during pregnancy.

Table 2.1. Dose-normalized pharmacokinetic parameters of metformin in pregnant and non-pregnant wild-type FVB mice.

Parameter	Unit	Non-pregnant	Pregnant	<i>p</i> -value
T_{\max}	min	45	30	--
C_{\max}	ng/ml/ μ g	9.01 ± 2.62	6.30 ± 1.50	N.S.
$AUC_{\text{dose-normalized}}$	μ g/ml*min/ μ g	1.82 ± 0.13	1.15 ± 0.029	<0.05
CL/F	μ l/min	0.55 ± 0.038	0.87 ± 0.022	<0.05
$T_{1/2,\beta}$	min	192.54	119.48	--
V_{β}/F	μ l	152.78 ± 21.11	150.00 ± 7.59	N.S.

Mice were given an oral dose of metformin (15 mg/kg containing 0.2 mCi/kg of [^{14}C] metformin). The average weights for non-pregnant (20 g) and pregnant (35 g) mice were used for dose normalization. The radioactivity in plasma was determined and converted to mass amounts. AUC, area under plasma concentration-time curve of metformin. CL/F value was calculated using Dose/AUC. V_{β}/F value was calculated using Dose/(AUC* β). N.S., not significant.

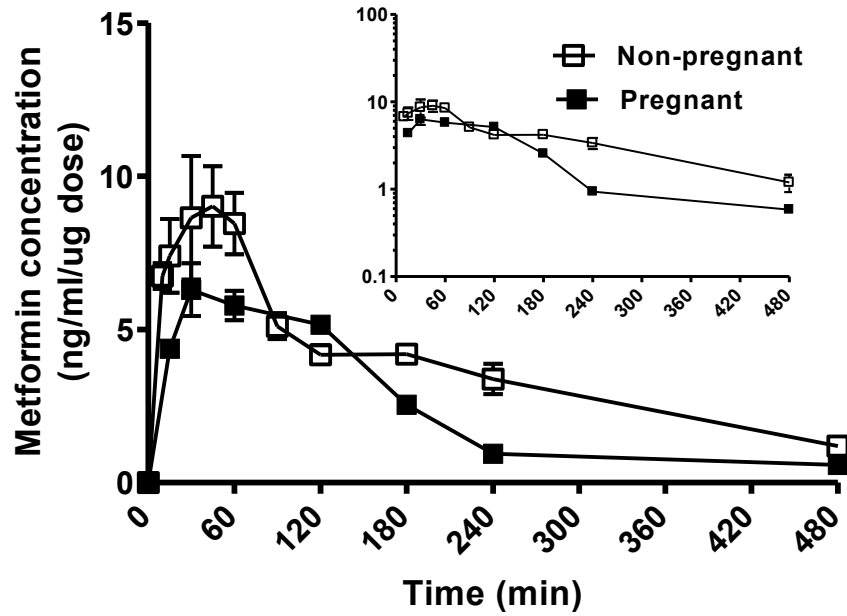


Figure 2.1. Dose-normalized plasma concentration-time profile of metformin in wild-type FVB non-pregnant (□) and pregnant (■) mice. Pregnant mice at gd 19 and non-pregnant (virgin) mice (8-10 weeks of age) were administered metformin (15 mg/kg metformin containing 0.2 mCi/kg of [14 C] labeled metformin) by oral gavage. Inset is the logarithmic plot. Data represented as mean \pm S.D. (n=3-5 mice at each time point).

Chapter 3. Effect of gestational age on mRNA and protein expression of polyspecific organic cation transporters during pregnancy

(This work was published in *Drug Metabolism and Disposition* 41(12): 2225-2232, 2013)

3.1. Introduction

Many drugs and toxins, such as metformin, histamine H₂ receptor blockers, and 1-methyl-4-phenylpyridinium (MPP⁺) and paraquat, are hydrophilic OCs that do not readily cross cell membranes by passive diffusion. Polyspecific OC transporters play important roles in the disposition, efficacy and toxicity of these cationic xenobiotics (Giacomini et al., 2010; Koepsell et al., 2007; Wright and Dantzler, 2004). These transporters are also likely to be involved in various physiological pathways through their action on endogenous bioactive amines (Giacomini et al., 2010; Koepsell et al., 2007; Wright and Dantzler, 2004). Known polyspecific OC transporters include the electrogenic organic cation transporters 1-3 (OCT1-3, SLC22A1-3), the proton/cation antiporters termed as multidrug and toxin extrusion proteins 1-2 (MATE1/2, SLC47A1/2), and the plasma membrane monoamine transporter (PMAT, SLC29A4). These transporters have largely overlapping substrate specificities and frequently work in concert to mediate transepithelial flux of OCs.

In humans, hOCT1 is predominantly expressed in the liver on the sinusoidal membrane of hepatocytes, mediating OC uptake into the hepatocytes (Giacomini et al., 2010). hMATE1, expressed at the canalicular membrane, further effluxes the OCs into the bile (Giacomini et al., 2010). In the human kidney, hOCT2 is primarily expressed and localized to the basolateral membrane of renal proximal tubular cells (Giacomini et al., 2010). hOCT2 concentrates OCs into the proximal tubular cells, where OCs can be further excreted into the urine by hMATE1

and hMATE2-K at the apical membrane. The third member of the human OCT family, hOCT3, is broadly distributed in tissues including placenta, skeletal muscle, heart, brain, kidney, liver, lung, and intestine (Koepsell et al., 2007). hOCT3 has been implicated in the clearance of endogenous monoamines, but could also be involved in transport of xenobiotic OCs. A new polyspecific OC transporter, termed the plasma membrane monoamine transporter (PMAT), is widely expressed in various tissues and has largely overlapping substrates and inhibitors with those of OCTs (Engel and Wang, 2005; Engel et al., 2004). hPMAT has been implicated in intestinal absorption of OCs (Zhou et al., 2007).

A number of medications used by pregnant women are substrates of the polyspecific OC transporters. For example, metformin, a positively charged biguanide transported by hOCT1-3, hMATE1/2, and hPMAT (Kimura et al., 2005; Nies et al., 2009; Tanihara et al., 2007; Zhou et al., 2007), is used to treat gestational diabetes mellitus in pregnant women (Eyal et al., 2010; Wensel, 2009). OCT1-mediated hepatic uptake of metformin is an important determinant of its glucose lowering effect as liver is the primary target of metformin action (Shu et al., 2007). Meanwhile, metformin is primarily eliminated by renal secretion via the OCT2/MATE1 pathway (Chen et al., 2009; Tsuda et al., 2009a). Metformin has been shown to cross the placenta barrier (Kovo et al., 2008), which most likely also involves specific OC transporters. Pregnant women undergo extensive physiological and hormonal changes not experienced by non-pregnant patients, making them unique with respect to drug therapy selection, dosage, efficacy and safety. Medication used during pregnancy may also cross the placenta and potentially result in fetal exposure and teratogenicity. Considerable data in the literature suggests that expression and activity of important drug metabolizing enzymes (e.g., hepatic CYP3A4, CYP2D6, CYP2C9) and transporters (e.g. placental P-gp and BCRP) are altered during pregnancy in a gestational

age-dependent manner (Hebert et al., 2008; Hodge and Tracy, 2007; Isoherranen and Thummel, 2013; Mathias et al., 2005). In a recent study performed by the Obstetric-fetal Pharmacology Research Unit Network at the University of Washington, a significant gestational stage-dependent change in metformin pharmacokinetics was seen during pregnancy (Eyal et al., 2010), suggesting a possibility that the expression of OC transporters in organs important for metformin disposition may be altered by pregnancy.

Little is known about the effect of pregnancy on the expression of polyspecific OC transporters in various tissues. Although the effect of pregnancy on mRNA expression of drug transporters has been analyzed in large scale microarray studies and/or in tissue-specific manners in pregnant animal models (Shuster et al., 2013; Yacovino et al., 2013), comprehensive and quantitative mRNA analysis of polyspecific OC transporters has not been performed. Furthermore, few studies have quantified and compared the protein levels of OC transporters between non-pregnant and pregnant states. In this study, we aim to investigate the effect of pregnancy and gestational age on mRNA expression of polyspecific OC transporters in pregnant mice and human placentas at various gestational stages. A quantitative liquid chromatography coupled with tandem mass spectrometry (LC–MS/MS) proteomics was used to quantify membrane expression of polyspecific OC transporter proteins in both mouse and human tissues.

3.2. Materials and methods

3.2.1. Animals and tissue harvest

Adult (8-10 weeks of age) wild-type FVB mice (Taconic) were housed in the specific pathogen free (SPF) facility at the University of Washington. The animal studies were approved

by the Institutional Animal Care and Use committee (IACUC) of the University of Washington. To obtain pregnant mice, timed mating was carried out. The date that a vaginal plug was observed was assigned as gestational day 1. Pregnant mice were sacrificed by gassing with CO₂. The kidneys, livers and placentas from pregnant mice at gestational days (gd) 10, 15, and 19 (term in mice is ~20-21 days) were immediately dissected, collected, and flash-frozen in liquid N₂. Tissues were stored at -80°C until use. Tissues from age-matched virgin mice were used as the non-pregnant control.

3.2.2. Human placenta source

The use of human placentae as biological specimens was approved by the Institutional Review Board at the University of Washington. Human term placentae from normal pregnancy were obtained from the Labor and Delivery Unit at the University of Washington. Normal first trimester (week 6-12) and second trimester (week 13-25) placentae were provided by the Birth Defects Research Laboratory at the University of Washington, which has Institutional Review Board approval to collect and distribute normal and diseased conceptual tissues for research use. All placental tissues were from healthy uncomplicated pregnancies and obtained from women (70% Caucasians and 30% other ethnicity) aged 16-38 years. Upon collection, a placenta was immediately snap frozen and stored at -80°C until use. The time interval from surgery or delivery to tissue preparation did not exceed 60-90 min, in order to minimize RNA degradation.

3.2.3. RNA isolation, cDNA synthesis and quantitative real-time PCR assays

Total RNA was extracted from the tissues using Trizol reagent (Invitrogen, Inc) or Qiagen Mini RNeasy kit according to the manufacturer's instruction. RNA integrity and purity

were verified by gel electrophoresis and UV spectrophotometry. Total RNA (2 µg) was reverse transcribed to first-strand cDNA using Superscript III reverse transcriptase (Invitrogen) according to the manufacturer's instructions and all cDNA samples were prepared in a final volume of 100 µl. Taqman real-time PCR reagents, assay primers and probes for human hOCT1-3 (SLC22A1-3), hMATE1 (SLC47A1), hPMAT (SLC29A4), hGUSB (beta glucuronidase), hGAPDH, mouse mOct1-3 (Slc22a1-3), mMate1-2 (Slc47a1-2), mPmat (Slc29a4), mGusb, mGapdh (glyceraldehyde 3-phosphate dehydrogenase), and mbeta-actin were purchased from Applied Biosystems. Taqman real-time PCR assays were carried out on an Applied Biosystems 7900HT fast real-time PCR system as described previously (Duan and Wang, 2010). To ensure the same amount of cDNA was loaded to the 96 well plates for the qRT-PCR analysis, 5 µl from each cDNA sample, which contains 100 ng RNA-equivalent cDNA, was added to the real-time reaction that contains 10 µl of 2X TaqMan Universal PCR Master Mix (Applied Biosystems), and 1 µl of 20x primer/probe mix in a final volume of 20 µl. Each sample was analyzed in duplicate or triplicate. To quantify the transcript numbers of genes of interest, comparative Ct method was used (Zhang et al., 2008). The mRNA levels of each tested gene was normalized to a house keeping gene according to the following formula: $Ct(\text{test gene}) - Ct(\text{housekeeping genes}) = \Delta Ct$. Thereafter, the relative mRNA levels of each gene was calculated using the $\Delta\Delta Ct$ method: $\Delta Ct(\text{test gene}) - \Delta Ct(\text{test gene in the calibrator}) = \Delta\Delta Ct(\text{test gene})$. The fold changes of mRNA levels were represented as a relative expression $2^{-\Delta\Delta Ct}$. For greater precision of the mRNA quantification by quantitative real-time PCR (qRT-PCR), expression of the commonly used house-keeping genes (mGusb, mbeta actin and mGapdh) were first analyzed in tissues at various gestational stages. Ct values of the house-keeping genes in the

tissues were determined and compared across the pregnancy stages using Student's *t* test. The house-keeping gene that showed least variation was chosen for normalization of target genes.

3.2.4. Membrane protein preparation and quantification of transporters by LC-MS/MS analysis

Total membrane proteins were prepared from mouse (kidney, liver and placenta) and human (placenta) tissues using the Proteo Extract native membrane protein extraction kit (Calbiochem) according to the manufacturer's instructions. Total membrane protein concentration was determined by a BCA protein assay kit (Pierce). The membrane fraction was digested by trypsin as per conditions described before (Prasad et al., 2013). Briefly, the isolated membrane proteins were denatured at 95°C, reduced with dithiothreitol and alkylated with iodoacetamide in ammonium bicarbonate buffer. The protein samples were digested at 37°C for 24 h by trypsin and the reaction was quenched and spiked with the internal standard (IS) solution and centrifuged at 5000 g for 5 min before analysis. Protein quantification was based on unique signature peptides as surrogates for quantification of these transporters and the corresponding isotopically ($[^{13}\text{C}_6, ^{15}\text{N}_4]$ -arginine or $[^{13}\text{C}_6, ^{15}\text{N}_2]$ lysine) labeled peptides as IS. Selected unique signature peptides for these transporters are shown in Table 3.1. These peptides were selected based on criteria previously described (Kamiie et al., 2008). Peptides with predicted transmembrane regions, single nucleotide polymorphisms (SNPs), posttranslational modifications or those susceptible to degradation were excluded. Continuous R and K sequences, i.e., RR, RK, KR and KK, were excluded to avoid miscleavages. Other characteristics, like stability and LC retention were also taken into consideration during peptide selection. LC-MS/MS parameters were optimized to quantify selected peptides in the tissues

samples. The analysis was performed using Agilent 6460A triple-quadrupole mass spectrometer coupled to Agilent 1290 Infinity LC system (Agilent Technologies, Santa Clara, CA) operated in ESI positive ionization mode. Approximately 2 μ g of the trypsin digest (5 μ l of LC injection volume) was injected onto the column (Kinetex™ 2.6 μ m, C18, 100 x 3 mm, Phenomenex, Torrance, CA). The LC flow rate was 0.4 ml/min, while two different mobile phase gradient programs were used to quantify above transporters. For mOct1, mOct2 and mMate1, the gradient program was: 97% A (water containing 0.1% v/v formic acid) and 3% B (acetonitrile containing 0.1% v/v formic acid) held for 4 min, followed by three steps of linear gradient of mobile phase B concentration of 3% to 12%, 12% to 25% and 25% to 30% over 4-8 min, 8-10 min and 10-14 min. This was followed by the washing step (90% mobile phase B) for 0.9 min, and re-equilibration for 4.5 min. Similarly, for mOct3 and hOCT3, the gradient program was: 97% A and 3% B held for 4.5 min, followed by two steps of linear gradient of mobile phase B concentration of 3% to 18% and 18% to 24% over 4.5-7.5 min and 7.5-11.5 min. This was followed by the washing step (80% mobile phase B) for 1 min, and re-equilibration for 5 min. The doubly charged parent to singly charged product transitions for the analyte peptides and their respective stable isotope labeled peptides were monitored using optimized MS/MS parameters (Table 3.1). The data were processed by integration of the peak areas generated from the reconstructed ion chromatograms for the analyte peptides and their respective IS using the MassHunter software (Agilent Technologies, Santa Clara, CA). For data analysis, peak response of multiple reaction monitoring (MRM) transitions from each peptide was averaged and the area ratio of analyte peptide versus IS peptide was obtained. Relative protein expression of individual OC transporters was presented as the area ratio of analyte peptide over IS peptide normalized by the total membrane protein amount in the injected tryptic digests. For absolute quantification of

hOCT3 in human placenta, the non-labeled signature peptide was synthesized as a calibrator. The amount of hOCT3 protein was calculated from the standard curve obtained from the quantitative data generated with the calibrator peptide.

3.2.5. Data analysis

For each mRNA or protein expression data point, data were obtained from mouse tissues from 3-6 animals and expressed as mean \pm S.D. Statistical significance in the expression in various mouse tissues was determined by unpaired Student's *t* test (GraphPad Prism 5.04, La Jolla, CA). The mRNA and protein expression were correlated using a linear regression, and the corresponding r^2 and *p* values were calculated. Expression data in human placentas was obtained from 6-16 placenta tissues per gestational stage. Due to the small sample size for each group, difference in the human placental expression was determined by a nonparametric method, Mann-Whitney U test (GraphPad Prism 5.04, La Jolla, CA). A *p*-value less than 0.05 was considered statistically significant.

3.3. Results

3.3.1. Fluctuation of house-keeping genes in various tissues during pregnancy

For greater precision of the mRNA quantification by qRT-PCR, we first determined the absolute Ct values for the house keeping genes in mouse kidney and liver from non-pregnant and pregnant mice at gd 10, 15 and 19 (Figure 3.1). The data showed that in the kidney mGusb expression was not affected by pregnancy and therefore was used for normalization for kidney expression. In the liver, mGapdh and mbeta actin were relatively stable and we used mGapdh for normalization. In human and mouse placentas, hGUSB/mGusb and hGAPDH/mGapdh were

both stable across gestational ages (data not shown). hGUSB for human placenta and either mGusb or mGapdh for mouse placenta were used for data normalization.

3.3.2. mRNA quantification of renal and hepatic mOct and mMate transporters in non-pregnant and pregnant mice at different gestational ages

Mice with timed pregnancies were used to investigate the influence of pregnancy and gestational age on OC transporter expression in the kidney and liver. It is not feasible to gather the same tissues from a human pregnancy. While many of the functional characteristics and tissue-distribution patterns of OC transporters are conserved between humans and rodents, there are also some species differences. Most notably, the human kidney predominantly expresses hOCT2 whereas both mOct1 and mOct2 are expressed in the rodent kidneys (Koepsell et al., 2007). In addition, the human kidney expresses both hMATE1 and hMATE2-K whereas mouse kidney expresses mMate1 only (Lickteig et al., 2008). As expected, qRT-PCR results showed that mOct1, mOct2 and mMate1 were highly expressed in the kidneys from non-pregnant and pregnant mice (Fig. 3.2A). In contrast, no significant expression was observed for mOct3, mMate2 or mPmat. There was no significant difference in renal mOct1 mRNA expression between non-pregnant and pregnant mice at gd 10, 15 and 19 (Fig. 3.2A). A trend of slight decrease in renal mOct2 mRNA expression was observed during pregnancy, but the decrease only became statistically significant ($p < 0.05$) at gd 10. A small but significant decrease (~30%) in renal mMate1 mRNA expression was observed at gd 10 and 15 (Fig. 3.2A).

In the mouse liver, mOct1 and mMate1 mRNA was highly expressed; whereas mRNA expression of other transporters (mOct2, mOct3, mMate2 and mPmat) was minimal or undetectable. Compared to non-pregnant mice, there were slight decreases in hepatic expression

of mOct1 mRNA at all three stages of pregnancy, but only the decrease at gd 15 (equivalent to the end of the second trimester in humans) was statistically significant (Fig. 3.2B). No significant change was observed in hepatic mMate1 mRNA expression from the pregnant mice as compared to the non-pregnant mice.

3.3.3. Protein quantification of renal and hepatic mOct and mMate transporters in non-pregnant and pregnant mice at different gestational ages

Next we used a novel LC-MS/MS targeted proteomics approach to determine the influence of pregnancy on renal and hepatic expression of mOct1, mOct2 and mMate1 proteins. Relative protein expression of each individual mouse OC transporters was measured across gestational age using transporter unique signature peptides (Table 3.1) and LC-MS/MS as detailed in Materials and Methods section. As shown in Fig. 3.2C, a marginal reduction in mOct1 and mOct2 proteins was observed in pregnant mouse kidneys, with gd 15 showing the most significant decrease. Notably, renal mMate1 protein expression showed 22%, 36% and 29% decrease at gd 10, 15 and 19 respectively. In the mouse liver, expression of Oct2 protein was negligible (Fig. 3.2D). mOct1 protein showed a minimal (10-15%) decrease at gd 15 and gd 19 whereas Mate1 protein expression was not affected by pregnancy (Fig. 3.2D). The overall impact of pregnancy on the expression of mOct and mMate proteins was consistent with mRNA expression of individual transporters during pregnancy (Fig. 3.2).

3.3.4. mRNA expression pattern of OC transporters in human and mouse placenta

Previous studies suggested a high expression of hOCT3/mOct3 in the placenta (Kekuda et al., 1998; Sata et al., 2005). However, the quantitative expression of other OC transporters in

the placenta has not been thoroughly investigated. Here, our qRT-PCR data showed that hOCT3 is expressed at a much greater level (> 30 -fold) than any other OC transporters (Fig. 3.3A). Similar expression pattern was also observed in late stage (gd 19) mouse placenta (Fig. 3.3B). Together, these data clearly demonstrated that in both humans and mice, hOCT3/mOct3 is the predominant polyspecific OC transporter expressed in term or near term placentas.

3.3.5. mOct3 mRNA and protein expression in mouse placenta at various gestational stages

The above study confirmed that mOct3 is the predominant polyspecific OC transporter in the mouse placenta. We next investigated whether placental mRNA expression levels of mOct3 change with gestational stages. The mRNA expressions of placental mOct3 at gd 15 and 19 were respectively 37-fold and 46-fold greater than that at gd 10 (Fig. 3.4A). Consistently, much stronger bands were observed at gd 15 and 19 when mOct3 transcripts were amplified from the mouse placentas by semi-quantitative PCR, (Fig. 3.4A). We then quantified the relative expression of mOct3 protein using LC-MS/MS. In agreement with the mRNA expression results, protein expressions of mOct3 at gd 15 and 19 were increased by 56- and 128-fold respectively (Fig 3B). The mOct3 mRNA expression at gd 19 appeared slightly higher than that at gd 15, but the difference was not statistically significant (Fig 3.4A). However, mOct3 protein expression at gd 19 was significantly higher than that at gd15 (Fig 3.4B). These data suggest that expression of the mOct3 gene in the mouse placenta is gestational-age dependent, and the expression of mOct3 mRNA and protein is greatly increased after gd 10 and reaches maximum at mid-to-late pregnancy. In addition to mOct3, we also examined the protein expression of mMate1 in the mouse placentas at gd 10, 15 and 19. Consistent with the mMate1 mRNA expression in mouse placenta at gd 19 (Fig 3.3B), there was no detectable mMate1 protein

expression in any of the placenta samples at all gestational ages (data not shown), further supporting that OCT3 protein is the major OC transporter in the placenta.

3.3.6. hOCT3 mRNA and protein expression in human placenta at different trimesters

The influence of gestational age on hOCT3 mRNA and protein expression in human placentas was measured in first trimester (T1, n=11), second trimester (T2, n=16), and term (n=6) placentas from normal uncomplicated pregnancies. To eliminate potential regional differences in hOCT3 mRNA expression, tissues from the outer surface (villus parenchyma) of the placenta were used in the study, as preliminary analysis showed little regional variation in hOCT3 mRNA expression in this area (data not shown). Different from the mouse, hOCT3 mRNA expression in human placentas did not show a significant increase in mid and late pregnancy (Fig. 3.5A), although there appeared a slight increase in hOCT3 mRNA expression in T2 placentas as compared to T1. A large inter-individual variability (> 20 fold) of hOCT3 mRNA expression was found in the placentas, especially those from T1 and T2 trimesters (Table 3.2). We then quantified the absolute amount of hOCT3 protein by LC-MS/MS in six randomly chosen placenta samples at each gestational age. The mean hOCT3 protein in T1, T2 and term placentas was quantified and found to be 0.23 ± 0.033 , 0.38 ± 0.072 and 0.36 ± 0.099 fmol/ μ g membrane protein respectively (Fig. 3.5B and Table 3.2). Compared to T1, hOCT3 protein levels showed ~65% and 56% increase at T2 and term respectively. In contrast to the large inter-individual variability in hOCT3 mRNA levels, a smaller variability (< 3 fold) was observed for hOCT3 protein in the human placenta samples. When comparative analysis was performed, protein levels were positively correlated with mRNA levels (Fig. 3.5C). However, the

correlation between hOCT3 mRNA and protein levels was weak, with an r^2 value of 0.21. Moreover, the slope deviated significantly from zero, with a p value of 0.049.

3.4. Discussion

This study evaluated the effects of pregnancy on mRNA and protein expression of polyspecific OC transporters in the kidney, liver and placenta, organs that are important for maternal disposition and fetal exposure to OC drugs. Since livers and kidneys of pregnant women are unavailable for gene analysis, we used a mouse model with timed pregnancies for our study. The gestational ages (gd 10, 15, 19) selected in this study represent critical times for placental and fetal development, and have been previously used to mimic the early, middle and late stages in human pregnancy (Wang et al., 2006; Zhang et al., 2008). For placenta, both human and mouse tissues at various gestational stages were analyzed and compared.

Our study showed that mRNA and protein expressions of mOct1 and mOct2 in the mouse kidney are marginally affected by pregnancy (Fig. 3.2A and 3.2C). Similarly, hepatic expression of mOct1 and mMate1 mRNA and protein is also minimally affected by pregnancy (Fig. 3.2B and 3.2D). However, in the kidney, mMate1 mRNA and protein expressions significantly declined by 20-40% throughout pregnancy with maximum down-regulation of mMate1 membrane protein observed at mid pregnancy (Fig. 3.2C). Our results are consistent with a recent report that also showed a down-regulation of renal apical drug efflux transporters (Mrp2, Mrp4, Mate1) in pregnant mice (Yacovino et al., 2013). The down-regulation of apical drug efflux transporters is anticipated to result in a reduced tubular secretory capacity during pregnancy. In addition, the significant down-regulation of apical efflux transporter (i.e. Mate1)

accompanied by less changes in the basolateral uptake transporters (i.e. Oct1/2) during pregnancy may, theoretically, lead to renal drug accumulation and increased risk of nephrotoxicity. These findings are somewhat counterintuitive, as urinary excretion of xenobiotics is generally enhanced during pregnancy in humans and rodents. We previously reported that metformin renal clearance increased significantly in mid- and late pregnancy as compared to postpartum (Eyal et al., 2010). Since we did not see an increase in Oct or Mate renal expression, altered renal expression of OC transporters may not be the reason underlying the observed increase in renal clearance of metformin during pregnancy. Other pregnancy-associated changes, such as elevations in renal blood flow and glomerular filtration, may contribute to the increased total renal clearance of metformin in pregnancy. However, it should be noted that since our study was conducted in mice, we cannot exclude the possibility that expression of hOCT2, hMATE1/2-K in the kidney is uniquely affected by human pregnancy.

Although OCT3/Oct3 is known for its high expression in placenta (Kekuda et al., 1998; Sata et al., 2005), the presence of other OC transporters in the placenta has been less well studied. Previous northern analysis found no expression of hMATE1 in the human placenta (Otsuka et al., 2005) whereas a high level of rMate1 expression was reported in the rat placenta (Ahmadimoghaddam et al., 2012; Terada et al., 2006). Here, we comprehensively analyzed the expression profiles of OCT1-3, MATE1-2 and PMAT in the same placental tissues obtained from healthy term human placenta and in mouse placenta at gd 19. Our data clearly showed that OCT3 is the predominant OC transporter expressed in the human and mouse placentas (Fig. 3.3). Previous membrane vesicle and immunostaining studies suggested a basal membrane localization of OCT3/Oct3 proteins in human and rat placentas (Ahmadimoghaddam et al., 2012; Sata et al., 2005). The precise role of OCT3 in OC transport at the placental barrier is presently

unclear. When pregnant Oct3-null mice were given intravenous MPP⁺, a model substrate for all OC transporters, a significant reduction in MPP⁺ accumulation was observed in homozygous Oct3^{-/-} embryos (Zwart et al., 2001b), suggesting that mOct3 mediates maternal-to-fetal OC transport. In contrast, Ahmadimoghaddam et al. showed high expression of rMate1 in rat placenta and suggested that rOct3 and rMate1 work together to sequentially mediate fetal-to-maternal transport of MPP⁺ (Ahmadimoghaddam et al., 2012). Here, we found that MATE1/Mate1 mRNA and protein are minimally expressed in mouse and human placentas (Fig. 3.3), which challenges an OCT3/MATE tandem transport model in these species. Clearly, more work is needed to elucidate OC transport mechanisms at the human placental barrier.

Recent studies showed that the placental expression of drug efflux transporters (e.g. P-gp, BCRP) change with gestational age, which may influence fetal drug exposure in a gestational-age dependent manner (Zhang et al., 2008; Zhou et al., 2008). Our data showed that mOct3 mRNA in mouse placenta at gd 15 and 19 was more than 35-fold higher than that seen at gd 10 (Fig. 3.4A). This apparent activation of mOct3 mRNA transcription in mouse placenta between early and mid pregnancy was also previously noticed by other investigators (Shuster et al., 2013; Zwart et al., 2001b). Using LC-MS/MS, we further showed that mOct3 protein levels in the mouse placenta also increased dramatically at gd 15 and 19 (Fig. 3.4B). Interestingly, such a dramatic change was not observed for hOCT3 in human placenta (Fig. 3.5). Despite a large inter-individual variation of mRNA levels, the mean hOCT3 mRNA expression did not show a gestational age-dependent change (Fig. 3.5A). When the absolute amount of protein was quantified, T2 and term human placenta only showed a moderate increase in hOCT3 protein (Fig. 3.5B). Together our data suggest while human and mouse term placenta share a similar expression pattern of polyspecific OC transporters and predominantly express OCT3/Oct3,

placental expression of the mouse mOct3 gene is regulated by gestational age and is transcriptionally activated after gd 10. Recently, the absolute membrane protein levels of drug transporters have been determined in several human tissues, especially the liver (Ohtsuki et al., 2012; Prasad et al., 2013; Uchida et al., 2011). The protein levels for the well-established drug transporters hOCT1, hMATE1, P-gp and BCRP in the human liver ranged from 0.14 to 7.35 fmol/ μ g by the LC-MS/MS method (Ohtsuki et al., 2012; Prasad et al., 2013). The hOCT3 protein amount in the human placenta determined in this study was 0.2-0.4 fmol/ μ g membrane protein. This value is comparable to those reported for the hepatic drug transporters. However, our absolute quantification of hOCT3 protein was performed using a single target peptide. We acknowledge that protein quantification by the LC-MS/MS method can be peptide-dependent, as variability in trypsin digestion might result in different protein yield when quantified using different target peptides. Nevertheless, this is the first report for absolute protein quantification for a human placental drug transporter by LC-MS/MS to our knowledge. Since it is more costly and time-consuming to measure absolute protein amount, only relative protein expression was performed for mOct1, mOct2, mOct3 and mMate1. While informative on pregnancy-induced changes in protein expression of a specific transporter, in the absence of authentic full-length protein standards, this value may not be used quantitatively for cross-comparison between different transporters, due to the peptide-dependent nature of the LC-MS/MS method.

Levels of mRNA expression have been widely used as a surrogate for protein expression or activity in biological samples. In this study, the overall patterns of OC transporter mRNA expression are generally consistent with their protein expression, especially in various mouse tissues that are collected and processed under highly controlled conditions. Transporters that were not detectable at the mRNA level were also not detected at the protein level (Figures 3.2

and 3.4). In human placenta, we observed a trend of increase of hOCT3 protein with its mRNA levels. However, the correlation between hOCT3 mRNA and protein levels was relatively weak (Fig. 3.5C). Poor correlations were also reported for other drug transporters in the human liver (Ohtsuki et al., 2012). A closer examination of Figure 4 revealed that the weak correlation can be traced down to a large variability (> 20 fold) in mRNA levels but a relatively small (< 3 fold) variability in hOCT3 protein levels in the human placenta samples. This may reflect the fact that proteins are more stable, whereas mRNAs are more prone to degradation during human sample preparation. mRNA instability could lead to noise in the correlation analysis. In addition, poor correlations might be due to the fact that mRNA is extracted from total lysate of tissue whereas protein is isolated plasma membrane fraction, as previously suggested (Ohtsuki et al., 2012).

In summary, we have determined the impact of pregnancy on mRNA and protein expression of polyspecific OC transporters in kidney, liver, and placenta. In mice, pregnancy has a marginal effect on renal expression of mOct1/2, but reduces mMate1 mRNA and protein expression by 20-40%. Hepatic expression of mOct1 and mMate1 were minimally affected by pregnancy. In the placenta, OCT3/Oct3 was the predominant isoform expressed in both human and mouse placentae. Oct3 expression in mouse placenta was gestational age-dependent and its expression is activated between early and mid-pregnancy. In contrast, expression of hOCT3 was high even in early stage human placenta, and hOCT3 protein only showed a moderate increase in second trimester and term placentas. Together, our studies provide new insights into the effect of pregnancy on the expression of polyspecific OC transporters and supported an important role of OCT3 in OC transport at the magtrenal-fetal interface.

Table 3.1. Optimized MS/MS parameters of proteotypic peptides selected for targeted analysis of mOct1, mOct2, mOct3, mMate1 and hOCT3.

Transporter	Peptide	Precursor Ion	Product Ions	Fragmentor	Collision Energy
mOct1	GVALPETIEEAENLGR	849.5	1357.7	160	20
		849.5	679.3	160	20
mOct1 (IS)	GVALPETIEEAENLGR	854.5	1367.7	160	20
		854.5	684.3	160	20
mOct2	LNPSFLDLVR	587.3	228.13	140	15
		587.3	946.54	140	15
mOct2 (IS)	LNPSFLDLVR	592.34	956.54	140	15
		592.34	228.13	140	15
mMate1	TEESAPGPGGADAASER	801.4	1084.5	160	18
		801.4	542.7	160	18
mMate1 (IS)	TEESAPGPGGADAASER	806.4	1094.5	160	18
		806.4	547.8	160	18
mOct3	GIALPETVEDVEK	700.4	1158.6	140	16
		700.4	1045.5	140	16
		700.4	579.8	140	18
mOct3 (IS)	GIALPETVDDVEK	697.5	1039.3	140	16
hOCT3	GIALPETVDDVEK	693.5	1031.3	140	16
		693.5	516.1	140	18
		693.5	355.1	140	13
hOCT3 (IS)	GIALPETVDDVEK	697.5	1039.3	140	16

IS = internal standard; arginine-¹³C₆, ¹⁵N₄ and lysine ¹³C₆, ¹⁵N₂ labeled residues are shown in bold and italic.

Because mouse and human Oct3/OCT3 surrogate peptides showed similar characteristics, single IS was used for both transporters.

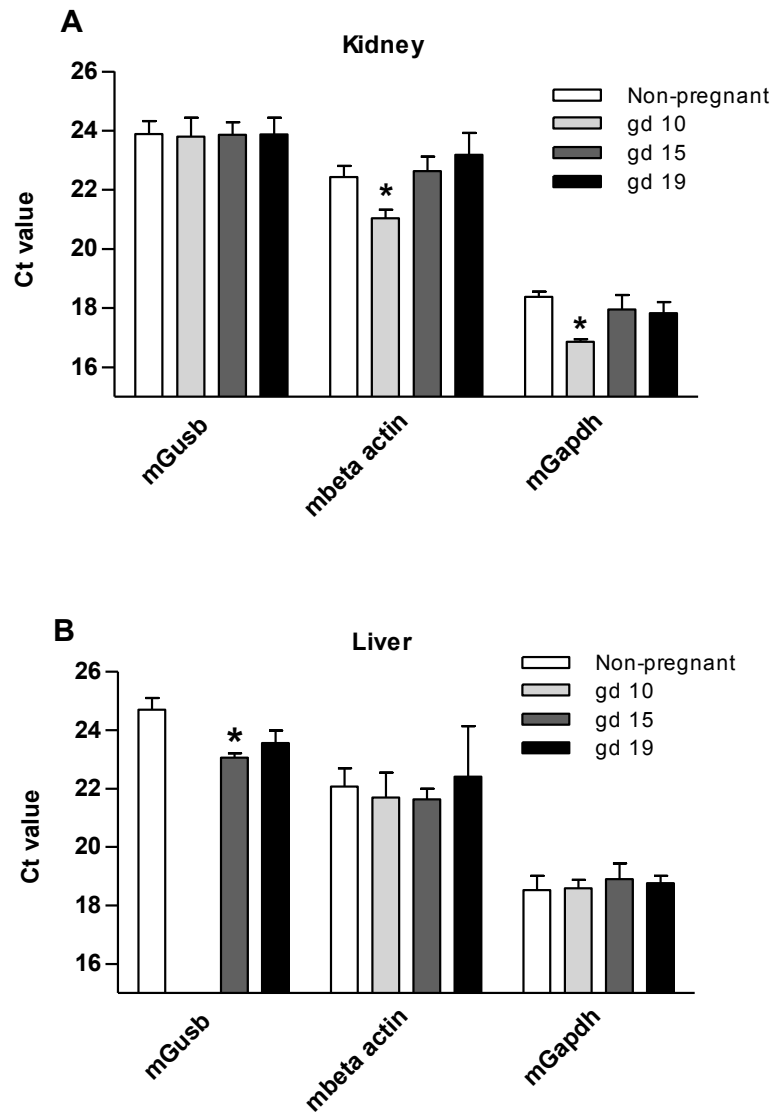


Figure 3.1. Ct values of different housekeeping genes in kidney and liver from pregnant mice at different gestational ages. The results represent mean \pm S.D for 3-6 mice at different gestational ages. Ct value of mGusb in mouse liver at gd 10 was not determined. * indicates a significant difference from the Ct values of non-pregnant mice ($p < 0.05$).

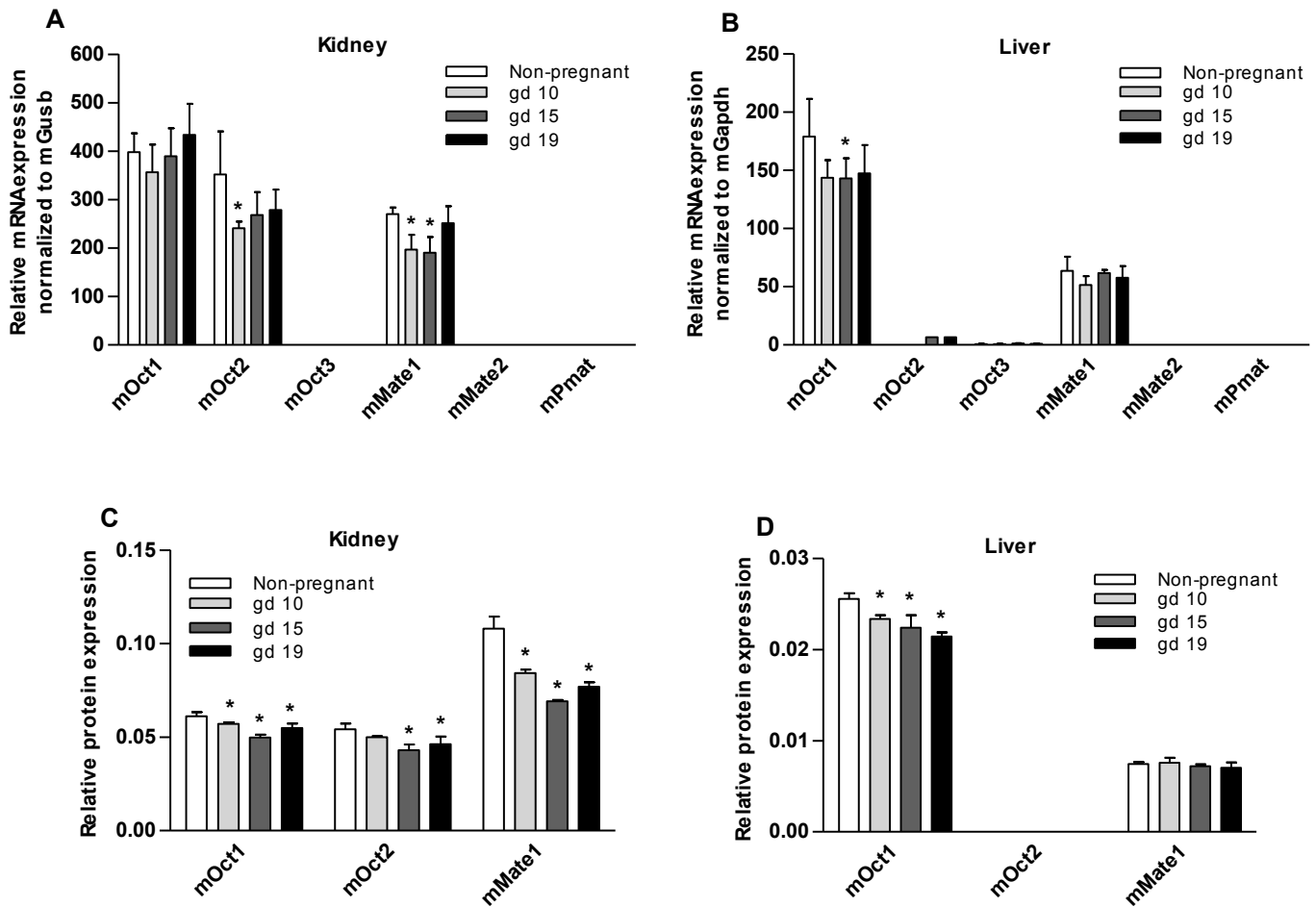


Figure 3.2. mRNA and protein expression of mouse OC transporters in kidney (A and C) and liver (B and D) at different gestational ages. Total RNA isolated from the kidneys and livers of non-pregnant (virgin) and pregnant mice at gd 10, 15 and 19 was reverse transcribed and mRNA levels of six OC transporters were determined by qRT-PCR. Relative protein expression of individual transporters across different gestational age was measured in the membrane protein prepared from kidney and liver using LC-MS/MS. The mRNA expression is normalized to mGusb in kidney and to mGapdh in liver. Data are expressed as mean \pm S.D from 3-6 mice at each gestational age. * indicates a significant difference from the expression at non-pregnant state ($p < 0.05$).

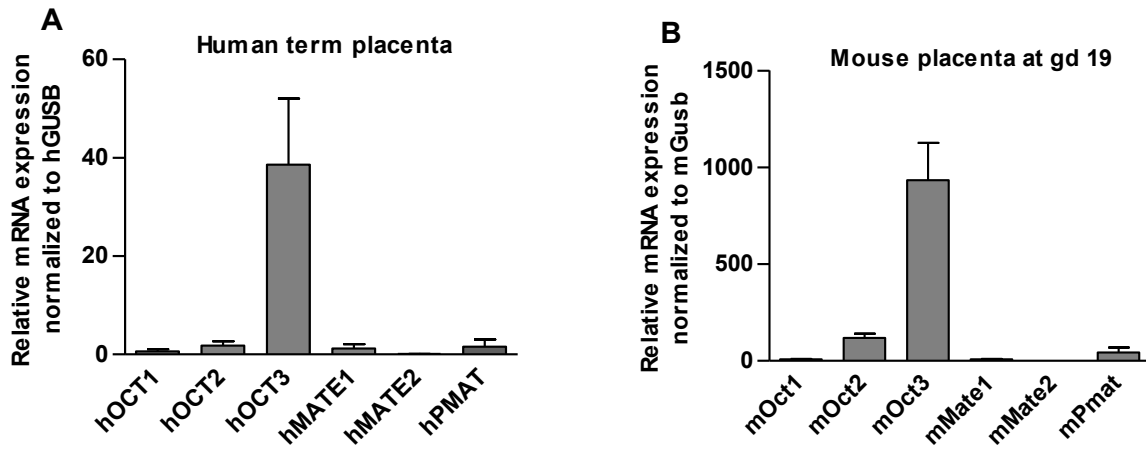


Figure 3.3. mRNA expression of various OC transporters in human term placenta (A) and mouse placenta at gd 19 (B). Total RNA was isolated from human term placentas (n=6) and mouse placentas at gd 19 (n=3). cDNA was synthesized by reverse transcriptase, and mRNA levels of hOCT1-3/mOct1-3, hMATE1/2/mMate1/2, and hPMAT/mPmat were determined by qRT-PCR. The results were normalized to hGUSB or mGusb and represent mean \pm S.D.

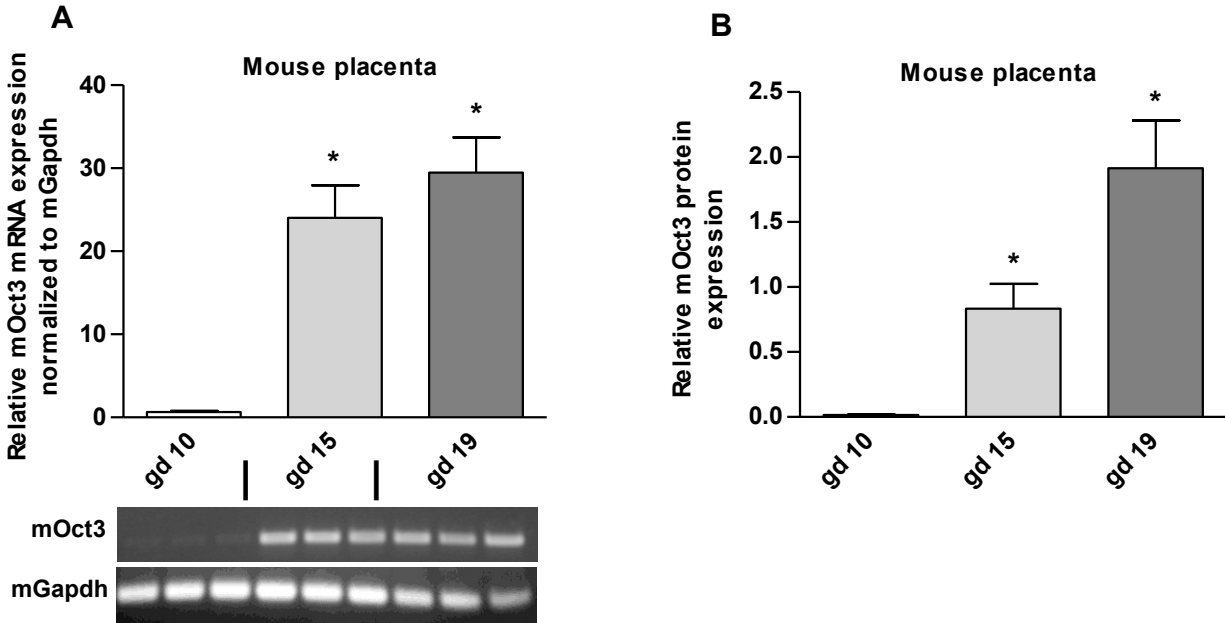


Figure 3.4. mOct3 mRNA and protein expression in mouse placenta at different gestational ages. Total RNA isolated from the placenta of non-pregnant (virgin) and pregnant mice at gd 10, 15 and 19 was reverse transcribed and mRNA levels of Oct3 were determined by semi-quantitative reverse transcriptase PCR and qRT-PCR (A). Relative protein expression of mOct3 in isolated membrane protein of mouse placentas was measured using LC-MS/MS (B). The mRNA levels determined by qRT-PCR were normalized to mGapdh. Data are mean \pm S.D (n=3 per group). * indicates a significant difference from the expression at gd 10 ($p < 0.05$).

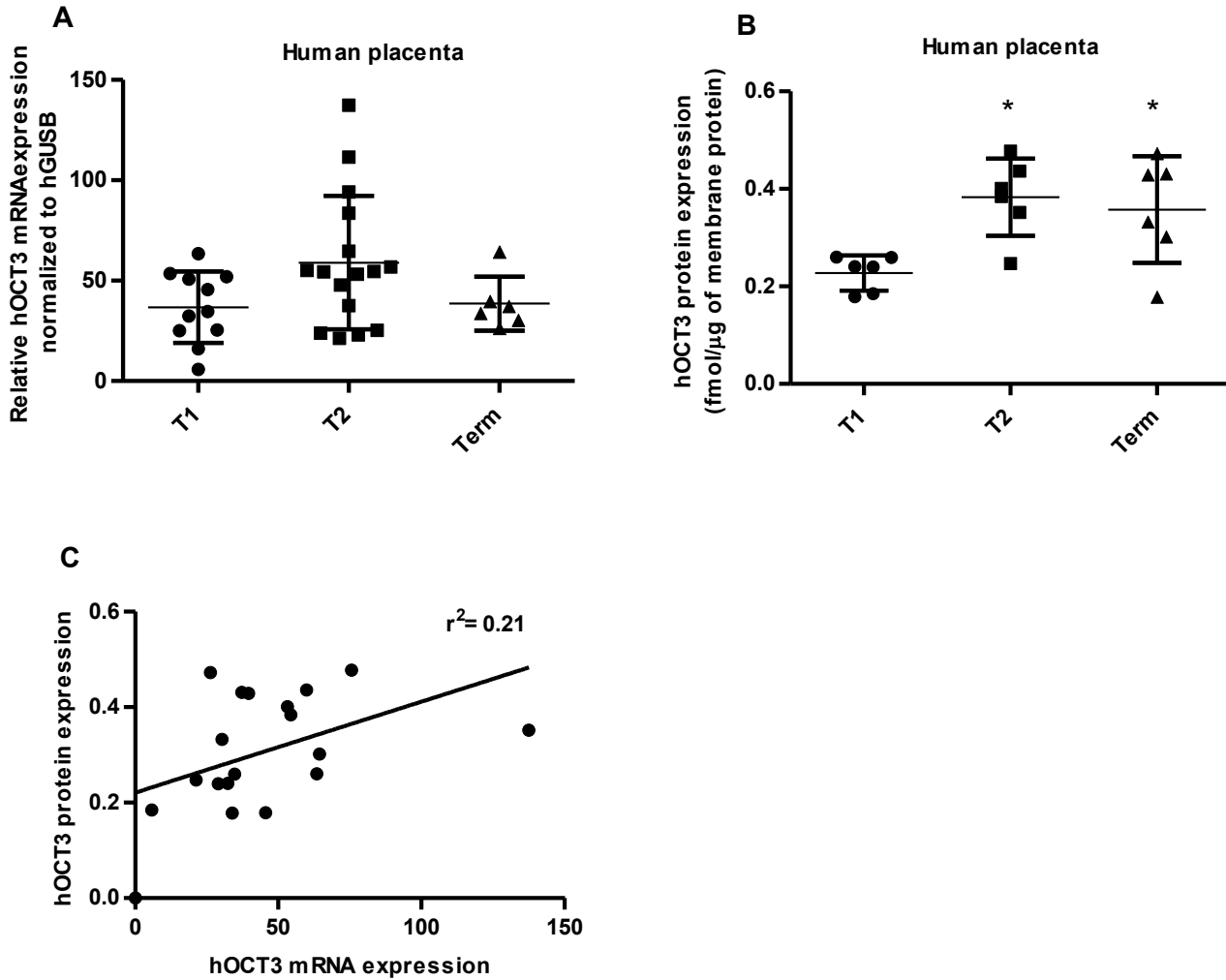


Figure 3.5. Quantification of hOCT3 mRNA (A) and protein (B) in human placentas at different gestational stages and correlation analysis of mRNA and protein expression (C).

Total RNA was isolated from first trimester (T1, n=11), second trimester (T2, n=16) and term (n=6) placentas, and mRNA levels were determined by qRT-PCR and normalized to hGUSB.

Membrane protein was isolated from T1, T2 and term placentas (n=6 for each gestation age placenta). hOCT3 protein levels were quantified using a LC-MS/MS method. Each data point represents an individual placenta. mRNA and protein expression of hOCT3 were correlated using linear regression.

Table 3.2. hOCT3 mRNA and protein quantification in human placentas from first, second trimesters and at term. Data are expressed as mean \pm S.D. Difference in the human placental expression was determined by nonparametric Mann-Whitney U test. * indicates a significant difference from the expression at T1 ($p < 0.05$).

Gestational Age	hOCT3 Transcript Expression mRNA/GUSB (arbitrary unit)		hOCT3 Protein Quantification (fmol/ μ g membrane protein)	
	Mean \pm S.D	Range	Mean \pm S.D	Range
T1	36.79 \pm 17.82 (n=11)	5.81 – 63.41	0.23 \pm 0.033 (n=6)	0.18 – 0.26
T2	58.93 \pm 33.22 (n=16)	21.20 – 137.40	0.38 \pm 0.072* (n=6)	0.25 – 0.48
Term	38.57 \pm 13.49 (n=6)	26.23 – 64.32	0.36 \pm 0.099* (n=6)	0.18 – 0.47

Chapter 4. Taste of pill: Organic cation transporter 3 mediates salivary gland accumulation of metformin

4.1. Introduction

Many medications, including antihypertensives, antidiabetics, antimicrobials and antidepressants, have the potential to adversely influence a patient's sense of taste and smell. In some cases, drug-induced chemosensory disturbances are persistent and cannot be quickly reversed by drug cessation. Taste-related adverse effects can significantly impact patient's quality of life, dietary choices, appetite, emotional state and compliance with medication regimens.

One medication that causes taste disturbance is metformin, a first line oral hypoglycemic widely prescribed for the treatment of type 2 diabetes mellitus (Hundal and Inzucchi, 2003; Lord et al., 2003; Wensel, 2009). As the prevalence of obesity and diabetes increases worldwide, metformin use also increases and has recently made it to the list of top 15 prescribed drugs in the US. Metformin acts as an insulin sensitizer and lowers blood glucose levels by suppressing hepatic gluconeogenesis, reducing intestinal glucose absorption, and stimulating glucose uptake and utilization in skeletal muscle and adipose tissues (Hundal and Inzucchi, 2003). The glycemic response to metformin is variable, with some patients responding extremely well whereas others showing no benefit (Inzucchi, 2002). The drug rarely causes lactic acidosis and has minimal risk of inducing hypoglycemia. The most common adverse effects of metformin are gastrointestinal in nature, including diarrhea, nausea, abdominal pain, taste disturbance and loss of appetite (Melchior and Jaber, 1996; Zolk, 2012). In particular, patients taking metformin

frequently complain of metallic and bitter taste in the mouth, which interferes with their normal sensation of food and quality of life.

The taste disturbance induced by metformin appears to result from a low but persistent secretion of the drug into the saliva which continually bathes the taste buds and receptors located on the upper surface of the tongue, soft palate, and upper esophagus. After a single oral or intravenous dose in man, metformin is easily detectable in the saliva (Pentikainen et al., 1979). The concentration of metformin in the saliva is considerably lower than that in the blood but declines much more slowly (Pentikainen et al., 1979). Animal studies further revealed that after metformin administration the drug is highly accumulated in salivary glands (Wilcock and Bailey, 1994).

In this Chapter, we report that OCT3/Oct3 (SLC22A3/Slc22a3), a member of the polyspecific organic cation transporter family, is responsible for the high accumulation of metformin in the salivary glands and might underly its adverse taste disturbance. We also show that OCT3/Oct3 impacts metformin pharmacokinetics and influence its distribution into other peripheral tissues including sites of metformin action. Together, our studies uncovered a unique molecular mechanism underlying drug-induced taste disturbance and identified an additional genetic factor that may contribute to variable disposition and response to a first line treatment drug for type 2 diabetes.

4.2. Methods and materials

4.2.1. Animals

The *Oct3 (Slc22a3)* null mice of the FVB inbred strain (Zwart et al., 2001b) were developed by Dr. Denise Barlow at the University of Vienna and maintained by Dr. Alfred Schinkel of the Netherlands Cancer Institute. After re-derivation in the Charles River Laboratories, a colony of *Oct3*^{-/-} and wild type (*Oct3*^{+/+}) inbred FVB mice were kindly provided to us by Dr. John Markowitz at the University of Florida with the consent of Dr. Schinkel. These mice were housed in the specific pathogen free (SPF) facility at the University of Washington. All animal studies were approved by the Institutional Animal Care and Use Committee (IACUC) at the University of Washington.

4.2.2. Human salivary glands

Human salivary gland total RNA (Clontech, Mountain View, CA), pooled from 24 male and female Caucasians with age of 16-60, was used for real-time PCR analysis. For immunostaining and protein quantification studies, freshly frozen salivary gland tissue, including parotid, submandibular, and sublingual glands, from a single healthy female donor (age 30) with no medical history was provided to us by National Disease Resource Interchange (NDRI).

4.2.3. RNA preparation and real-time PCR

For mRNA expression, 10-12 week old female *Oct3* ^{+/+} and *Oct3* ^{-/-} mice were used (n=4). Liver, kidney, small intestine, heart, salivary gland, and skeletal muscle were collected and the tissues were flash-frozen in liquid N₂ and stored at -80°C until use.

Total RNA was extracted from mouse and human tissues using Trizol reagent (Invitrogen, Inc) or Qiagen Mini RNeasy Kit according to the manufacturer's instructions. RNA integrity and purity were verified by gel electrophoresis and UV spectrophotometer. Mouse and

human total RNA (1-2 µg) was reverse transcribed to first-strand cDNA using Superscript III reverse transcriptase (Invitrogen) according to the manufacturer's instructions. Taqman real-time PCR reagents, assay primers and probes for human and mouse OCT1/Oct1 (SLC22A1/Slc22a1), hOCT2/mOct2 (SLC22A2/Slc22a2), hOCT3/mOct3 (SLC22A3/Slc22a3), hMATE1/mMate1 (SLC47A1/Slc47a1), hPMAT/mPmat (SLC29A4/Slc29a4), and hGUSB/mGusb (beta glucuronidase), were purchased from Applied Biosystems (Foster City, CA). Taqman real-time PCR assays were carried out according to the manufacturer's protocols on an Applied Biosystems 7900HT fast real-time PCR system. The real-time reaction contained 10 µl of 2X TaqMan Universal PCR Master Mix (Applied Biosystems), 20 ng of RNA-equivalent cDNA, and 1 µl of 20x primer/probe mix in a final volume of 20 µl. Each sample was analyzed in triplicate. To quantify the transcript numbers of genes of interest, the comparative CT method was used (Zhang et al., 2008). The mRNA levels of each test gene was normalized to hGUSB/mGusb, according to the following formula: $CT(\text{test gene}) - CT(\text{mGusb}) = \Delta CT$. Thereafter, the relative mRNA levels of each gene was calculated using the $\Delta\Delta CT$ method: $\Delta CT(\text{test gene}) - \Delta CT(\text{test gene in the calibrator}) = \Delta\Delta CT(\text{test gene})$. The fold changes of mRNA levels were represented as a relative expression $2^{-\Delta\Delta CT}$.

4.2.4. Drug uptake in hOCT3 expressing cells

Human OCT3-expressing HEK cells (Flp-In-293) were previously generated (Duan and Wang, 2010). Cells were maintained in D-MEM media containing 10% fetal bovine serum, 1% L-Glutamine, 1% penicillin/streptomycin, and hygromycin B (150 µg/ml) at 37 °C in 5% CO₂ and 95% humidity. Cells were seeded in 24-well plates and allowed to grow for 2-3 days. Growth medium was aspirated and each well was rinsed with Krebs-Rinber-Henseleit (KRH)

buffer (5.6 mM glucose, 125 mM NaCl, 4.8 mM KCl, 1.2 mM KH_2PO_4 , 1.2 mM CaCl_2 , 1.2 mM MgSO_4 , and 25 mM HEPES), and preincubated in KRH buffer for 15 min at 37°C and pH 7.4. Transport was started by the addition of [^{14}C] labeled metformin (Moravek Biochemicals and Radiochemicals, Brea, CA) and terminated by washing the cells three times with ice-cold KRH buffer. Cells were then solubilized with 1N NaOH, and neutralized with 1 N HCl. Radioactivity was quantified by liquid scintillation counting, and the protein content was measured using BCA protein assay kit (Pierce). Time-dependant uptake was carried out with 10 μM of metformin to identify initial rate period and verify the linear range uptake of metformin. Then, 4-5 min uptake was chosen, and kinetic studies were performed with various concentrations of metformin. Specific uptake activity was calculated by subtracting the uptake in the pcDNA5 vector transfected cells. Using GraphPad Prism (version 5: GraphPad Software, La Jolla, CA), the kinetic parameters V_{max} and K_m were determined by nonlinear least square regression by fitting the data to the Michaelis-Menten equation: $V = V_{\text{max}} * [S] / (K_m + [S])$, where $[S]$ is the substrate concentration, and V is the initial rate of uptake. V_{max} is the maximum rate of uptake, expressed as pmol/min/mg or nmol/min/mg; and K_m , expressed as mM, is the concentration where the rate of uptake is a half of V_{max} .

4.2.5. Membrane protein preparation and LC-MS/MS analysis

Total membrane proteins were isolated from the human salivary glands including parotid, submandibular, and sublingual glands and hOCT3 stably transfected cells using the Proteo Extract native membrane protein extraction kit (Calbiochem) according to the manufacturer's instructions (Prasad et al., 2013). Total protein concentration was determined by the BCA protein assay kit (Pierce). The membrane fraction was digested by trypsin as per conditions

described before (Prasad et al., 2013). Briefly, the isolated membrane proteins were denatured at 95° C, reduced with dithiothreitol and alkylated with iodoacetamide in ammonium bicarbonate buffer. The protein samples were digested at 37°C for 24 h by trypsin and the reaction was quenched by adding internal standard (IS) solution and centrifuged at 5000 g for 5 min before LC-MS/MS analysis.

Absolute quantification of OCT3 in total membrane fraction isolated from the hOCT3 expressed cells and human salivary glands was performed using an unique signature peptide as a surrogate and the corresponding isotopically ($[^{13}\text{C}_6, ^{15}\text{N}_2]$ lysine) labeled peptide as IS. The signature peptide was selected based on criteria previously discussed (Kamiie et al., 2008). The selected peptide was GIALPETVDDVEK and used as a calibrator. The LC-MS/MS parameters were optimized to quantify the selected peptide in the tissues samples. The analysis was performed using an Agilent 6460A triple-quadrupole mass spectrometer coupled to an Agilent 1290 Infinity LC system (Agilent Technologies, Santa Clara, CA) operated in ESI positive ionization mode. Approximately 2 μg (or less) of the trypsin digest (5 μl of LC injection volume) was injected onto the column (Kinetex™ 2.6 μm , C18, 100 x 3 mm, Phenomenex, Torrance, CA). The LC flow rate was 0.4 ml/min. The gradient program was: 97% A and 3% B held for 4.5 min, followed by two steps of linear gradient of mobile phase B concentration of 3% to 18% and 18% to 24% over 4.5-7.5 min and 7.5-11.5 min. This was followed by the washing step (80% mobile phase B) for 1 min, and re-equilibration for 5 min. The parent-to-product transitions for the OCT3 peptide monitored were doubly charged parent ion of m/z 700.4 or 693.5 to single-charged product ions of m/z 1031.3, 516.1 and 355.1. The transitions selected for the stable isotope labeled peptides (SIL) peptide were m/z 697.5 (parent) to m/z of 1039.3 (product). The data were processed by integrating the peak areas generated from the ion

chromatograms for the analyte peptides and their respective internal standards using the MassHunter software (Agilent Technologies, Santa Clara, CA). For data analysis, peak response of MRM transitions from each peptide was averaged and the area ratio of analyte peptide vs IS peptide was performed. The measurements were performed in triplicate.

4.2.6. *In vivo* study in mice

To determine pharmacokinetics and tissue distribution of metformin in the absence of Oct3, 10-12 week old female and male Oct3^{+/+} and Oct3^{-/-} mice were used (n=3-5 per time points). The mice were fasted for 5-10 hours and administered 15 mg/kg metformin containing 0.2 mCi/kg of [¹⁴C] labeled metformin by oral gavage. At time points of 10, 15, 30, 45, 60, 90, 120, 180, 240, and 480 min, animals were sacrificed by CO₂. Blood samples were obtained by cardiac puncture using the heparin coated syringe (Smiths Medical) and plasma was separated by centrifugation for 5 minute at 5000 x g. Tissues including liver, kidney, skeletal muscle, heart, salivary gland and brain were collected at each time point.

Metformin concentrations in the plasma and tissues were determined by scintillation counting using the method described by Wilcock et al. with minor modification (Wilcock and Bailey, 1994). In brief, plasma and tissues were placed in scintillation vials with 1 mL 1 M NaOH and incubated at 55~70°C for 1~2 hours. After cooling, H₂O₂ was added to decolorize the samples. After several hours, 15 mL of Eco-scintillation buffer was added first, and then 1 mL 1 M HCL was added to neutralize the solutions. The samples were stored overnight before counting. The amounts of radioactivity were expressed as ng/g tissue for tissues and ng/ml for plasma.

4.2.7. Immunofluorescent labeling of hOCT3 in human submandibular salivary gland

Snap frozen human submandibular glands were processed to frozen section by the Pathology Research Services at the University of Washington. The sections were fixed in ice-cold acetone for 5 min and immersed in PBS for 5 min. The sections were blocked in PBS containing 5% goat serum for 45 min at room temperature. Then, the sections were incubated overnight at 4°C with polyclonal rabbit anti-OCT3 (1:125) (Genway), co-labeled with anti-human Na⁺/K⁺-ATPase α subunit (1:500) (Sigma). After antibody incubation, the sections were washed with PBS; and Alexa Fluor tagged secondary antibodies, Alexa 488 and Alexa 568 (1:500), were applied for 1 hr at room temperature. After washing with PBS, ProLong Gold antifade medium with DAPI was mounted on the slides and cover-slipped. The fluorescence images were obtained with a Zeiss Axiovert 200 fluorescence microscope.

4.2.8. Pharmacokinetic data analysis

For one point sampling data (one blood sample from one individual mouse), we used a bootstrap method to obtain confidence intervals for pharmacokinetic parameter estimates of maternal plasma and fetal tissue. Area under the curve (AUC), oral clearance (CL/F), terminal half-life ($t_{1/2, \beta}$), and volume of distribution at terminal phase (V_{β}) were calculated using the following equations,

$$AUC_{0-t} = \int_0^t C(t)dt$$

$$AUC_{0-\infty} = AUC_{0-t} + \frac{C(T)}{\beta}$$

$$\frac{CL}{F} = \frac{Dose}{AUC_{0-\infty}}$$

$$t_{\frac{1}{2},\beta} = \frac{\ln 2}{\beta}$$

$$V_{\beta} = \frac{CL}{F \cdot \beta}$$

Terminal slope (β) was calculated by performing a linear regression of concentrations at the last three to five time points. T indicates last time point (i.e. 480 min), and C(T) is the concentration at the last time point. The 95% confidence intervals for PK parameters were generated using the bootstrap method as described by Mager and Göller (Mager and Göller, 1998) with modification. Briefly, plasma or tissue concentrations were resampled with random replacement of 26 mice. This resampling with random replacement was performed using the R program developed by Jason Liang in the Department of Biostatistics at the University of Washington. The resampling was repeated 10,000 times to create 10,000 pseudo concentration-time profiles. For each profile, the concentrations at each nominal time point were averaged and the PK parameters were calculated using the equations defined above. The 95% confidence intervals for each parameter were calculated by taking the 2.5% and 97.5% quantiles, i.e. the 251th and 97501th AUC values of 10,000 bootstrap AUC values.

4.2.9. Statistical analysis

Data are expressed as mean \pm S.D or S.E. Uptake experiments were performed in triplicate and repeated at least three times. Statistical significance for uptake experiments was determined by Student's t test. A p-value less than 0.05 was considered significant. *In vivo*

study data were analyzed and 95% confidence intervals for each PK parameter were determined using the bootstrap method as described in the previous section.

4.3. Results

4.3.1. Metformin transport kinetics by OCT3

When time dependent uptake of [^{14}C] metformin was examined at 10 μM , human OCT3-mediated metformin uptake was linear up to 5 min. hOCT3-expressing cells exhibited significantly greater uptake activity as compared to the empty vector transfected cells (Figure 4.1A). Based on these data, kinetic studies with various metformin concentrations were carried out using 4-5 min as the incubation time. hOCT3-mediated metformin uptake was saturable with an apparent affinity (K_m) of 3.67 ± 0.25 mM, which is comparable to those of previous reports of metformin K_m in hOCT1 or hOCT2 expressing cells (Figure 4.1B) (Dresser et al., 2002; Kimura et al., 2005; Suhre et al., 2005; Wang et al., 2002). A maximum velocity (V_{\max}) was estimated to be 43.37 ± 4.14 pmol/ μg membrane protein/min. Using a LC-MS/MS targeted proteomics method, hOCT3 protein expression in the cells was determined to be 21.44 ± 3.00 fmol/ μg membrane protein. Accordingly, the maximum metformin turnover number (k_{cat}) for OCT3 was calculated to be 33.71 ± 7.00 s $^{-1}$ and the single transporter catalytic efficiency (k_{cat}/K_m) was 9.19 ± 2.37 s $^{-1}\text{mM}^{-1}$.

4.3.2. Predominant expression of OCT3 in salivary glands

Previous expression profiling studies in human tissues reported a wide distribution of OCT3 mRNA in various human tissues with major expression found in skeletal muscle, cardiac myocytes, placenta, liver, adrenal gland, salivary gland, and prostate (Wu et al., 2000). As Oct3

expression was less studied in mice, we first quantified mRNA expression of Oct3 and other known metformin transporters (Oct1, Oct2, Mate1, Pmat) in various mouse tissues that are most relevant to metformin disposition, response and adverse reactions. As previously reported (Koepsell et al., 2007), mouse liver predominantly expressed Oct1 and Mate1 and mouse kidney predominantly expressed Oct1, Oct2 and Mate1 (Fig. 4.2). In the small intestine, Oct1 and Mate1 predominated in all segments although Oct3 and Pmat were also significantly expressed in the ileum (Fig. 4.2). Mouse heart and skeletal muscle had a very high expression of Mate1 together with a significant expression of Oct3 (Fig. 4.2). Among the mouse tissue analyzed, the highest expression of Oct3 was observed in salivary glands (Fig. 4.3A), where other organic cation and biogenic amine transporters, including Oct1, Oct2, Mate1, Pmat, Sert, Net, and Dat, were minimally expressed (Fig. 4.3B). A similar and predominant expression of OCT3 was also observed in human salivary glands (Fig. 4.4A). A further analysis revealed that OCT3 mRNA is expressed in all three major locations of human salivary glands including parotid, sublingual and submandibular glands (Fig. 4.4B). Among the different types of salivary glands, the submandibular gland, which is responsible for generating 70% of all saliva produced in the oral cavity, has the highest OCT3 expression.

4.3.3. OCT3 protein expression and localization in salivary glands

Using targeted proteomics, hOCT3 protein in human parotid, submandibular, and sublingual glands were quantified to be 0.42 ± 0.11 , 1.53 ± 0.015 and 0.43 ± 0.29 fmol per μg total membrane protein respectively (Fig. 4.5A). Consistent with mRNA data, OCT3 protein in submandibular gland was higher than in parotid and sublingual glands. Human submandibular gland cryostat section was immunolabeled for OCT3 and Na^+/K^+ -ATPase. hOCT3 staining was

primarily found on the plasma membranes of acinar and ductal epithelial cells, and largely overlapped with the basolateral membrane marker Na^+/K^+ -ATPase (Fig. 4.5B). Besides basolateral membrane labeling, strong immunostaining was also observed on the apical membrane lining the canaliculi of acinar cells. These data revealed that OCT3 is present on both the basolateral (blood-facing) and the apical (salivary fluid-facing) membranes of the secretory cells of the salivary glands. A cellular model was presented to show OCT3 location and transport direction in the salivary epithelial cells (Fig. 4.11).

4.3.4. Altered metformin pharmacokinetics in Oct3^{-/-} mice

To assess the role of Oct3 in metformin disposition *in vivo*, we determined metformin pharmacokinetics and tissue distribution in Oct3^{+/+} and Oct3^{-/-} mice. Prior to the *in vivo* studies, we confirmed by qRT-PCR that there were no significant compensatory changes in the expression of other metformin transporters (Oct1, Oct2, Mate1, Pmat) in tissues of interest in Oct3^{-/-} mice (Fig. 4.2). Age- and gender-matched Oct3^{+/+} and Oct3^{-/-} mice were given 15 mg/kg metformin containing a trace amount of ¹⁴C-metformin by oral gavage. Mice (n=3-5) were sacrificed at each time point, and metformin plasma and tissue concentrations were determined. The plasma concentration-time profiles and the pharmacokinetic parameters of metformin in female Oct3^{+/+} and Oct3^{-/-} mice were shown in Fig. 4.7 and Table 4.1. While the overall systemic exposure ($\text{AUC}_{0-480 \text{ min}}$) was comparable between Oct3^{+/+} and Oct3^{-/-} mice, clear difference was observed in metformin plasma levels in the first 60 min between the two genotypes (Fig 4.7B). The peak concentration (C_{max}) of metformin in female Oct3^{-/-} mice increased by 67% and $\text{AUC}_{0-60 \text{ min}}$ increased by 41% (Table 4.1). Similar pharmacokinetic changes were also observed in male Oct3^{-/-} mice (Fig. 4.8 and Table 4.2). These data suggest

that Oct3 influences metformin disposition *in vivo* and has a significant impact on metformin plasma levels in the early exposure phase following drug administration.

4.3.5. Depleted metformin accumulation in salivary glands of Oct3^{-/-} mice

We next examined metformin concentrations in salivary glands of Oct3^{+/+} and Oct3^{-/-} mice. Because rodent salivary glands exhibit significant sexual dimorphism (Pinkstaff, 1998), metformin concentration was measured in two separate cohorts of male and female adult animals. Metformin concentrations were much lower in salivary glands of Oct3^{-/-} mice in both females and males at all time-points between 15-480 min (Fig. 4.9). At 60 min post dosing, average metformin concentration in the salivary glands of Oct3^{-/-} mice was only one sixth of that in wild type mice. Compared to Oct3^{+/+} mice, tissue metformin exposure (AUC_{0-480 min}) in salivary glands showed 65% and 54% reduction in female and male Oct3^{-/-} mice, respectively (Table 4.3). These data suggest that Oct3 actively transports metformin from blood into salivary glands. The concentrative nature of this process is evident when metformin concentrations were compared between salivary glands and plasma. In wild type mice, metformin tissue concentrations in salivary glands peaked around 60-90 min and then started to decline after 120 min. However, salivary gland metformin concentrations (ng/g tissue) in both male and female mice were consistently higher (2-4 fold) than its corresponding plasma concentrations (ng/mL) after 30 min (Fig. 4.10A), suggesting an active, uphill transport process from the blood into the salivary gland epithelial cell. The intracellular metformin concentrations could be even greater after adjusting to cytosolic volume or tissue water contents which typically range between 67-73% in mouse salivary glands (Menghi et al., 1989). In contrast, this concentrative transport

process is abolished in Oct3^{-/-} mice as metformin salivary gland concentrations rarely exceeded its plasma concentrations in the knockout mice (Fig. 4.10B).

In addition to salivary glands, Oct3^{-/-} mice also exhibited altered metformin exposure in several other tissues (Table 4.3). Consistent with a significant expression of Oct3 in the heart (Fig. 4.2), metformin AUC_{0-480 min} in this tissue was reduced by 34-35% ($p < 0.05$) in both male and female Oct3^{-/-} mice (Table 4.3). Male and female Oct3^{-/-} mice also showed 34% (not significant; N.S.) and 10% (N.S.) reduction in metformin exposure in skeletal muscle, respectively. Unexpectedly, liver metformin exposure increased by 36% ($p < 0.05$) and 12% (N.S.) in male and female Oct3^{-/-} mice, respectively. No significant change in metformin AUC_{0-480 min} was observed in the kidney. Tissue exposure in the gastrointestinal track could not be accurately measured due to significant contamination of unabsorbed metformin that remained in the intestinal lumen.

4.4. Discussion

Patients receiving medications frequently report a variety of drug-induced adverse effects including taste disturbance. In most cases there is limited mechanistic information regarding drug-induced taste disturbance. In order to minimize or prevent this problem, it is important to identify the underlying molecular mechanisms leading to this adverse effect. In this Chapter, we uncovered a novel molecular mechanism leading to taste disturbance of metformin. We also demonstrated the *in vivo* roles of OCT3 in tissue distribution of metformin.

Metformin, a first-line oral therapy for the treatment of type 2 diabetes, has several common side effects that include gastrointestinal upset and taste disturbance (Melchior and Jaber, 1996; Zolk, 2012). This drug is also known to highly accumulate in various tissues including liver, kidney, small intestine and salivary glands (Hundal and Inzucchi, 2003; Scheen, 1996; Wilcock and Bailey, 1994). In addition, there are large variations in interpatient pharmacokinetics and response to metformin.

Metformin, a polar soluble biguanide, is a substrate of multiple polyspecific organic cation transporters. Our study and others demonstrated that metformin can be transported by OCT3 (Chen et al., 2010; Nies et al., 2009). OCT3 is known to be expressed in various tissues including placenta, skeletal muscle, kidney, liver, heart, lung, and brain. In our study, we found high expression of OCT3/Oct3 in human and mouse salivary glands in both mRNA and protein levels. Using LC-MS/MS method, our group quantified the absolute OCT3 protein expression in the human salivary glands and estimated its catalytic efficiency. OCT3 protein expression in the human submandibular glands was 1.53 fmol/ μ g membrane protein. In agreement with the OCT3 expression data in salivary glands, there was markedly reduced metformin accumulation in salivary glands in both female and male Oct3^{-/-} mice. Our immunolocalization data in human submandibular glands suggest that OCT3 is expressed at both apical and basolateral membranes of salivary gland epithelial cells. This localization would suggest that driven by the inside-negative membrane potential, OCT3 on the basolateral membrane actively concentrates metformin from the blood into the salivary gland epithelial cells, resulting in high accumulation of metformin in the salivary glands. However, once metformin is highly concentrated inside the cells, due to the bi-directional nature of OCT3, a fraction of metformin inside the salivary gland

cells can be further effluxed into the saliva by apically localized OCT3, leading to metformin's presence in the saliva fluid and its taste disturbance.

In addition to salivary glands, Oct3^{-/-} mice also exhibited altered metformin exposure in several other tissues. Consistent with a significant expression of Oct3 in the heart, the AUCs of metformin was reduced in both female and male Oct3^{-/-} mice. Similarly, in a previous study Oct3^{-/-} mice showed decreased MPP⁺ uptake in the heart when mice were given MPP⁺ intravenously (Zwart et al., 2001b). Another tissue that showed altered metformin exposure was skeletal muscle. Both male and female Oct3^{-/-} mouse skeletal muscle showed reduction in its AUCs although statistical difference was not significant. While metformin exerts its pharmacological effect primarily in the liver, other peripheral tissues including the skeletal muscle are also known as secondary sites of action. Chen et al. reported that the cells expressing *OCT3* genetic variants showed decreased uptake activity and inhibition of OCT3 resulted in reduced phosphorylation of AMP-activated protein kinase (AMPK) in the skeletal muscle cells treated with metformin (Chen et al., 2010). Thus, altered metformin exposure in skeletal muscle in the absence of OCT3 or by *OCT3* genetic polymorphisms may affect metformin response. Collectively, our data suggest that OCT3/Oct3 is an important determinant of metformin uptake into peripheral tissues.

Oct3^{-/-} mice also exhibited altered plasma kinetics of metformin. Although the overall exposure of metformin did not change, peak concentration (C_{\max}) and early exposure ($AUC_{0-60\text{ min}}$) to metformin significantly increased in Oct3^{-/-} mice greater in Oct3^{-/-} mice in early time points. This finding may be clinically relevant if altered peak concentration and time to peak concentration affect the onset of metformin action. The change in plasma kinetics in early time

points could be due to change in tissue distribution or/and intestinal absorption. In our study, Oct3^{-/-} mice showed reduced metformin exposures in various tissues. Most distinctively, we found significant decrease in salivary concentration in Oct3^{-/-} mice. Like liver, kidney and small intestine, the salivary glands may serve as a deep compartment, and a change in distribution in these peripheral tissues may affect volume of distribution and alter the plasma pharmacokinetic profiles. Another possible explanation for the observed change in early plasma kinetic could be due to a change in rate of absorption of metformin. In our study, tissue exposure in the gastrointestinal track could not be accurately measured due to significant contamination of unabsorbed metformin that remained in the intestinal lumen. Further study will be necessary in order to elucidate whether Oct3 plays a role in intestinal absorption of metformin.

In summary, we demonstrated that OCT3 mediates metformin accumulation in salivary gland and is an important determinant of peripheral metformin uptake and distribution. Together, our studies identified a novel molecular mechanism underlying drug-induced taste disturbance and provided an additional genetic factor that may contribute to variable disposition and response to metformin.

Table 4.1. Metformin pharmacokinetic parameters from female Oct3^{+/+} and Oct3^{-/-} mice.

Parameters	Oct3 ^{+/+}	Oct3 ^{-/-}	% change	<i>p</i> -value
C _{max} (µg/ml)	2.70 ± 0.79	4.51 ± 0.99	67%↑	<0.05
AUC _{0-1hr} (µg/ml*min)	135.85 (118.79, 155.07)	190.95 (169.60, 210.87)	41%↑	<0.05
AUC _{0-8hr} (µg/ml*min)	545.75 (475.08, 598.84)	553.36 (494.17, 601.66)	--	N.S.
CL/F (ml/min/kg) ^a	27.49 (25.05, 31.57)	27.11 (24.93, 30.35)	--	N.S.
Terminal t _{1/2} (min)	164.20 (125.60, 283.68)	113.01 (89.39, 141.53)	--	N.S.
V/F (L/kg) ^b	6.51 (4.83, 11.04)	4.42 (3.45, 5.94)	--	N.S.

Data are presented as mean ± SD (C_{max}) or with 95 % confidence interval in the parenthesis. AUC, area under the plasma concentration-time curve of metformin. ^a CL/F value was calculated using Dose/AUC₀₋

_{8hr}. ^b V/F is terminal volume of distribution. N.S., not significant.

Table 4.2. Metformin pharmacokinetic parameters from male Oct3^{+/+} and Oct3^{-/-} mice.

Parameters	Oct3 ^{+/+}	Oct3 ^{-/-}	% change	<i>p</i> -value
C _{max} (μg/ml)	2.63 ± 1.33	4.23 ± 0.26	61%↑	<0.05
AUC _{0-1hr} (μg/ml*min)	139.00 (124.56, 154.19)	167.03 (145.08, 181.08)	20%↑	<0.05
AUC _{0-8hr} (μg/ml*min)	529.28 (383.84, 569.16)	432.82 (373.18, 494.66)	--	N.S.
CL/F (ml/min/kg) ^a	28.34 (26.35, 39.08)	34.66 (30.32, 47.36)	--	N.S.
Terminal t _{1/2} (min)	143.10 (114.85, 182.54)	98.10 (71.21, 124.47)	--	<0.05
V/F (L/kg) ^b	5.85 (4.68, 8.06)	4.91 (3.71, 6.19)	--	N.S.

Data are presented as mean ± SD (C_{max}) or with 95% confidence interval in the parenthesis. AUC, area under the curve of plasma concentration-time of metformin. ^a CL/F value was calculated using

Dose/AUC_{0-8hr}. ^b V/F is terminal volume of distribution. N.S., not significant.

Table 4.3. Tissue AUC_{0-8hr} from female and male Oct3^{+/+} and Oct3^{-/-} mice.

Tissues	Gender	Oct3 ^{+/+}	Oct3 ^{-/-}	% change	<i>p</i> -value
Salivary gland	Female	1881.35 (1671.53, 2087.20)	677.26 (593.44, 756.54)	↓64	<0.05
	Male	1374.89 (921.00, 1508.84)	629.85 (422.01, 772.24)	↓54	<0.05
Heart	Female	389.13 (350.61, 426.09)	261.74 (228.65, 291.36)	↓33	<0.05
	Male	316.74 (226.53, 339.99)	208.14 (170.51, 260.11)	↓34	<0.05
Skeletal muscle	Female	318.20 (268.62, 364.77)	285.70 (234.83, 326.35)	↓10	N.S.
	Male	283.57 (145.55, 317.51)	188.20 (121.76, 223.48)	↓34	N.S.
Liver	Female	995.05 (849.49, 1123.01)	1110.75 (982.70, 1241.99)	--	N.S.
	Male	912.40 (730.20, 1028.80)	1242.41 (1044.62, 1411.73)	↑36	<0.05
Kidney	Female	1938.48 (1724.90, 2143.43)	1761.07 (1486.04, 2076.49)	--	N.S.
	Male	1770.01 (1215.02, 1994.06)	1722.93 (1417.29, 2015.32)	--	N.S.

Data are presented mean with 95% confidence interval in the parenthesis. The units of AUCs is µg/g*min.

N.S., not significant.

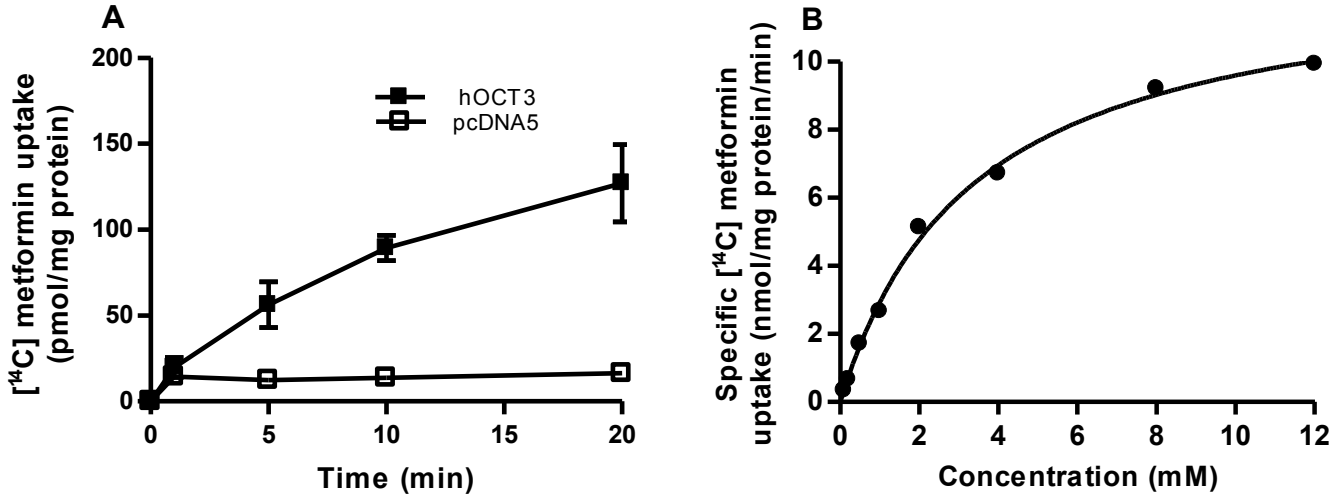


Figure 4.1. Metformin transport kinetics in human OCT3-expressing HEK cells. The uptake experiments were carried in hOCT3 or pcDNA transfected cells at 10 μ M of metformin in a time-dependent manner (A). The kinetic experiments were performed with various concentrations for 4-5 minutes and the specific uptake was calculated by subtracting the transport activity in control cells (B). Using Michaelis-Menten equation, the kinetic parameters of K_m and V_{max} were respectively determined as 3.67 ± 0.25 mM and 43.37 ± 4.14 pmol/ μ g membrane protein/min.

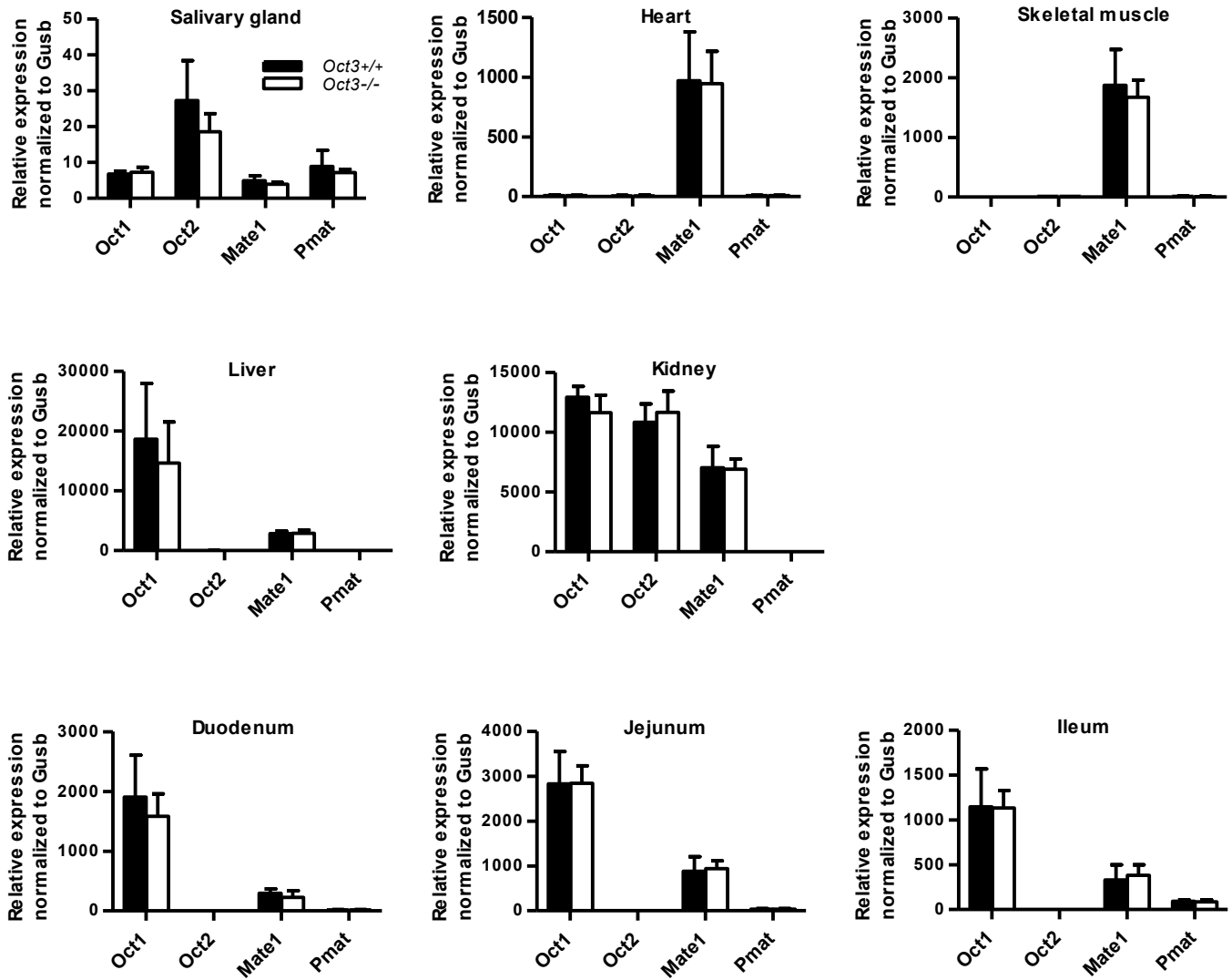


Figure 4.2. Expression of polyspecific organic cation transporters in various tissues of *Oct3*^{+/+} (solid bar) and *Oct3*^{-/-} (open bar) mice. Total RNA of eight tissues, including salivary gland, heart, skeletal muscle, liver, kidney, duodenum, jejunum, and ileum, were isolated from female *Oct3*^{+/+} and *Oct3*^{-/-} mice (n=4 per group), and reverse transcribed to cDNA. mRNA expressions of Oct1, Oct2, Mate1, and Pmat were determined using real-time PCR and normalized by Gusb.

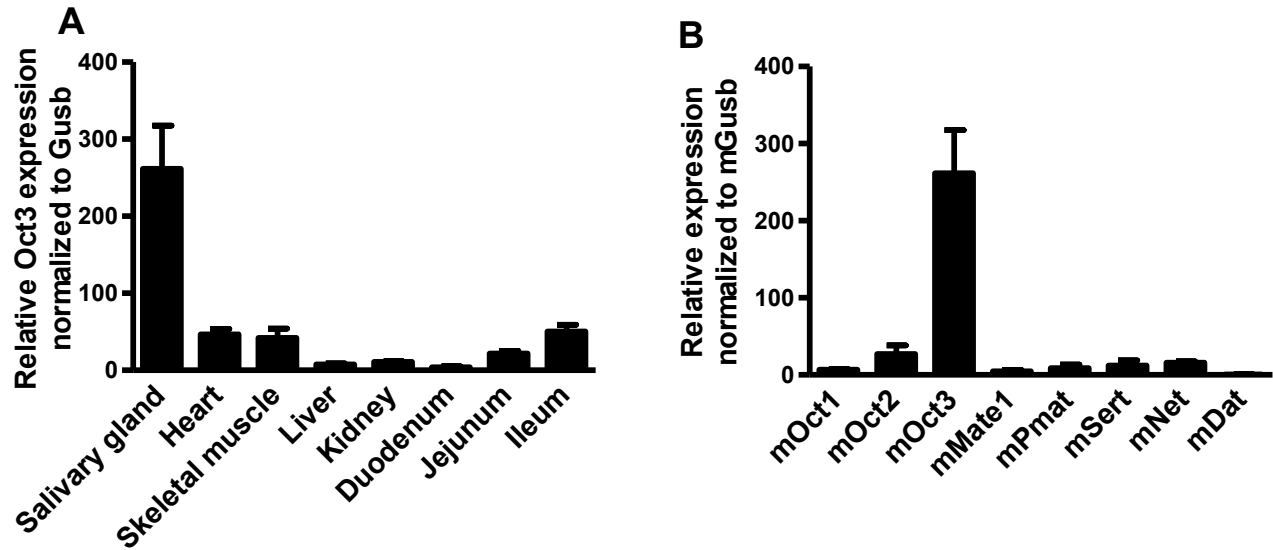


Figure 4.3. Oct3 mRNA expression in various mouse tissues (A) and mRNA expression of various transporters in mouse salivary glands (B). Using real-time PCR, mRNA expression of Oct3 was examined in various tissues of female Oct3^{+/+} mice (n=4). Then, mRNA expressions of Oct1-3, Mate1, Pmat, Sert, Net and Dat were measured in mouse salivary glands.

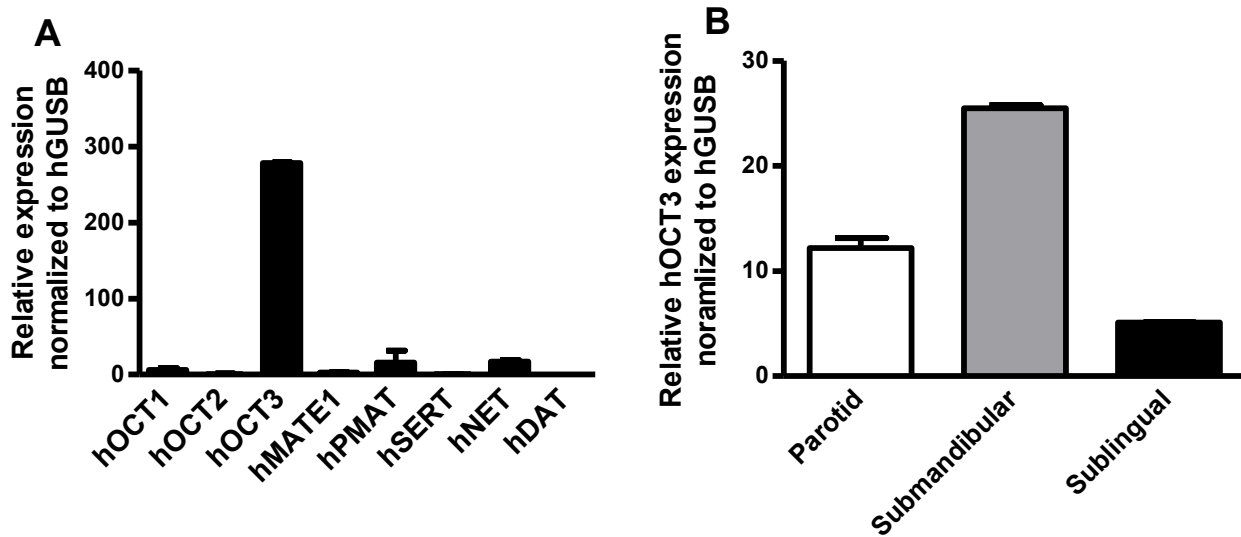


Figure 4.4. mRNA expression of various transporters in human salivary glands (A) and OCT3 mRNA expression in three human salivary gland regions (B). In (A), mRNA expressions of OCT1-3, MATE1, PMAT, SERT, NET and DAT were determined in pooled (n=24) human salivary glands using real-time PCR. In (B), mRNA expression of OCT3 was examined in parotid, submandibular, and sublingual glands obtained from a single donor.

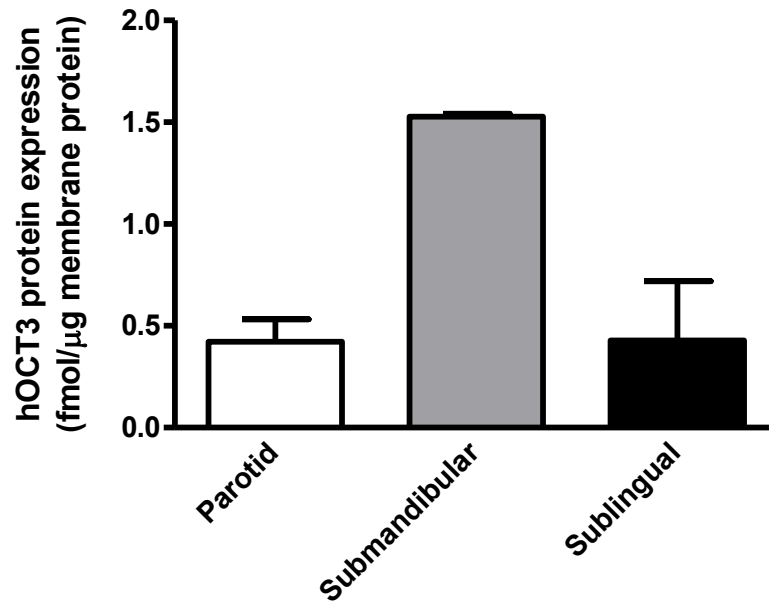


Figure 4.5. Protein expression of OCT3 in three human salivary glands regions. Using LC-MS/MS method, absolute protein expression of OCT3 was quantified in parotid, submandibular, and sublingual glands from a single donor. The protein levels were determined to be 0.42 ± 0.11 , 1.53 ± 0.015 and 0.43 ± 0.29 fmol per μg total membrane protein in parotid, submandibular and sublingual glands respectively.

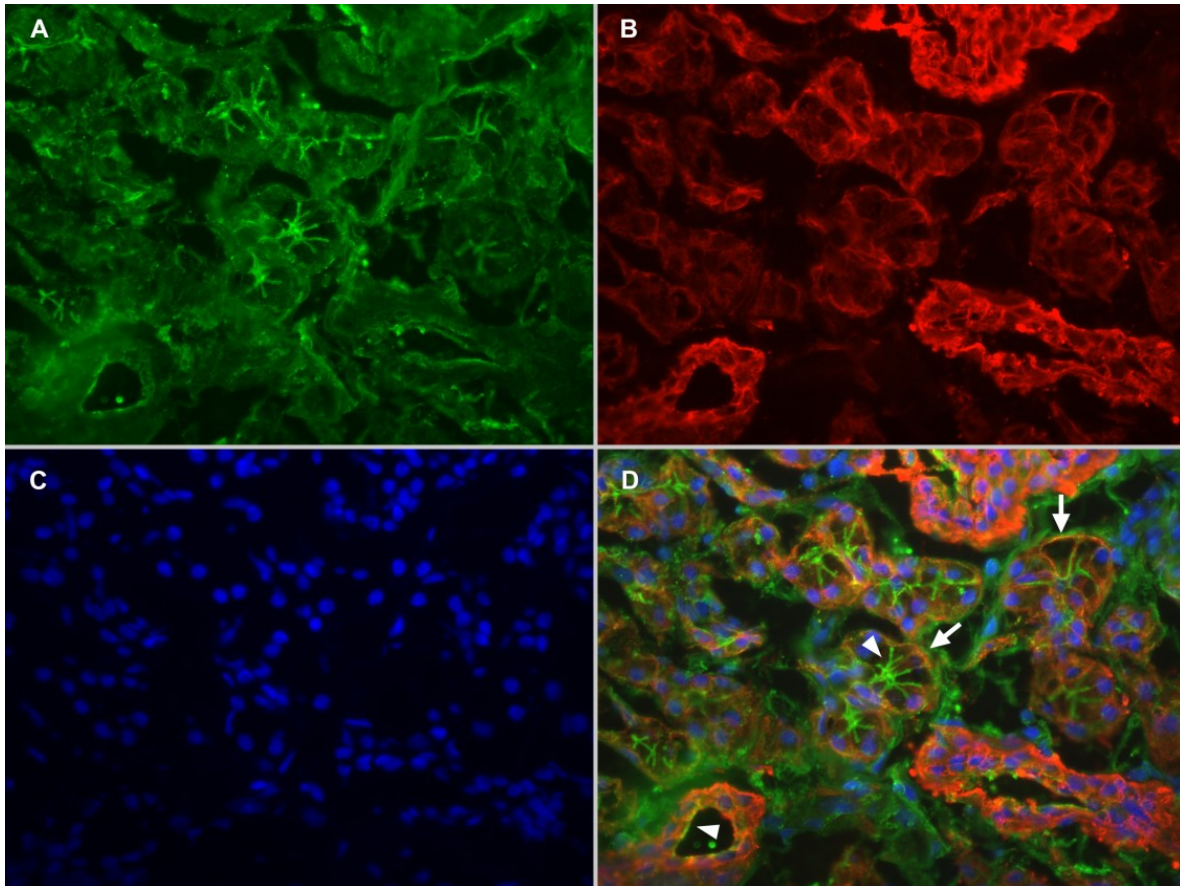


Figure 4.6. Dual-color immunofluorescence staining in human submandibular glands.

Human submandibular glands sections were co-labeled with OCT3 shown in green (A) and a basolateral membrane marker, Na⁺/K⁺-ATPase shown in red (B). The nuclei are shown in blue (C). In a merged image (D), arrows and arrow heads respectively indicate the basolateral membrane and apical membrane of epithelial cells.

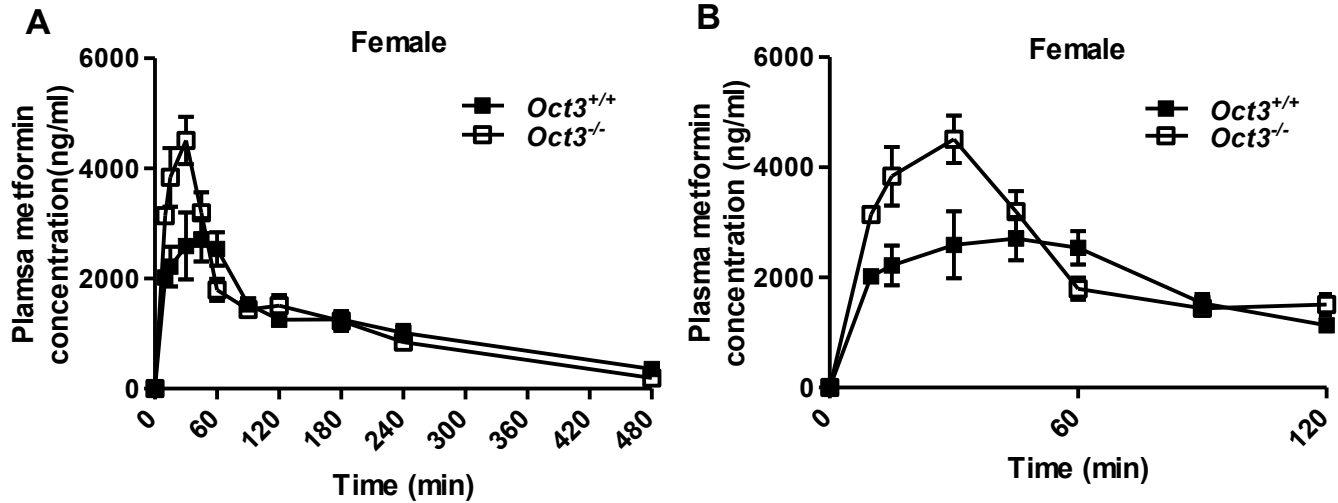


Figure 4.7. Metformin plasma kinetics in female *Oct3*^{+/+} and *Oct3*^{-/-} mice. Female mice (n = 3-5 per group at each time point) were given an oral dose of 15 mg/kg containing 0.2 mCi/kg of [¹⁴C] metformin, and the plasma concentrations of metformin were measured from 0 to 8 hours (A) or 0 to 2 hours (B) after metformin treatment. The radioactivity in plasma was determined by scintillation counting and converted to mass amounts. Data represent mean \pm SE.

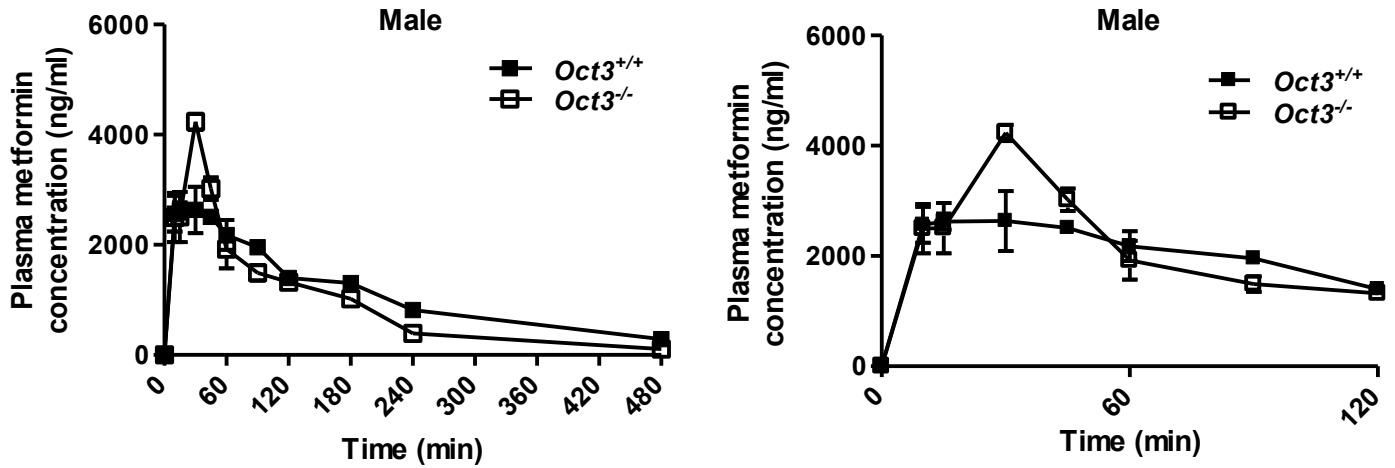


Figure 4.8. Metformin plasma kinetics in male *Oct3*^{+/+} and *Oct3*^{-/-} mice. Male mice (n = 3-5 per group at each time point) were given an oral dose of 15 mg/kg containing 0.2 mCi/kg of [¹⁴C] metformin, and the plasma concentrations of metformin were measured from 0 to 8 hours (A) or 0 to 2 hours (B) after metformin treatment. The radioactivity in plasma was determined by scintillation counting and converted to mass amounts. Data represent mean \pm SE.

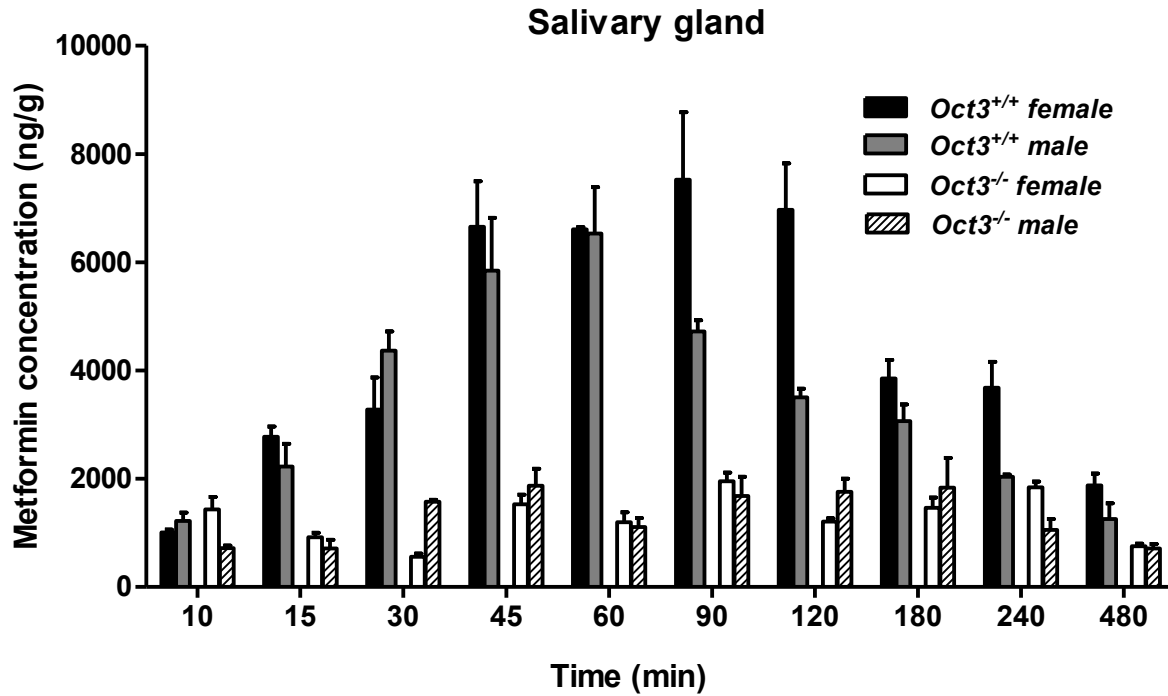


Figure 4.9. Accumulation of metformin in salivary glands of female and male *Oct3*^{+/+} and *Oct3*^{-/-} mice. Female and male mice (n = 3-5 per group at each time point) were given an oral dose of 15 mg/kg containing 0.2 mCi/kg of [¹⁴C] metformin. At each time point, salivary glands were collected and the metformin concentrations were measured. The radioactivity in plasma was determined by scintillation counting and converted to mass amounts. Data represent mean \pm SE.

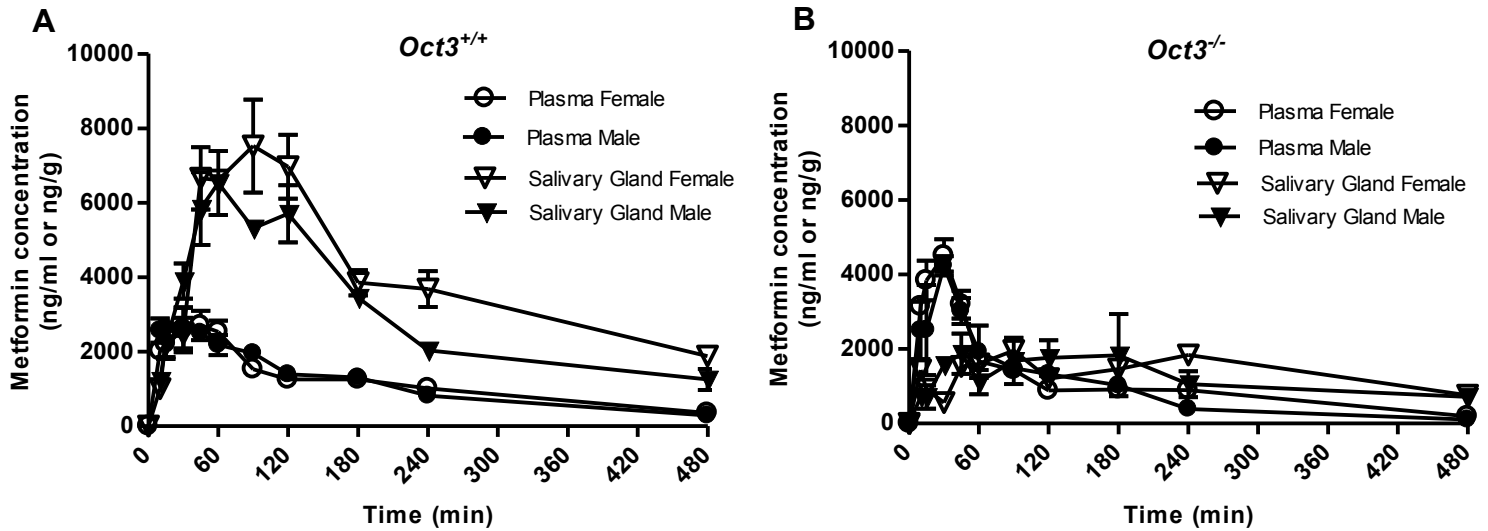


Figure 4.10. Plasma and salivary glands metformin concentration in female and male *Oct3*^{+/+} (A) and *Oct3*^{-/-} (B) mice. Female and male mice (n = 3-5 per group at each time point) were given an oral dose of 15 mg/kg containing 0.2 mCi/kg of [¹⁴C] metformin. Metformin concentrations in plasma and salivary glands were measured from 0-8 hours. The radioactivity in plasma was determined by scintillation counting and converted to mass amounts. Data represent mean \pm SE.

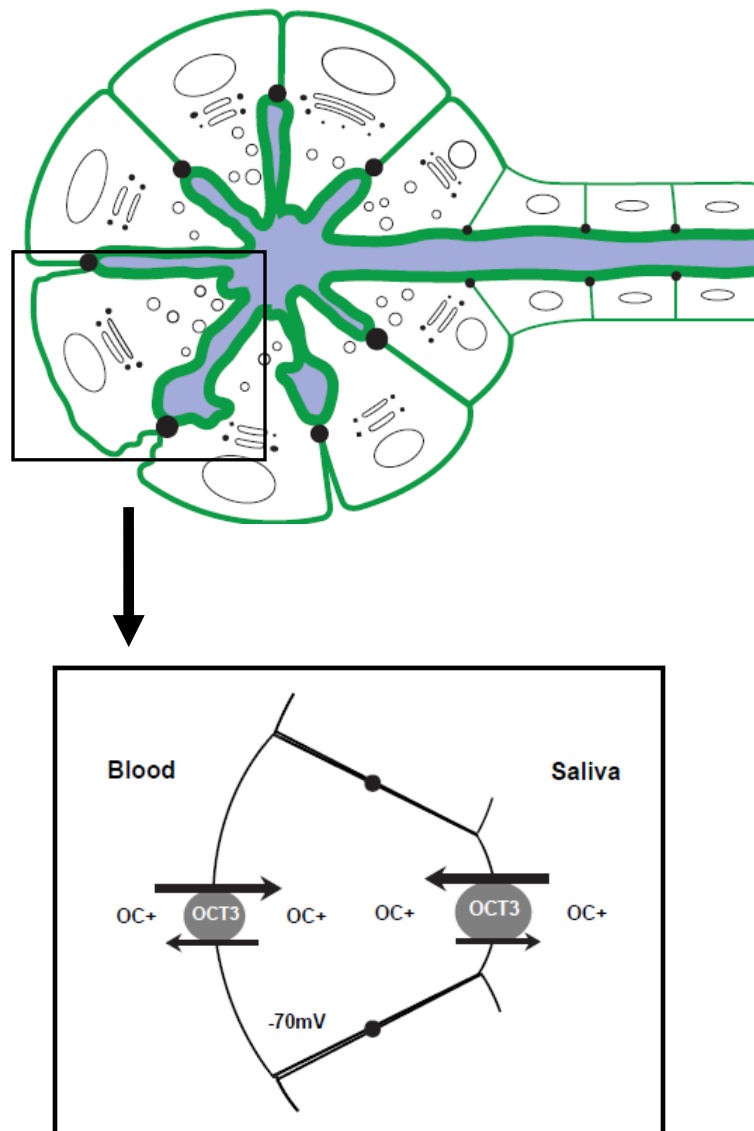


Figure 4.11. Proposed model for OCT3-mediated organic cation transport in salivary gland epithelial cells. OCT3 on the basolateral membrane of epithelial cells mediates metformin uptake from the blood into the cells. Once metformin is highly concentrated inside the cells, OCT3 on the apical membrane facilitates excretion of metformin into the saliva.

Chapter 5. Organic cation transporter 3 facilitates fetal disposition of metformin during pregnancy

5.1. Introduction

The biguanide derivative, metformin is an oral hypoglycemic drug widely used in the treatment of type 2 diabetes (Hundal and Inzucchi, 2003). Metformin has recently been used to treat polycystic ovary syndrome (PCOS) and gestational diabetes mellitus (GDM) in pregnant women (Lord et al., 2003; Wensel, 2009). Oral antihyperglycemic agents such as glyburide and metformin have been recently considered alternative therapy for insulin in achievement of glycemic control in the pregnant diabetic population. However, there are challenges in the safe and effective use of these agents in pregnant women due to the large variability in response and pharmacokinetic changes of drugs. Furthermore, fetal drug exposure during pregnancy needs to be considered as it may have harmful effects to the developing fetus.

Previous clinical studies have shown that metformin concentrations at the time of delivery in umbilical cord plasma can be as high as maternal concentrations, suggesting that metformin crosses the placental barrier and is transferred to the fetal compartment (Charles et al., 2006; Eyal et al., 2010; Vanky et al., 2005). Insulin is known to be an important factor for fetal growth during pregnancy. Metformin can increase insulin sensitivity and it is unclear how this can affect the fetal growth and development. In addition, long-term outcome and complications following in utero exposure to metformin remain to be evaluated.

Metformin, which is polar and positively charged at physiological pH, has very low passive membrane permeability and requires carrier-mediated transport to penetrate the cell membrane. Metformin is a known substrate for multiple polyspecific organic cation transporters

including the organic cation transporters (OCT)1-3, and multi-drug and toxin extrusion transporter (MATE)1-2 (Kimura et al., 2005; Masuda et al., 2006; Tanihara et al., 2007). The drug is predominantly eliminated by the kidney with negligible hepatic metabolism and exerts its pharmacological effect mainly in the liver (Hundal and Inzucchi, 2003). OCT2 and MATE1/2 play an important role in secretion of metformin in the kidney because OCT2 mediates metformin uptake from the blood to the kidney cells and MATE1/2 complete the excretion process by effluxing the drug from the renal cells into the urine. OCT1, which mediates hepatic uptake of metformin has a direct influence on metformin's glucose lowering effect (Shu et al., 2008; Shu et al., 2007; Wang et al., 2002). In recent studies, MATE1/2 are also shown to be important determinants of metformin response (Choi et al., 2011; Stocker et al., 2013).

OCT3, a third member of SLC22A family, is a bi-directional transporter and displays substrate specificity similar to OCT1 and OCT2 (Wu et al., 2000). OCT3 is broadly expressed in various tissues including placenta (Wu et al., 2000). Among all known organic cation transporters, OCT3 is the one most highly expressed in human placenta (Lee et al., 2013). However, the role of OCT3 in metformin fetal disposition is unknown. In an ex vivo perfusion study, metformin was shown to freely cross the human placenta through a carrier-mediated pathway (Kovo et al., 2008). When pregnant Oct3 knockout mice were administered intravenously with MPP⁺, a model substrate for Oct1-3, there was a decrease in MPP⁺ concentration in the fetus, suggesting a possible involvement of Oct3 in transport of organic cations at the maternal-fetal interface (Zwart et al., 2001a). Yet, the role of OCT3 in metformin disposition across the placental barrier has not been established.

In this Chapter, to investigate the molecular and cellular mechanism of metformin transport at the placental barrier, we first determined the membrane localization of OCT3 in

human term placenta using immunofluorescence labeling. This work was followed by a pharmacokinetic study in pregnant Oct3^{+/+} and Oct3^{-/-} mice to assess the *in vivo* significance of Oct3 in the fetal disposition of metformin.

5.2. Materials and methods

5.2.1. Animals and tissue harvest

For gene expression profiling, adult (8-10 weeks of age) wild-type FVB mice were purchased from Taconic. Oct3^{+/+} and Oct3^{-/-} mice, originally generated by Dr. Denise Barlow at the University of Vienna and back-crossed to FVB strain (Zwart et al., 2001a). This mouse strain was maintained by Dr. Alfred Schinkel of the Netherlands Cancer Institute and generously provided to us by Dr. John Markowitz from the University of Florida. These mice were housed in the specific pathogen free (SPF) facility at University of Washington. The animal studies were approved by the Institutional Animal Care and Use committee (IACUC) at the University of Washington. To obtain pregnant mice at gestational day (gd) 19 (term in mice is ~20-21 days), timed mating was carried out. The date that a vaginal plug was observed was assigned as gestational day 1. For placental tissue collection, wild type FVB pregnant mice at gd 19 were sacrificed using CO₂, and the placentas were immediately collected and flash-frozen in liquid N₂. Tissues were stored at -80°C until use.

5.2.2. Human placenta source

The use of biological specimen was approved by the Institutional Review Board at the University of Washington. Six human term placentas were obtained at the University of Washington medical center Labor and Delivery Unit. All placenta tissues were from healthy

uncomplicated pregnancies. Placenta tissue was processed within 60-90 min after delivery. The umbilical cords and large vessels were removed and the placenta was rinsed with ice cold phosphate buffered saline (PBS) 1-2 times. The parenchyma of placenta was cut to a large piece of about 100-150 g (10 cm x 5 cm). The cut tissue was immediately wrapped with the aluminum foil and was immersed in the liquid nitrogen. The tissue was stored at -80°C until use.

5.2.3. Immunolocalization studies in human placenta

Snap-frozen human term placentas underwent frozen section by the Pathology Research Services at the University of Washington. The human term placenta sections were fixed in ice cold acetone for 5 min and immersed in PBS for 5 min. The sections were blocked in PBS containing 5% goat serum for 45 min at room temperature. Then, the sections were incubated overnight at 4°C with polyclonal rabbit anti-OCT3 (1:125) (Genway), co-labeled with either anti-human CD31-PECAM1 (1:50) (R&D Systems), anti-human laminin (1:1000) (Sigma), or anti-human CD71 (transferrin receptor) (1:200) (Abbiotec). After antibody incubation, the sections were washed with PBS, and florescent secondary antibodies Alexa 488 and Alexa 568 (1:500) were applied for 1 hr at room temperature. After washing with PBS, ProLong Gold antifade medium with DAPI was mounted on the slides and cover-slipped. The fluorescence images were obtained with a Zeiss Axiovert 200 fluorescence microscope.

5.2.4. Expression of organic cation transporters and monoamine transporters in mouse placenta

Total RNA was extracted from Oct3^{+/+} and Oct3^{-/-} mouse placentas using Trizol reagent (Invitrogen, Inc) or Qiagen Mini RNeasy Kit according to the manufacturer's instructions. RNA

integrity and purity were verified by gel electrophoresis and UV spectrophotometry. Total RNA (2 µg) was reverse transcribed to first-strand cDNA using Superscript III reverse transcriptase (Invitrogen) according to the manufacturer's instructions. Taqman real-time PCR reagents, assay primers and probes for mouse Oct1-3 (Slc22a1-3), mMate1-2 (Slc47a1-2), mPmat (Slc29a4), mSert (Slc6a4), mNet (Slc6a2), and mDat (Slc6a3), and mGusb were purchased from Applied Biosystems (Foster City, CA). Taqman real-time PCR assays were carried out according to the manufacturer's protocols on an Applied Biosystems 7900HT fast real-time PCR system as described previously (Duan and Wang, 2010). The real-time reaction contained 10 µl of 2X TaqMan Universal PCR Master Mix (Applied Biosystems), 5 µl of RNA-equivalent cDNA (100 ng), and 1 µl of 20x primer/probe mix in a final volume of 20 µl. Each sample was analyzed in duplicate or triplicate. To quantify the transcript expression levels of genes of interest, comparative CT method was used (Zhang et al., 2008). The mRNA levels of each test gene was normalized to either hGUSB or mGusb, according to the following formula: CT (test gene) - CT (house keeping genes) = Δ CT. Thereafter, the relative mRNA levels of each gene was calculated using the $\Delta\Delta$ CT method: Δ CT (test gene) - Δ CT (test gene in the calibrator) = $\Delta\Delta$ CT (test gene). The fold changes of mRNA levels were represented as a relative expression $2^{-\Delta\Delta CT}$.

5.2.5. *In vivo* study

Pregnant Oct3^{+/+} and Oct3^{-/-} mice at gd 19 were fasted for 5-10 hours and administered 15 mg/kg metformin containing 0.2 mCi/kg of [¹⁴C] labeled metformin by oral gavage. At 15, 30, 45, 60, 120, 180, 240, and 480 min, animals were euthanized by CO₂. The blood samples were collected in heparinized microhematocrit capillary tubes (Fisher) by cardiac puncture and

plasma was separated by centrifugation for 1 minute at 5000 x g. Fetus, placenta and other tissues (heart, skeletal muscle, salivary gland, liver, and kidney) were collected at each time point. The metformin concentrations in the plasma and tissues were determined by scintillation counting using the method described by Wilcock et al. with minor modification (Wilcock et al., 1994). In brief, plasma and tissues were placed in scintillation vials with 1 mL 1M NaOH and incubated at 55~70 °C for 1~2 hours. After cooling, H₂O₂ was added to decolorize the samples. After several hours, 15 mL of Eco-scintillation buffer was added first, and then 1 mL 1 M HCL was added to neutralize the solutions. The samples were stored overnight before counting. The amounts of radioactivity were expressed as ng/g tissue for tissues and ng/ml for plasma. For each time point, 3-5 mice were used and a total of 26 mice were used for each genotype group.

5.2.6. Pharmacokinetic data analysis

For one point sampling data (one blood sample from each mouse), we used a bootstrap method to obtain confidence intervals for pharmacokinetic parameter estimates of maternal plasma and fetal tissue. Area under the curve (AUC), oral clearance (CL/F), terminal half-life ($t_{1/2, \beta}$), volume of distribution at terminal phase (V_{β}), area under the moment curve (AUMC), and mean residence time (MRT) were calculated using the following equations,

$$AUC_{0-t} = \int_0^t C(t) dt$$

$$AUC_{0-\infty} = AUC_{0-t} + \frac{C(T)}{\beta}$$

$$\frac{CL}{F} = \frac{Dose}{AUC_{0-\infty}}$$

$$t_{\frac{1}{2},\beta} = \frac{\ln 2}{\beta}$$

$$V_{\beta} = \frac{CL}{F \cdot \beta}$$

$$AUMC_{0-t} = \int_0^t C(t) \cdot t \, dt$$

$$AUMC_{0-\infty} = AUMC_{0-t} + \frac{C(T)}{\beta^2} + \frac{C(T)}{\beta} \cdot T$$

$$MRT = \frac{AUMC}{AUC}$$

Terminal slope (β) was calculated by performing a linear regression of concentrations at the last three to five time points. T indicates last time point (i.e. 480 min), and C(T) is the concentration at the last time point. The 95% confidence intervals for PK parameters were generated using the bootstrap method as described by Mager and Göller (Mager and Göller, 1998) with modification. Briefly, plasma or tissue concentrations were resampled with random replacement of 26 mice. This resampling with random replacement was performed using the R program developed by Jason Liang in the Department of Biostatistics at the University of Washington. The resampling was repeated 10,000 times to create 10,000 pseudo concentration-time profiles. For each profile, the concentrations at each nominal time point were averaged and the PK parameters were calculated using the equations defined above. The 95 % confidence intervals for each parameter were calculated by taking the 2.5% and 97.5% quantiles, i.e. the 251th and 97501th AUC values of 10,000 bootstrap AUC values.

5.3. Results

5.3.1. Localization of OCT3 in human term placenta. To identify the membrane localization of OCT3 in human placenta, frozen sections of human term placentas were prepared and stained with anti-OCT3 together with cellular membrane markers for endothelium, basolateral and apical membranes. CD31-PECAM1 is known to be expressed in fetal vascular endothelium, and laminin is expressed in the basal membrane of syncytiotrophoblast and fetal vascular endothelium (Figure 5.1C and G). The transferrin receptor is localized to the apical membrane of syncytiotrophoblast (Figure 5.1K). When the sections were co-labeled with an OCT3 antibody, co-localization was observed at the fetal vascular endothelium and basal membrane of syncytiotrophoblast (Figure 5.1D and H). On the other hand, OCT3 did not co-localize with the transferrin receptor (Figure 5.1L). These data suggest that OCT3 is localized to the basal membrane of placental epithelial cells and is also expressed in fetal vascular endothelium.

5.3.2. Expression of polyspecific organic cation transporters and monoamine transporters in placenta of pregnant Oct3^{+/+} and Oct3^{-/-} mice

Before carrying out *in vivo* study, mRNA expression of various organic cation and monoamine transporters was measured in the placentas of pregnant Oct3^{+/+} and Oct3^{-/-} mice at gd 19. Consistent with our previous findings (Lee et al., 2013), wild type mice showed predominant placental expression of Oct3 with lower or minimal expression of other organic cation and monoamine transporters. When the placental expressions of other transporters including Oct1-2, Mate1-2, Pmat, Set and Dat were compared between Oct3^{+/+} and Oct3^{-/-} mice, placental expression was not significantly different between the Oct3^{+/+} and Oct3^{-/-} genotype, suggesting

that there is no compensatory change in the expression of other organic cation transporters and monoamine transporters in the placenta of the knockout mice (Figure 5.2).

5.3.3. Maternal plasma kinetics of metformin in Oct3^{+/+} and Oct3^{-/-} mice

To determine the role of OCT3 in metformin disposition at the maternal-fetal interface, pregnant Oct3^{+/+} and Oct3^{-/-} mice were administered [¹⁴C] labeled metformin by oral gavage, and maternal and fetal concentrations of metformin were measured at various time points. Consistent with our previous findings from *in vivo* study (Chapter 4), the pregnant Oct3^{-/-} mice exhibited higher peak concentration (C_{\max}) and early exposure (0-1hr). The overall AUC ($AUC_{0-480\text{min}}$) was slightly lower in the pregnant Oct3^{-/-} mice as compared to the pregnant Oct3^{+/+} mice (Figure 5.3 and Table 5.1). Other PK parameters including CL/F, terminal half life, V_{β} , AUMC, and MRT were also estimated. Most of estimates of these parameters were comparable between pregnant Oct3^{+/+} and Oct3^{-/-} mice with exception for AUMC, which was found to be higher in the pregnant Oct3^{+/+} mice (Table 5.1).

5.3.4. Fetal exposure to metformin in Oct3^{+/+} and Oct3^{-/-} mice

Fetal concentrations of metformin in Oct3^{-/-} mice were lower than those in Oct3^{+/+} mice throughout the time course (Figure 5.4). At 2 and 3 hour time points, fetal concentrations from Oct3^{-/-} mice were about 2 fold lower than those from Oct3^{+/+} mice. Fetal metformin $AUC_{0-480\text{ min}}$ in the Oct3^{-/-} mice decreased by about 40% as compared with that in the Oct3^{+/+} mice. When fetal AUC was extrapolated to infinity, there was about 47% reduction in fetal $AUC_{0-\infty}$ in Oct3^{-/-} mice. Even after normalizing to maternal AUCs, Oct3^{-/-} mice still showed a 30% and 44%

decrease in fetal $AUC_{0-480 \text{ min}}$ and $AUC_{0-\infty}$ respectively as compared with $Oct3^{+/+}$ mice (Table 5.2).

5.3.5. Peripheral tissue distribution of metformin in $Oct3^{+/+}$ and $Oct3^{-/-}$ mice

Metformin concentrations in other tissues including placenta, heart, salivary gland, skeletal muscle, liver and kidney were also measured and AUCs ($AUC_{0-480 \text{ min}}$ and $AUC_{0-\infty}$) were calculated. Pregnant $Oct3^{-/-}$ mice showed about a 30% decrease in placental $AUC_{0-480 \text{ min}}$. Consistent with the previous *in vivo* findings from the non-pregnant female or male mice (Chapter 4), pregnant $Oct3^{-/-}$ mice showed a 50% and 70% decrease in $AUC_{0-480 \text{ min}}$ in heart and salivary gland respectively. $AUC_{0-480 \text{ min}}$ in the skeletal muscle and liver did not show significant difference between the two genotypes during pregnancy. However, there was about a 20% decrease in $AUC_{0-480 \text{ min}}$ in the kidney of $Oct3^{-/-}$ mice (Table 5.3). The magnitude of changes in the tissue $AUC_{0-\infty}$ between $Oct3^{+/+}$ and $Oct3^{-/-}$ mice was similar to the changes in tissue $AUC_{0-480 \text{ min}}$.

5.4. Discussion

Metformin, an oral hypoglycemic agent, is recently recognized as an alternative therapy for the treatment of gestational diabetes mellitus. Because there are two lives represented in the pregnant women, distribution of drug to and from the fetus must be evaluated to ensure its safety. Previous clinical reports have shown that umbilical cord concentrations of metformin at the time of delivery were comparable to maternal concentrations, suggesting an involvement of drug transporters in metformin transport at the maternal-fetal interface. Here we hypothesized that OCT3 in the placenta plays an important role in mediating metformin entry into the fetal

compartment, resulting in high concentrations of metformin in the fetal blood circulation during pregnancy.

OCT3 is known to be expressed in various human tissues including placenta (Wu et al., 2000). Consistently, our group found high expression of OCT3 mRNA and protein in human term placentas (Lee et al., 2013). Placental expression of other functionally related transporters, including OCT1, OCT2, MATE1, MATE2 and PMAT, was much lower than for OCT3. A similar expression profile was observed in mouse placenta at gd 19. A recent study suggested a high expression of Oct3 and Mate1 in rat placentas (Ahmadimoghaddam and Staud, 2013). In contrast, we found little expression of MATE1 or Mate1 in human and mouse placentas (Lee et al., 2013). Humans and mice seem to share a similar placental expression profile of organic cation transporters, suggesting that mice may serve as a more relevant animal model to investigate the mechanism of metformin transport at the maternal-fetal interface in humans.

To determine the exact role of OCT3 in metformin transport at the placental barrier, it is important to know the membrane localization of OCT3 in the syncytiotrophoblast. Syncytiotrophoblasts are multi-nucleated, terminally differentiated epithelial cells that form the placental barrier between the maternal and the fetal circulations. These cells express a number of drug transporters. In the brush border membrane facing the maternal blood, multiple transporters including Pgp, BCRP, MRP2, OCTN2, ENT1, MCTs, SERT and NET are expressed (Ganapathy et al., 2000; Vahakangas et al., 2009). The basal membrane facing the fetal blood is also known to express several transporters including MRP1, MRP5, MCTs, OAT4, OATP 2B1, and RFT-1) (Ganapathy et al., 2000; Vahakangas and Myllynen, 2009). OCT3 was generally thought to be expressed on the basal membrane of syncytiotrophoblast; however, the exact membrane localization of OCT3 in the human placenta has not been established. Previous membrane

vesicle studies using human placenta suggested OCT3 expression in the basal membrane vesicles, but not in the microvillous membrane vesicles (Sata et al., 2005). Recently, Oct3 expression was found at the basal membrane of the rat term placenta (Ahmadimoghaddam et al., 2012). Here in the human term placenta, we found that OCT3 was localized to the basal membrane of syncytiotrophoblast facing the fetal compartment, suggesting that OCT3 can play a role in transport of organic cations from the placental cells to the fetal blood.

When the pregnant mice were administered [^{14}C] metformin, Oct3^{-/-} mice exhibited altered maternal plasma kinetics profile at early time points with a higher C_{max} but only a slightly lower overall AUC. This is similar to the PK profile observed in the non-pregnant Oct3 knockout mice (Chapter 3). There were decreased AUCs in peripheral tissues including heart and salivary glands, suggesting that Oct3 mediates metformin uptake into these peripheral tissues (Table 5.4). Whether the absence of Oct3 in the small intestine contributes to change in the absorption kinetics of metformin is unclear. More investigation will be necessary to elucidate involvement of OCT3 in metformin absorption.

Previously, Zwart et al. provided evidence that Oct3 may play a role in maternal-to-fetal transfer of organic cations (Zwart et al., 2001). However, there has never been any complete pharmacokinetic study to examine the impact of Oct3 on fetal exposure. In the current study, we demonstrated that when the pregnant Oct3^{+/+} and Oct3^{-/-} mice were given metformin orally, there was significant decrease in fetal metformin AUC in pregnant Oct3^{-/-} mice. Fetal AUC_{0-∞} and AUC_{0-480 min} in the Oct3 knockout mice was reduced by 44 % and 29 % after normalization with maternal AUC. The reduced fetal exposure to metformin in mice with targeted deletion of the *Oct3* gene demonstrates that OCT3/Oct3 at the basal membrane facilitates metformin transport from syncytiotrophoblast to the fetal compartment. OCT3 is a bi-directional transporter,

indicating that high intracellular concentration can drive OCT3 to mediate transport a substrate from the cell interior to the extracellular space. To have high concentrations of metformin in the syncytiotrophoblast, there has to be initial uptake of metformin from maternal blood to the syncytiotrophoblast. The apical membrane transporters responsible for the transport of metformin from the maternal blood to the placental cells are currently unknown. Our group recently found that the apically localized SERT and NET can transport metformin in transfected cells (unpublished data), suggesting that SERT or/and NET may mediate metformin transport at the apical membrane of placental cells.

Ahmadimoghaddam et al. recently studied transport of metformin and MPP⁺ in the rat term placenta using a perfused placenta model. Their results suggested a protective mechanism as Oct3 takes up the molecules from fetal blood to the placental cells and Mate 1 at the apical membrane effluxes them into the maternal blood (Ahmadimoghaddam et al., 2012; Ahmadimoghaddam and Staud, 2013). However, in contrast to rat, the humans and mice showed very low placental expression of MATE1/Mate1, indicating that the underlying mechanisms of metformin placental transport differs between species. In addition, our findings are consistent with previous clinical studies which reported high fetal metformin concentrations at the time of delivery, suggesting a net flux of metformin from maternal blood to the fetal blood.

Recently, when we examined the OCT3/Oct3 expression in human and mouse placentas at different gestational ages, both human and mouse placentas exhibited increased expression of OCT3/Oct3 at mid-late pregnancy (Lee et al., 2013). These finding suggest that the developing fetus may be susceptible to higher exposure to metformin and other organic cations at later pregnancy than at early pregnancy. Further investigation will be necessary to fully understand

the mechanisms of metformin transport at the placental barrier and the effect of gestational age on fetal exposure to metformin.

In conclusion, the current study demonstrated that OCT3 is expressed at the basal membrane of syncytiotrophoblasts in human placenta and mice with targeted deletion of the *Oct3* gene exhibits reduced fetal exposure to metformin. Together, these results suggest that OCT3/Oct3 in the placenta facilitates metformin transport from the placental cells to the fetal compartment (Figure 5.5). This is the first study to clearly demonstrate the membrane localization of OCT3 in human placenta and the impact of Oct3 in fetal disposition of metformin in the Oct3 knockout mouse model. Our results provide strong evidence that OCT3 is an important determinant of fetal exposure to metformin and possibly other organic cation drugs during pregnancy. In the future, it would be interesting to evaluate whether gestational age-dependent placental expression and genetic polymorphism of OCT3 could have an effect on the extent to which the developing fetus are exposed to organic cation drugs during pregnancy.

Table 5.1. Maternal metformin pharmacokinetic parameters from pregnant Oct3^{+/+} and Oct3^{-/-} mice. The mice were given an oral dose of metformin (15mg/kg body weight). AUC from 0 to 480 min (AUC_{0-480min}) and that from 0 to infinity (AUC_{0-∞}), CL/F, t_{1/2, β}, V_β, AUMC and MRT were estimated using the equations as described under *Materials and methods*. Data are mean with 95 % confidence intervals (CI). Using the bootstrap method, 95 % CI and *p* value were calculated to assess the statistical significant difference of the pharmacokinetic parameters between pregnant Oct3^{+/+} and Oct3^{-/-} mice.

	Oct3 ^{+/+}	Oct3 ^{-/-}	<i>p</i> -value
AUC _{0-480min} (μg/ml*min)	608.84 (564.42, 697.85)	512.88 (451.53, 569.35)	<0.05
AUC _{0-∞} (μg/ml*min)	661.17 (616.23, 752.54)	555.98 (493.81, 614.95)	<0.05
CL/F (ml/min/kg)	24.64 (21.49, 26.58)	29.25 (26.35, 33.22)	N.S.
t _{1/2, β} (min)	118.50 (107.21, 194.71)	154.21 (99.20, 233.54)	N.S.
V _β (L/kg)	4.21 (3.60, 7.11)	6.51 (4.23, 10.32)	N.S.
AUMC (mg/ml*min ²)	81.30 (74.51, 95.85)	61.25 (50.46, 71.37)	<0.05
MRT (min)	133.53 (125.64, 140.07)	119.43 (106.57, 130.10)	N.S.

N.S., not significant.

Table 5.2. Fetal exposure to metformin in Oct3^{+/+} and Oct3^{-/-} pregnant mice. Fetal AUCs and the ratio of fetal AUC to maternal AUC were calculated. Data are mean with 95% confidence intervals (CI). Using the bootstrap method, 95% CI, % change and *p* value were calculated to assess the statistical significant differences in fetal metformin exposure between Oct3^{+/+} and Oct3^{-/-} mice.

	Oct3 ^{+/+}	Oct3 ^{-/-}	% change	<i>p</i> -value
AUC _{fetal, 0-480min} (μg/g*min)	127.18 (82,63, 145.97)	77.16 (66.85, 87.40)	↓39%	<0.05
AUC _{fetal, 0-∞} (μg/g*min)	181.09 (136.16, 204.25)	95.74 (86.19, 104.32)	↓47%	<0.05
AUC _{fetal, 0-480min} / AUC _{maternal, 0-480min}	0.21 (0.14, 0.25)	0.15 (0.13, 0.18)	↓29%	<0.05
AUC _{fetal, 0-∞} / AUC _{maternal, 0-∞}	0.27 (0.20, 0.32)	0.17 (0.15, 0.20)	↓44%	<0.05

Table 5.3. Various tissue AUCs in Oct3^{+/+} and Oct3^{-/-} pregnant mice.

AUC _{0-480min} (µg/g*min)	Oct3 ^{+/+}	Oct3 ^{-/-}	% change	<i>p</i> -value
AUC _{0-∞} (µg/g*min)				
Placenta	730.71 (603.75, 832.09)	487.23 (444.40, 529.70)	↓33%	<0.05
	1092.58 (806.02, 1771.21)	558.78 (510.68, 619.07)	↓49%	<0.05
Heart	618.75 (534.23, 711.15)	296.44 (250.63, 344.46)	↓52%	<0.05
	704.11 (598.13, 792.53)	339.72 (291.19, 401.63)	↓52%	<0.05
Salivary gland	2740.44 (2239.29, 3155.49)	830.99 (760.36, 893.74)	↓70%	<0.05
	3453.06 (2663.72, 5153.04)	1309.47 (1043.77, 1699.99)	↓62%	<0.05
Skeletal muscle	447.73 (372.07, 522.17)	367.57 (311.15, 424.68)	--	N.S.
	540.14 (474.06, 619.19)	573.61 (398.97, 1730.19)	--	N.S.
Liver	875.55 (711.08, 1051.32)	1033.66 (858.00, 1215.27)	--	N.S.
	948.68 (788.67, 1171.27)	1080.49 (904.08, 1268.00)	--	N.S.
Kidney	2241.05 (2024.75, 2416.32)	1756.10 (1505.10, 1968.37)	↓22%	<0.05
	2730.23 (2413.30, 3133.49)	1872.33 (1640.83, 2092.90)	↓31%	<0.05

N.S., not significant.

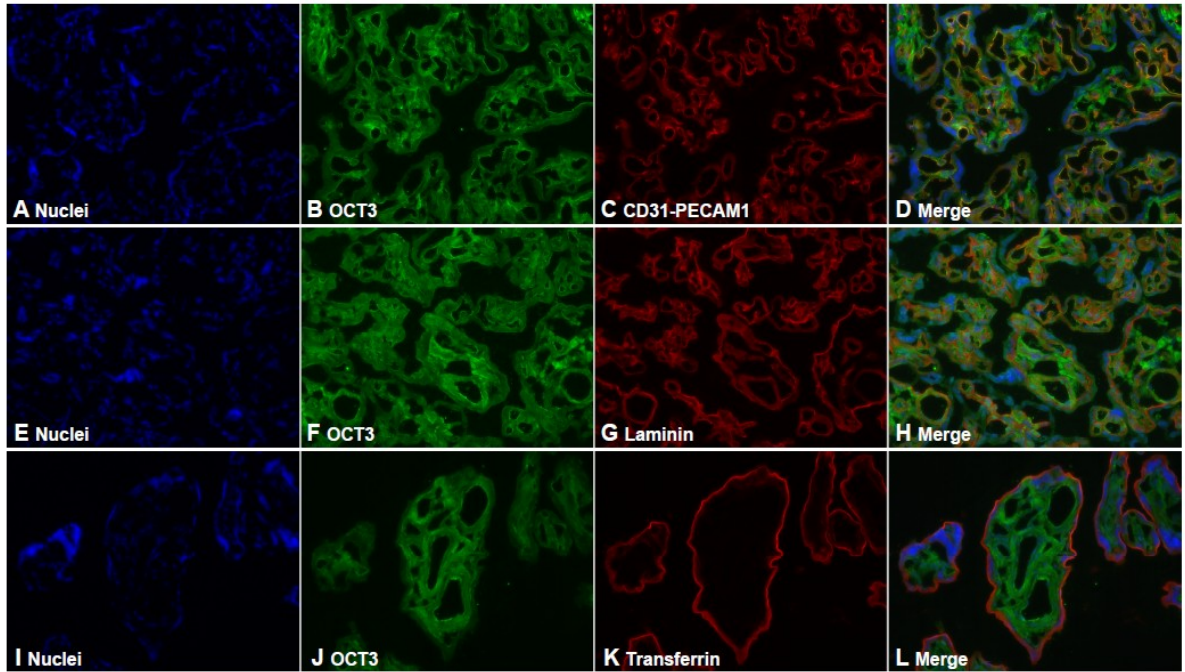


Figure 5.1. Dual-color immunofluorescence staining in human term placenta. Human term placenta sections were co-labeled with OCT3 and membrane markers including CD31-PECAM1 (endothelium), laminin (basal membrane and endothelium), and CD71-transferrin receptor (apical membrane). The nuclei were shown in blue (A, E, and I). OCT3 was labeled with green fluorescence (B, F, and J). The membrane markers were labeled with red fluorescence (C, G, and K). Merged images are shown in D, H, and L.

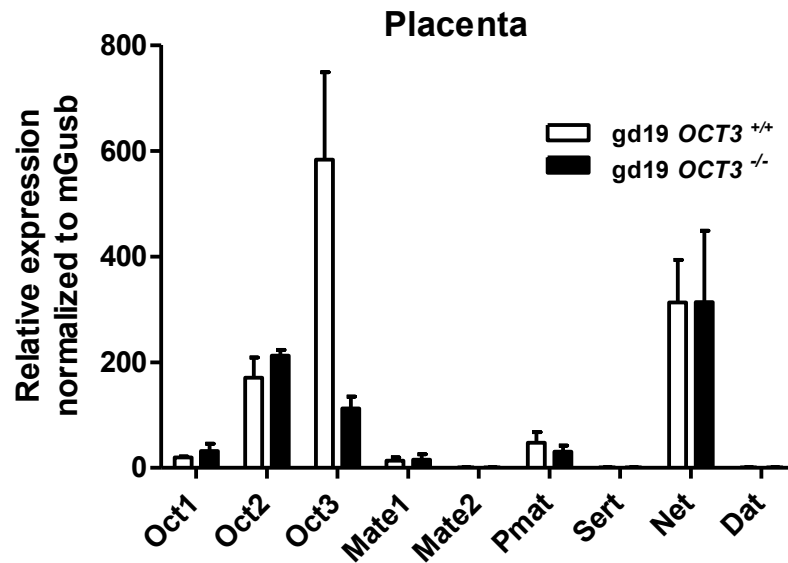


Figure 5.2. Expression of various organic cation transporters in the placentas of Oct3^{+/+} and Oct3^{-/-} mice. mRNA transcript expression of various organic cation transporters in the Oct3^{+/+} (n=3) and Oct3^{-/-} (n=3) mouse placentas at gd 19 was determined using real-time PCR.

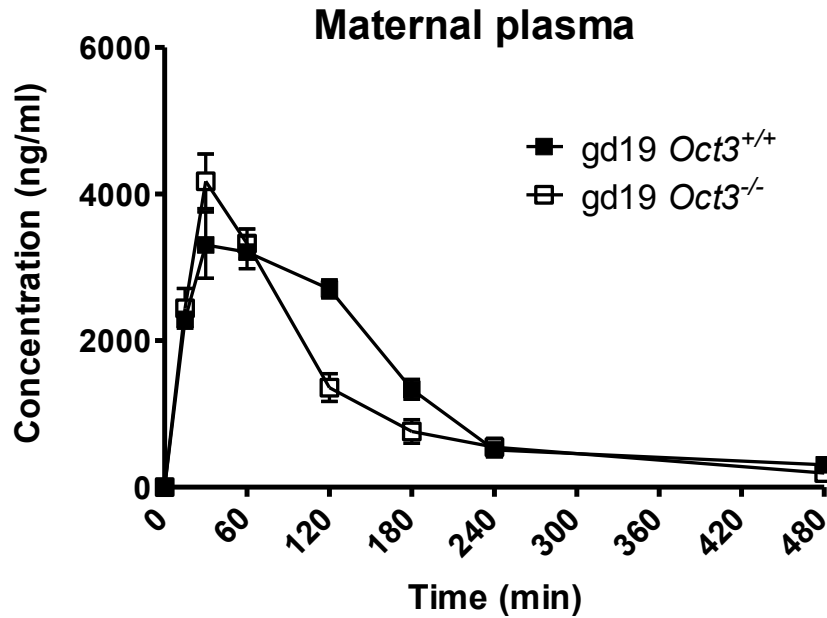


Figure 5.3. The plasma concentration-time curve of metformin after an oral dose in pregnant *Oct3*^{+/+} mice (□) and *Oct3*^{-/-} mice (■) (n=3-5 at each time point) at gd 19. The pregnant mice at 19 days of gestation were given an oral dose of 15 mg/kg metformin containing 0.2 mCi/kg of [¹⁴C] metformin. Plasma was collected up to 8 hours, and metformin concentrations were measured by liquid scintillation counter. Data represent mean ± SD.

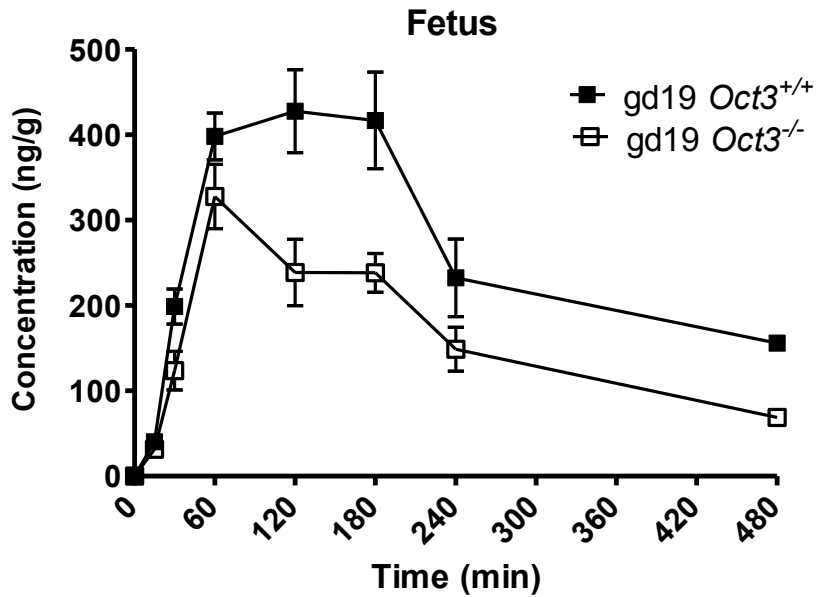


Figure 5.4. Fetal concentration-time curve of metformin after an oral dose in pregnant *Oct3*^{+/+} mice (■) and *Oct3*^{-/-} mice (□) (n=3-5 at each time point) at gd 19. The pregnant mice at 19 days of gestation were given an oral dose of 15 mg/kg with 0.2 mCi/kg of [¹⁴C] metformin. Fetus was collected up to 8 hours, and metformin concentrations were measured by liquid scintillation counter. Data represent mean ± SD.

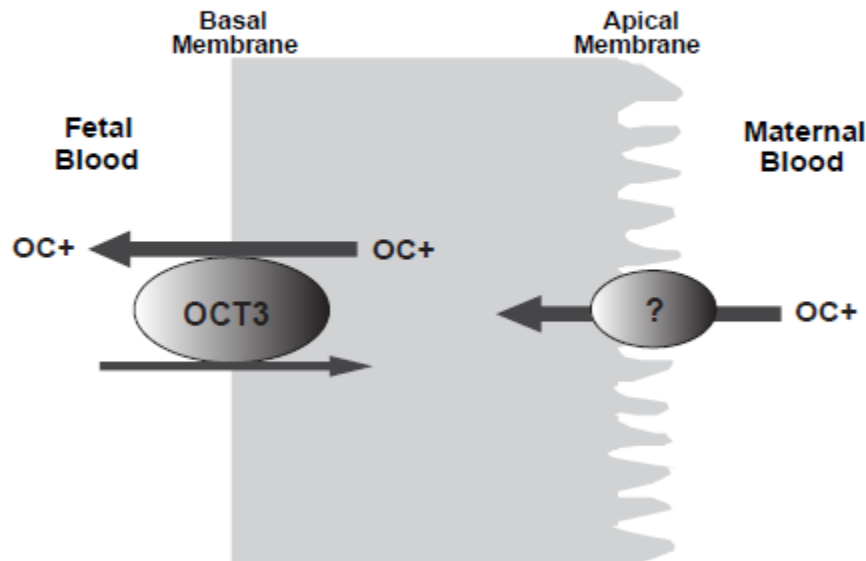


Figure 5.5. Proposed cellular model of metformin transport at the maternal-fetal interface.

OCT3 is shown in the basal membrane of syncytiotrophoblast cells and facilitates metformin transport from the placental cells to the fetal blood circulation. An unknown transporter depicted in the apical membrane of syncytiotrophoblast may transport metformin from the maternal blood circulation into the syncytiotrophoblast cell.

Chapter 6. Conclusions and future direction

Pregnancy-induced changes in drug disposition and potential teratogenicity present unique challenges for safe and effective drug therapy in pregnant women. Understanding the changes in drug metabolism and transport during pregnancy is important for optimizing drug efficacy and minimizing potential adverse effects for pregnant women and their developing fetuses. This dissertation research was focused on understanding mechanisms that influence maternal and fetal exposure to metformin, a drug currently used to treat gestational diabetes mellitus. The studies were designed to 1) determine the mechanism of altered maternal metformin disposition during pregnancy; 2) elucidate the role of OCT3 in fetal metformin disposition and in metformin tissue distribution in both pregnant and non-pregnant states.

In Chapter 2, we showed that similar to human pregnancy pregnant mice had increased apparent oral clearance of metformin, suggesting that mechanisms involved in metformin disposition are similarly affected by pregnancy in the two species. Therefore, the mouse may represent a reasonable animal model to study the effect of pregnancy on the expression of various polyspecific organic cation transporters involved in metformin disposition during pregnancy. In Chapter 3, we examined mRNA and protein expression levels of Oct1-2, Mate1-2, and Pmat in the kidneys and livers of pregnant mice at different gestational ages. Our results revealed that mRNA and protein expressions of mOct1 and mOct2 in the mouse kidney are marginally affected by pregnancy. Similarly, hepatic expression of mOct1 and mMate1 mRNA and protein is also minimally affected by pregnancy. However, in the kidney, mMate1 mRNA and protein expressions significantly declined by 20%–40% throughout pregnancy, with maximum down-regulation of mMate1 membrane protein observed at mid-pregnancy. Because we did not observe an increase in Oct or Mate renal expression, altered renal expression of

organic cation transporters may not be the reason underlying the observed increase in renal clearance of metformin during pregnancy. Other pregnancy-associated changes, such as elevation in renal blood flow and glomerular filtration, may contribute to the increased total renal clearance of metformin in pregnancy. However, it should be noted that our study was conducted in mice, so we cannot exclude the possibility that expressions of hOCT2 and hMATE1/2-K in the human kidney are uniquely affected by pregnancy.

With regard to fetal metformin disposition, we particularly focused on OCT3 (Chapters 3 and 5). Both human and mouse placentas showed high expression of OCT3/Oct3 with minimal expression of other organic cation transporters. Interestingly, mouse placental Oct3 expression significantly increased after early gestational age while OCT3 expression in human placenta showed a modest increase in mid-to-late pregnancy. In human term placenta, OCT3 was localized to the basal membrane of syncytiotrophoblast cells, facing the fetal compartment. Our *in vivo* study further showed a significant decrease in metformin fetal exposure in pregnant Oct3 knockout mice. Together our data suggest that OCT3/Oct3 facilitates metformin transport from placental epithelial cells to the fetus and is an important determinant for fetal exposure to metformin and possibly other organic cation drugs. To fully understand the molecular mechanism of fetal disposition of metformin from maternal-to-fetal compartments, future research should be directed towards identifying the apical membrane transporter(s) responsible for metformin uptake from the maternal blood into the placental cells. In addition, *in vivo* studies may be necessary to examine if the increased Oct3 placental expression in mid-to-late pregnancy translates to an increase in fetal exposure to metformin at the later stage of gestation.

In this dissertation research, we examined the role of OCT3 in fetal disposition of metformin during pregnancy, as well as investigated the significance of OCT3 in tissue

distribution of metformin in non-pregnant state (Chapter 4). Results from an *in vivo* study in non pregnant wild type and Oct3 knockout mice suggested that OCT3/Oct3 plays an important role in the plasma PK and peripheral tissue distribution of metformin. Oct3 knockout mice exhibited altered plasma concentrations during the first 1 hour following dosing and showed reduced metformin accumulation in heart, salivary gland and skeletal muscle. The change in salivary gland concentration was remarkable, suggesting that OCT3/Oct3 is responsible for high accumulation of metformin in the salivary glands, potentially leading to the taste disturbance, a common adverse effect of metformin. It would be interesting to know if OCT3 plays a physiological role in salivary glands (e.g. saliva generation, salivary recycling, etc); and if OCT3 is also involved in the taste disturbance of other organic cation drugs.

In conclusion, my dissertation research has contributed greatly to our understanding of the role of OCT3 in metformin disposition. My research has demonstrated that OCT3 facilitates the metformin disposition from the placenta to the fetal compartment and plays an important role in peripheral tissue distribution of metformin. In particular, OCT3-mediated high accumulation of metformin in the salivary glands potentially underlies taste disturbance of metformin. Several genetic polymorphisms of the *OCT3* gene have been reported. In the future, it would be important to determine if genetic variants of OCT3 contribute to inter-individual variations in metformin disposition, response and adverse reactions. In addition, my thesis research provided the first ever information on the effect of pregnancy on mRNA and protein expression of various polyspecific organic cation transporters in kidney, liver and placenta. These findings contribute to our understanding of molecular mechanisms involved in maternal and fetal disposition of metformin and will help to pave the way for optimizing metformin pharmacotherapy to treat gestational diabetes mellitus in the pregnant population.

Bibliography

- Adam MP, Polifka JE and Friedman JM (2011) Evolving knowledge of the teratogenicity of medications in human pregnancy. *American journal of medical genetics Part C, Seminars in medical genetics* **157**(3): 175-182.
- Ahmadimoghaddam D, Hofman J, Zemankova L, Nachtigal P, Dolezelova E, Cervený L, Ceckova M, Micuda S and Staud F (2012) Synchronized Activity of Organic Cation Transporter 3 (OCT3/Slc22a3) and Multidrug and Toxin Extrusion 1 (MATE1/Slc47a1) Transporter in Transplacental Passage of MPP⁺ in Rat. *Toxicol Sci* **128**(2): 471-481.
- Ahmadimoghaddam D and Staud F (2013) Transfer of metformin across the rat placenta is mediated by organic cation transporter 3 (OCT3/SLC22A3) and multidrug and toxin extrusion 1 (MATE1/SLC47A1) protein. *Reprod Toxicol* **39**: 17-22.
- Andrade SE, Gurwitz JH, Davis RL, Chan KA, Finkelstein JA, Fortman K, McPhillips H, Raebel MA, Roblin D, Smith DH, Yood MU, Morse AN and Platt R (2004) Prescription drug use in pregnancy. *American journal of obstetrics and gynecology* **191**(2): 398-407.
- Barnes K, Dobrzynski H, Foppolo S, Beal PR, Ismat F, Scullion ER, Sun L, Tellez J, Ritzel MW, Claycomb WC, Cass CE, Young JD, Billeter-Clark R, Boyett MR and Baldwin SA (2006) Distribution and functional characterization of equilibrative nucleoside transporter-4, a novel cardiac adenosine transporter activated at acidic pH. *Circ Res* **99**(5): 510-519.
- Berggren EK and Boggess KA (2013) Oral Agents for the Management of Gestational Diabetes. *Clinical obstetrics and gynecology*.
- Charles B, Norris R, Xiao X and Hague W (2006) Population pharmacokinetics of metformin in late pregnancy. *Ther Drug Monit* **28**(1): 67-72.
- Chen L, Pawlikowski B, Schlessinger A, More SS, Stryke D, Johns SJ, Portman MA, Chen E, Ferrin TE, Sali A and Giacomini KM (2010) Role of organic cation transporter 3 (SLC22A3) and its missense variants in the pharmacologic action of metformin. *Pharmacogenet Genomics* **20**(11): 687-699.
- Chen Y, Li S, Brown C, Cheatham S, Castro RA, Leabman MK, Urban TJ, Chen L, Yee SW, Choi JH, Huang Y, Brett CM, Burchard EG and Giacomini KM (2009) Effect of genetic variation in the organic cation transporter 2 on the renal elimination of metformin. *Pharmacogenet Genomics* **19**(7): 497-504.
- Chen Y, Zhang S, Sorani M and Giacomini KM (2007) Transport of paraquat by human organic cation transporters and multidrug and toxic compound extrusion family. *J Pharmacol Exp Ther* **322**(2): 695-700.
- Choi JH, Yee SW, Ramirez AH, Morrissey KM, Jang GH, Joski PJ, Mefford JA, Hesselson SE, Schlessinger A, Jenkins G, Castro RA, Johns SJ, Stryke D, Sali A, Ferrin TE, Witte JS, Kwok PY, Roden DM, Wilke RA, McCarty CA, Davis RL and Giacomini KM (2011) A common 5'-UTR variant in MATE2-K is associated with poor response to metformin. *Clin Pharmacol Ther* **90**(5): 674-684.
- Dresser MJ, Xiao G, Leabman MK, Gray AT and Giacomini KM (2002) Interactions of n-tetraalkylammonium compounds and biguanides with a human renal organic cation transporter (hOCT2). *Pharm Res* **19**(8): 1244-1247.
- Duan H and Wang J (2010) Selective transport of monoamine neurotransmitters by human plasma membrane monoamine transporter and organic cation transporter 3. *J Pharmacol Exp Ther* **335**(3): 743-753.
- Dunn CJ and Peters DH (1995) Metformin. A review of its pharmacological properties and therapeutic use in non-insulin-dependent diabetes mellitus. *Drugs* **49**(5): 721-749.
- Engel K and Wang J (2005) Interaction of organic cations with a newly identified plasma membrane monoamine transporter. *Mol Pharmacol* **68**(5): 1397-1407.

- Engel K, Zhou M and Wang J (2004) Identification and characterization of a novel monoamine transporter in the human brain. *J Biol Chem* **279**(48): 50042-50049.
- Eyal S, Easterling TR, Carr D, Umans JG, Miodovnik M, Hankins GD, Clark SM, Risler L, Wang J, Kelly EJ, Shen DD and Hebert MF (2010) Pharmacokinetics of metformin during pregnancy. *Drug metabolism and disposition: the biological fate of chemicals* **38**(5): 833-840.
- Fujita T, Urban TJ, Leabman MK, Fujita K and Giacomini KM (2006) Transport of drugs in the kidney by the human organic cation transporter, OCT2 and its genetic variants. *J Pharm Sci* **95**(1): 25-36.
- Ganapathy V, Prasad PD, Ganapathy ME and Leibach FH (2000) Placental transporters relevant to drug distribution across the maternal-fetal interface. *J Pharmacol Exp Ther* **294**(2): 413-420.
- Giacomini KM, Huang SM, Tweedie DJ, Benet LZ, Brouwer KL, Chu X, Dahlin A, Evers R, Fischer V, Hillgren KM, Hoffmaster KA, Ishikawa T, Keppler D, Kim RB, Lee CA, Niemi M, Polli JW, Sugiyama Y, Swaan PW, Ware JA, Wright SH, Yee SW, Zamek-Gliszczynski MJ, Zhang L and Consortium IT (2010) Membrane transporters in drug development. *Nat Rev Drug Discov* **9**(3): 215-236.
- Glover DD, Amonkar M, Rybeck BF and Tracy TS (2003) Prescription, over-the-counter, and herbal medicine use in a rural, obstetric population. *American journal of obstetrics and gynecology* **188**(4): 1039-1045.
- Gui J, Liu Q and Feng L (2013) Metformin vs insulin in the management of gestational diabetes: a meta-analysis. *PloS one* **8**(5): e64585.
- Hebert MF, Easterling TR, Kirby B, Carr DB, Buchanan ML, Rutherford T, Thummel KE, Fishbein DP and Unadkat JD (2008) Effects of pregnancy on CYP3A and P-glycoprotein activities as measured by disposition of midazolam and digoxin: a University of Washington specialized center of research study. *Clin Pharmacol Ther* **84**(2): 248-253.
- Hiasa M, Matsumoto T, Komatsu T and Moriyama Y (2006) Wide variety of locations for rodent MATE1, a transporter protein that mediates the final excretion step for toxic organic cations. *Am J Physiol Cell Physiol* **291**(4): C678-686.
- Hodge LS and Tracy TS (2007) Alterations in drug disposition during pregnancy: implications for drug therapy. *Expert Opin Drug Metab Toxicol* **3**(4): 557-571.
- Hundal RS and Inzucchi SE (2003) Metformin: new understandings, new uses. *Drugs* **63**(18): 1879-1894.
- Inzucchi SE (2002) Oral antihyperglycemic therapy for type 2 diabetes: scientific review. *JAMA : the journal of the American Medical Association* **287**(3): 360-372.
- Isoherranen N and Thummel KE (2013) Drug metabolism and transport during pregnancy: how does drug disposition change during pregnancy and what are the mechanisms that cause such changes? *Drug metabolism and disposition: the biological fate of chemicals* **41**(2): 256-262.
- Johnson JA, Majumdar SR, Simpson SH and Toth EL (2002) Decreased mortality associated with the use of metformin compared with sulfonylurea monotherapy in type 2 diabetes. *Diabetes Care* **25**(12): 2244-2248.
- Kamiie J, Ohtsuki S, Iwase R, Ohmine K, Katsukura Y, Yanai K, Sekine Y, Uchida Y, Ito S and Terasaki T (2008) Quantitative atlas of membrane transporter proteins: development and application of a highly sensitive simultaneous LC/MS/MS method combined with novel in-silico peptide selection criteria. *Pharm Res* **25**(6): 1469-1483.
- Kekuda R, Prasad PD, Wu X, Wang H, Fei YJ, Leibach FH and Ganapathy V (1998) Cloning and functional characterization of a potential-sensitive, polyspecific organic cation transporter (OCT3) most abundantly expressed in placenta. *J Biol Chem* **273**(26): 15971-15979.
- Kimura N, Masuda S, Tanihara Y, Ueo H, Okuda M, Katsura T and Inui K (2005) Metformin is a superior substrate for renal organic cation transporter OCT2 rather than hepatic OCT1. *Drug Metab Pharmacokinet* **20**(5): 379-386.
- Koepsell H (2004) Polyspecific organic cation transporters: their functions and interactions with drugs. *Trends Pharmacol Sci* **25**(7): 375-381.

- Koepsell H, Lips K and Volk C (2007) Polyspecific organic cation transporters: structure, function, physiological roles, and biopharmaceutical implications. *Pharm Res* **24**(7): 1227-1251.
- Koepsell H, Schmitt BM and Gorboulev V (2003) Organic cation transporters. *Rev Physiol Biochem Pharmacol* **150**: 36-90.
- Koh KH, Xie H, Yu AM and Jeong H (2011) Altered cytochrome P450 expression in mice during pregnancy. *Drug metabolism and disposition: the biological fate of chemicals* **39**(2): 165-169.
- Kovo M, Kogman N, Ovadia O, Nakash I, Golan A and Hoffman A (2008) Carrier-mediated transport of metformin across the human placenta determined by using the ex vivo perfusion of the placental cotyledon model. *Prenat Diagn* **28**(6): 544-548.
- Langer O, Conway DL, Berkus MD, Xenakis EM and Gonzales O (2000) A comparison of glyburide and insulin in women with gestational diabetes mellitus. *N Engl J Med* **343**(16): 1134-1138.
- Langer O, Yogev Y, Most O and Xenakis EM (2005) Gestational diabetes: the consequences of not treating. *American journal of obstetrics and gynecology* **192**(4): 989-997.
- Lautatzis ME, Goulis DG and Vrontakis M (2013) Efficacy and safety of metformin during pregnancy in women with gestational diabetes mellitus or polycystic ovary syndrome: A systematic review. *Metabolism: clinical and experimental*.
- Lee N, Hebert MF, Prasad B, Easterling TR, Kelly EJ, Unadkat JD and Wang J (2013) Effect of Gestational Age on mRNA and Protein Expression of Polyspecific Organic Cation Transporters during Pregnancy. *Drug metabolism and disposition: the biological fate of chemicals* **41**(12): 2225-2232.
- Li M, Anderson GD and Wang J (2006) Drug-drug interactions involving membrane transporters in the human kidney. *Expert Opin Drug Metab Toxicol* **2**(4): 505-532.
- Lickteig AJ, Cheng X, Augustine LM, Klaassen CD and Cherrington NJ (2008) Tissue distribution, ontogeny and induction of the transporters Multidrug and toxin extrusion (MATE) 1 and MATE2 mRNA expression levels in mice. *Life Sci* **83**(1-2): 59-64.
- Lord JM, Flight IH and Norman RJ (2003) Metformin in polycystic ovary syndrome: systematic review and meta-analysis. *BMJ* **327**(7421): 951-953.
- Mager H and Göller G (1998) Resampling methods in sparse sampling situations in preclinical pharmacokinetic studies. *J Pharm Sci* **87**(3): 372-378.
- Masuda S, Terada T, Yonezawa A, Tanihara Y, Kishimoto K, Katsura T, Ogawa O and Inui K (2006) Identification and functional characterization of a new human kidney-specific H⁺/organic cation antiporter, kidney-specific multidrug and toxin extrusion 2. *J Am Soc Nephrol* **17**(8): 2127-2135.
- Mathias AA, Hitti J and Unadkat JD (2005) P-glycoprotein and breast cancer resistance protein expression in human placentae of various gestational ages. *American journal of physiology Regulatory, integrative and comparative physiology* **289**(4): R963-969.
- Melchior WR and Jaber LA (1996) Metformin: an antihyperglycemic agent for treatment of type II diabetes. *Ann Pharmacother* **30**(2): 158-164.
- Menghi G, Curini R and Materazzi S (1989) Characterization of mouse salivary glands by water content and type. *Cellular and molecular biology* **35**(4): 391-398.
- Mesdaghinia E, Samimi M, Homaei Z, Saberi F, Moosavi SG and Yaribakht M (2013) Comparison of newborn outcomes in women with gestational diabetes mellitus treated with metformin or insulin: a randomised blinded trial. *International journal of preventive medicine* **4**(3): 327-333.
- Moriyama Y, Hiasa M, Matsumoto T and Omote H (2008) Multidrug and toxic compound extrusion (MATE)-type proteins as anchor transporters for the excretion of metabolic waste products and xenobiotics. *Xenobiotica; the fate of foreign compounds in biological systems* **38**(7-8): 1107-1118.
- Nies AT, Koepsell H, Winter S, Burk O, Klein K, Kerb R, Zanger UM, Keppler D, Schwab M and Schaeffeler E (2009) Expression of organic cation transporters OCT1 (SLC22A1) and OCT3 (SLC22A3) is affected by genetic factors and cholestasis in human liver. *Hepatology* **50**(4): 1227-1240.

- Ohtsuki S, Schaefer O, Kawakami H, Inoue T, Liehner S, Saito A, Ishiguro N, Kishimoto W, Ludwig-Schwellinger E, Ebner T and Terasaki T (2012) Simultaneous absolute protein quantification of transporters, cytochromes P450, and UDP-glucuronosyltransferases as a novel approach for the characterization of individual human liver: comparison with mRNA levels and activities. *Drug metabolism and disposition: the biological fate of chemicals* **40**(1): 83-92.
- Otsuka M, Matsumoto T, Morimoto R, Arioka S, Omote H and Moriyama Y (2005) A human transporter protein that mediates the final excretion step for toxic organic cations. *Proc Natl Acad Sci U S A* **102**(50): 17923-17928.
- Pentikainen PJ, Neuvonen PJ and Penttila A (1979) Pharmacokinetics of metformin after intravenous and oral administration to man. *Eur J Clin Pharmacol* **16**(3): 195-202.
- Pinkstaff CA (1998) Salivary gland sexual dimorphism: a brief review. *European journal of morphology* **36 Suppl**: 31-34.
- Prasad B, Lai Y, Lin Y and Unadkat JD (2013) Interindividual variability in the hepatic expression of the human breast cancer resistance protein (BCRP/ABCG2): effect of age, sex, and genotype. *J Pharm Sci* **102**(3): 787-793.
- Qaseem A, Humphrey LL, Sweet DE, Starkey M and Shekelle P (2012) Oral pharmacologic treatment of type 2 diabetes mellitus: a clinical practice guideline from the American College of Physicians. *Ann Intern Med* **156**(3): 218-231.
- Rowan JA, Hague WM, Gao W, Battin MR and Moore MP (2008) Metformin versus insulin for the treatment of gestational diabetes. *N Engl J Med* **358**(19): 2003-2015.
- Sata R, Ohtani H, Tsujimoto M, Murakami H, Koyabu N, Nakamura T, Uchiumi T, Kuwano M, Nagata H, Tsukimori K, Nakano H and Sawada Y (2005) Functional analysis of organic cation transporter 3 expressed in human placenta. *J Pharmacol Exp Ther* **315**(2): 888-895.
- Scheen AJ (1996) Clinical pharmacokinetics of metformin. *Clin Pharmacokinet* **30**(5): 359-371.
- Shehata HA and Nelson-Piercy C (2001) Drugs in pregnancy. Drugs to avoid. *Best practice & research Clinical obstetrics & gynaecology* **15**(6): 971-986.
- Shu Y, Brown C, Castro RA, Shi RJ, Lin ET, Owen RP, Sheardown SA, Yue L, Burchard EG, Brett CM and Giacomini KM (2008) Effect of genetic variation in the organic cation transporter 1, OCT1, on metformin pharmacokinetics. *Clin Pharmacol Ther* **83**(2): 273-280.
- Shu Y, Sheardown SA, Brown C, Owen RP, Zhang S, Castro RA, Ianculescu AG, Yue L, Lo JC, Burchard EG, Brett CM and Giacomini KM (2007) Effect of genetic variation in the organic cation transporter 1 (OCT1) on metformin action. *J Clin Invest* **117**(5): 1422-1431.
- Shuster DL, Bammler TK, Beyer RP, Macdonald JW, Tsai JM, Farin FM, Hebert MF, Thummel KE and Mao Q (2013) Gestational age-dependent changes in gene expression of metabolic enzymes and transporters in pregnant mice. *Drug Metab Dispos* **41**(2): 332-342.
- Song IS, Shin HJ, Shim EJ, Jung IS, Kim WY, Shon JH and Shin JG (2008) Genetic variants of the organic cation transporter 2 influence the disposition of metformin. *Clin Pharmacol Ther* **84**(5): 559-562.
- Stocker SL, Morrissey KM, Yee SW, Castro RA, Xu L, Dahlin A, Ramirez AH, Roden DM, Wilke RA, McCarty CA, Davis RL, Brett CM and Giacomini KM (2013) The effect of novel promoter variants in MATE1 and MATE2 on the pharmacokinetics and pharmacodynamics of metformin. *Clin Pharmacol Ther* **93**(2): 186-194.
- Suhre WM, Ekins S, Chang C, Swaan PW and Wright SH (2005) Molecular determinants of substrate/inhibitor binding to the human and rabbit renal organic cation transporters hOCT2 and rbOCT2. *Molecular pharmacology* **67**(4): 1067-1077.
- Tanihara Y, Masuda S, Sato T, Katsura T, Ogawa O and Inui K (2007) Substrate specificity of MATE1 and MATE2-K, human multidrug and toxin extrusions/H(+)-organic cation antiporters. *Biochem Pharmacol* **74**(2): 359-371.
- Terada T, Masuda S, Asaka J, Tsuda M, Katsura T and Inui K (2006) Molecular cloning, functional characterization and tissue distribution of rat H⁺/organic cation antiporter MATE1. *Pharm Res* **23**(8): 1696-1701.

- Tracy TS, Venkataramanan R, Glover DD, Caritis SN, National Institute for Child H and Human Development Network of Maternal-Fetal-Medicine U (2005) Temporal changes in drug metabolism (CYP1A2, CYP2D6 and CYP3A Activity) during pregnancy. *American journal of obstetrics and gynecology* **192**(2): 633-639.
- Tsuda M, Terada T, Mizuno T, Katsura T, Shimakura J and Inui K (2009a) Targeted disruption of the multidrug and toxin extrusion 1 (mate1) gene in mice reduces renal secretion of metformin. *Molecular pharmacology* **75**(6): 1280-1286.
- Tsuda M, Terada T, Ueba M, Sato T, Masuda S, Katsura T and Inui K (2009b) Involvement of human multidrug and toxin extrusion 1 in the drug interaction between cimetidine and metformin in renal epithelial cells. *J Pharmacol Exp Ther* **329**(1): 185-191.
- Tzvetkov MV, Vormfelde SV, Balen D, Meineke I, Schmidt T, Sehr D, Sabolic I, Koepsell H and Brockmoller J (2009) The effects of genetic polymorphisms in the organic cation transporters OCT1, OCT2, and OCT3 on the renal clearance of metformin. *Clin Pharmacol Ther* **86**(3): 299-306.
- Uchida Y, Ohtsuki S, Katsukura Y, Ikeda C, Suzuki T, Kamiie J and Terasaki T (2011) Quantitative targeted absolute proteomics of human blood-brain barrier transporters and receptors. *J Neurochem* **117**(2): 333-345.
- Vahakangas K and Myllynen P (2009) Drug transporters in the human blood-placental barrier. *Br J Pharmacol* **158**(3): 665-678.
- Vanky E, Zahlén K, Spigset O and Carlsen SM (2005) Placental passage of metformin in women with polycystic ovary syndrome. *Fertil Steril* **83**(5): 1575-1578.
- Wang DS, Jonker JW, Kato Y, Kusuhashi H, Schinkel AH and Sugiyama Y (2002) Involvement of organic cation transporter 1 in hepatic and intestinal distribution of metformin. *J Pharmacol Exp Ther* **302**(2): 510-515.
- Wang H, Wu X, Hudkins K, Mikheev A, Zhang H, Gupta A, Unadkat JD and Mao Q (2006) Expression of the breast cancer resistance protein (Bcrp1/Abcg2) in tissues from pregnant mice: effects of pregnancy and correlations with nuclear receptors. *Am J Physiol Endocrinol Metab* **291**(6): E1295-1304.
- Wang ZJ, Yin OQ, Tomlinson B and Chow MS (2008) OCT2 polymorphisms and in-vivo renal functional consequence: studies with metformin and cimetidine. *Pharmacogenet Genomics* **18**(7): 637-645.
- Wensel TM (2009) Role of metformin in the treatment of gestational diabetes. *Ann Pharmacother* **43**(5): 939-943.
- Wilcock C and Bailey CJ (1994) Accumulation of metformin by tissues of the normal and diabetic mouse. *Xenobiotica; the fate of foreign compounds in biological systems* **24**(1): 49-57.
- Wright SH and Dantzer WH (2004) Molecular and cellular physiology of renal organic cation and anion transport. *Physiol Rev* **84**(3): 987-1049.
- Wu X, Huang W, Ganapathy ME, Wang H, Kekuda R, Conway SJ, Leibach FH and Ganapathy V (2000) Structure, function, and regional distribution of the organic cation transporter OCT3 in the kidney. *Am J Physiol Renal Physiol* **279**(3): F449-458.
- Xia L, Engel K, Zhou M and Wang J (2007) Membrane localization and pH-dependent transport of a newly cloned organic cation transporter (PMAT) in kidney cells. *Am J Physiol Renal Physiol* **292**(2): F682-690.
- Yacovino LL, Gibson CJ and Aleksunes LM (2013) Down-regulation of brush border efflux transporter expression in the kidneys of pregnant mice. *Drug Metab Dispos* **41**(2): 320-325.
- Zhang H, Wu X, Wang H, Mikheev AM, Mao Q and Unadkat JD (2008) Effect of pregnancy on cytochrome P450 3a and P-glycoprotein expression and activity in the mouse: mechanisms, tissue specificity, and time course. *Mol Pharmacol* **74**(3): 714-723.
- Zhou L, Naraharisetti SB, Wang H, Unadkat JD, Hebert MF and Mao Q (2008) The breast cancer resistance protein (Bcrp1/Abcg2) limits fetal distribution of glyburide in the pregnant mouse: an

- Obstetric-Fetal Pharmacology Research Unit Network and University of Washington Specialized Center of Research Study. *Mol Pharmacol* **73**(3): 949-959.
- Zhou L, Zhang Y, Hebert MF, Unadkat JD and Mao Q (2010) Increased glyburide clearance in the pregnant mouse model. *Drug metabolism and disposition: the biological fate of chemicals* **38**(9): 1403-1406.
- Zhou M, Xia L and Wang J (2007) Metformin transport by a newly cloned proton-stimulated organic cation transporter (plasma membrane monoamine transporter) expressed in human intestine. *Drug metabolism and disposition: the biological fate of chemicals* **35**(10): 1956-1962.
- Zolk O (2012) Disposition of metformin: variability due to polymorphisms of organic cation transporters. *Ann Med* **44**(2): 119-129.
- Zwart R, Sleutels F, Wutz A, Schinkel AH and Barlow DP (2001a) Bidirectional action of the Igf2r imprint control element on upstream and downstream imprinted genes. *Genes Dev* **15**(18): 2361-2366.
- Zwart R, Verhaagh S, Buitelaar M, Popp-Snijders C and Barlow DP (2001b) Impaired activity of the extraneuronal monoamine transporter system known as uptake-2 in Orct3/Slc22a3-deficient mice. *Mol Cell Biol* **21**(13): 4188-4196.